Development of a Model using Machine Learning Intended to be Embedded in a Wearable Device to Detect Muscle Fatigue based on sEMG Data Associated with a Sustained Single 80% Maximum Voluntary Contraction

by

Md Manirul Islam

A thesis submitted in partial fulfillment of the requirements for the degree of

Master of Science

in

Rehabilitation Science

Faculty of Rehabilitation Medicine
University of Alberta

ABSTRACT

Background: Muscle fatigue is the progressive reduction in a muscle's ability to contract and exert force when performing a sustained task. Muscle fatigue may prevent the task from being complete and increase the risk of injury. Eventually, the performance of individuals during athletic activities can be limited due to fatigue. Individuals typically have to rely on their own perception of muscle fatigue and often report this to their trainer subjectively. Fatigue onset may occur differently from day to day due to the factors such as dehydration and electrolyte balance. As a result, constant vigilance is required to optimize exertion levels completing a task. Obtaining a balance between enhancing performance and preventing injury is essential in planning the desired exercise and training program for a specific activity. A wearable device to detect muscle fatigue in real-time can help define training strategies for optimal test-specific activities and exercises.

Objective: The overall objective of this thesis was to develop a model using machine learning that can be embedded in a wearable device to detect muscle fatigue in real-time based on the sEMG data associated with a sustained single 80% maximum voluntary contraction (MVC).

Five specific objectives were undertaken sequentially to accomplish the overall objective. The individual specific objectives included: 1) To conduct a scoping review to identify all machine learning algorithms that are potentially capable of detecting muscle fatigue in a real-time and computationally adaptable to be embedded in a wearable device, 2) To extract features from the previously recorded sEMG data, and select the most promising features that are associated with a pattern of fatigue, 3) To evaluate the performance of the algorithms selected in Objective 1 using the extracted features identified in Objective 2, 4) To then select the most promising algorithm

based its accuracy in classifying fatigue state, and 5) To develop a model using the identified ML algorithm that has the potential to be embedded in a wearable device.

Methods: To address our first objective, a scoping review involving six different electronic databases was undertaken, where a total of 67 studies were included.

To address objectives 2-5, an sEMG dataset from 100 participants who performed a sustained single 80% MVC was evaluated. The Fast Fourier Transform was used to estimate the power spectrum. Several frequency and time domain features (RMS, IEMG, Power, Median and Mean Frequency) from the sEMG signal were extracted. The Neighbourhood Component Analysis (NCA) was applied to select promising features. After training each algorithm utilizing selected features, their performance in fatigue classification was evaluated. The most promising algorithm was selected to develop our proposed model based on the classification performance and adaptability to integrate the algorithm in a wearable device.

Finally, a new model was developed, and its potential to be embedded in a wearable device detecting muscle fatigue in real-time was assessed.

Results: The scoping review suggested four potential algorithms (LDA, LR, SVMs, and Ensemble) that had the potential to be integrated into a wearable device with the goal of fatigue detection in real-time.

From the extracted sEMG features, NCA selected 14 features that were used to train the ML algorithm. Comparing the performance of each algorithm with selected features, the proposed OSVM model achieved the highest classification accuracy of 99.2% with a sensitivity of 99% and specificity of 99.2%. The area under the curve (AUC) for both fatigue and non-fatigue conditions

achieved a maximum unity of 1.00. Further testing of the trained model with new data demonstrated a 100% fatigue classification accuracy, an outstanding performance in the current literature. Additionally, our developed OSVM model showed a 92% fatigue classification accuracy when using only the 5 most prominent features.

Conclusion: This research represents a comprehensive automated method where the developed model can be used in the laboratory setting as well as a wearable device to detect muscle fatigue in real-time during a sustained single isometric task. Furthermore, the features reduction mechanism facilitates the model to perform adaptively on the criteria of fatigue forecasting time and performance accuracy. Based on the technical requirements, the model is suitable for embedding into the 'Raspberry Pi Zero-W' microcontroller. Deploying into the microcontroller, it is possible to be used as a wearable device to detect muscle in real-time.

Keywords: *Surface EMG, MVC, Muscle fatigue, Algorithm, Feature extraction and selection, Model, Wearable device, Real-time.*

PREFACE

This thesis is an original work by Md. Manirul Islam. The research project, of which this thesis is a part, received research ethics approval from the University of Alberta Research Ethics Board for the following project:

Project Name: **Real-Time Algorithm to Detect Muscle Fatigue in Biceps Brachii Muscles**.

Project ID No. : **Pro00063851** dated: 01/07/2016

The related materials shown in this work are original research conducted in the Rehabilitation Robotics Lab (RRL) at the University of Alberta.

The 100 participants' dataset used in this research were collected previously by Mr. Adam Pinkoski and his team, under the direct supervision of Professor Dr. Martin Ferguson-Pell.

The analysis of this dataset is my original work.

Chapters 2 and 3 are intended to be submitted for publication. The anticipated journals for publishing the research work of Chapter 2 and Chapter 3 are the 'IEEE Journal of Biomedical and Health Informatics, and the 'IEEE Sensors Journal'.

Chapter 1 introduces the context of this study, and Chapter 4 discusses the outcomes of this study and considers the potential for creating a wearable device that can accurately assess muscle fatigue in real-time.

This thesis is an original work by Md. Manirul Islam. No part of this thesis has been previously published.

DEDICATION

It is my absolute pleasure to dedicate this thesis to my parents, brothers, sister, niece (Khushi), nephew (Dolon), and all of the family members.

Throughout my life, they have always been my shadow.

"There is no success in research, only welfare for the universe."

*_M_*

ACKNOWLEDGEMENTS

I feel incredibly grateful to think how my parents and my family have laid the base of where I stand now in here. Their dedication and motivation have thrived my journey from a small town in Bangladesh to this dream destiny through time and space. They are my constant inspiration to execute at my best possible level.

I would like to express my reply to the Rajshahi University of Engineering & Technology (RUET), Bangladesh, allowing me to come here with study leave.

I am thankful to all of the faculty members, staff, and students in the Department of Mechatronics Engineering, RUET. The values and experience I gathered there were critical to my growth. I would like to convey my gratitude to my colleagues for their incessant support.

The contribution of the University of Alberta and the Faculty of Rehabilitation Medicine to my life is irreplaceable. They have allowed me the opportunity to discover myself in the journey to acquire knowledge and expertise for serving through excellence. I am wordless to convey my gratitude for the financial assistance and scholarship they provided me during my studies.

I am indebted to all of my fellow labmates at the RRL lab for their magnanimous support that have shielded me during this ongoing pandemic. Although we work from home, we meet virtually and look after each other regularly. They are like my second family to me.

I would also like to extend my appreciation to Mr. Adam Pinkoski and colleagues for access to the data that they had previously collected. My research would not have been possible without the data.

My sincere gratitude goes out to all the participants who selflessly donated their time during data collection for the study. You were all amazing.

I wish to acknowledge my committee members and external member for their helpful recommendations and encouragement. I firmly believe that their feedback has assisted in making this thesis more impactful.

I concede to put in words that how grateful I am to my supervisors Professor Dr. Martin Ferguson-Pell and Professor Dr. Greg Kawchuk, for they have paved the way for my journey and its destination. I thank them from the core of my heart for believing me in the opportunity and for drawing a distinctive mark in my life. It is a huge privilege for me to get a chance to work with such great Professors. It was the very first ever 11,000 km away from my home. Besides the ongoing pandemic, and even though the situation was different, they always cared for me and provided me with support no matter what. My professors make me feel as though we are a part of the family. I must say with absolute certainty that they are true gentlemen beyond academia. I would like to express my sincere gratitude to them for their financial support as a research assistant.

Finally, I would like to thank the Government of Canada and the people of Canada. I am humbled by their support and assistance. I have found comfort and home here in Canada, for it is a beautiful country with wonderful people.

I would like to thank my friends and roommates. Whenever I need help with my study, you never deny listening to my things, even my silly kinds of stuff.

I feel the motivation to thrust to my limit for all the people who have made my journey as worthy as it is.

TABLE OF CONTENTS

LIST OF TABLES

LIST OF FIGURES

LIST OF ABBREVIATIONS

AD	Anterior deltoid
ANN	Artificial neural network
ANCOVA	Analysis of covariance
ANOVA	Analysis of variance
AUC	Area under the curve
AUC-F	Area under the curve for fatigue state
AUC-NF	Area under the curve for non-Fatigue state
BB	Biceps brachii
CNN	Convolutional neural network
CV	Conduction velocity
CON	Concentric contraction
ECC	Eccentric contraction
EMG	Electromyography
EMD	Empirical mode decomposition
FFT	Fast Fourier transform
FT	Fourier Transform
FPR	False positive rate
IA	Instantaneous amplitude
ICA	Independent component analysis
IEMG	Integrated EMG
IE	Instantaneous energy
IF	Instantaneous frequency
IMF	Instantaneous mean Frequency
IMDB	Instantaneous median frequency band
IMDF	Instantaneous median frequency
ISE	Instantaneous spectral entropy
ISO	Isometric contraction
HMS	Hilbert marginal spectrum
HHT	Hilbert-Huang transform
LDA	Linear discriminant analysis
LR	Logistic regression
MD	Middle deltoid
MDF	Median frequency

MF	Mean frequency
MPF	Mean power frequency
MUAP	Motor unit action potential
MVC	Maximum voluntary contraction
NCA	Neighborhood component analysis
NSM	Normalized spectral moment
NI	National instruments
OSVM	Optimized support sector machine
PCI	The first principal component
PCII	The second principal component
PCA	Principal component analysis
PM	Pectoralis major
sEMG	Surface electromyography
SCI	Spinal cord injury
SVM	Support vector machine
SVMs	Support vector machine with polynomial and radial basis kernel
SVD	Singular value decomposition
TPR	True positive rate
TB	Triceps brachii
ROC	Receiver operating characteristics
RMS	Root mean square
UT	Upper trapezius
WL	Wavelength
WT	Wavelet transform

CHAPTER 1: **GENERAL OVERVIEW OF THE THESIS**

1.1: Introduction

Muscle fatigue is a non-specific symptom experienced by people in everyday life and an exercise-induced common physiological phenomenon associated with several health conditions (Wan et al., 2017). Recent advances in physiological research have increased the understanding of how muscle-intensive activities and strenuous exercises cause a deterioration in performance, identified as fatigue (Allen & Westerblad, 2001; Kumar et al., 2003), which leads to a reduction in muscle contraction and a decrease in force production (Bilgin et al., 2015; Koutsos et al., 2016; Wu et al., 2016). Fatigue is manifested as a state of exhaustion when completing strenuous voluntary, physical tasks.

Figure 1.1: Different types of exercises and activities causing muscle fatigue (Google photos)

Physical exercises and activities are beneficial to health. However, activities like construction work, wheelchair propulsion, running, weightlifting, cycling, and physical workouts can result in muscle fatigue that reduces the endurance of the individual (Al-Mulla & Sepulveda, 2010; Kumar et al., 2003). Under these stressful and heavy work conditions, muscle fatigue can be dangerous (Mitra & Cumming, 2017), causing significant injuries and work-related disorders (Caffier et al., 1993). Fatigue is mainly measured as a reduction in maximal force generated during a muscle contraction (Wan et al., 2017; Wu et al., 2016). It is challenging to determine a fatigue threshold for an individual due to the heterogeneity of muscle properties and functional capacities from one person to another (Al-Mulla et al., 2011b; Kumar et al., 2003). Failure to detect muscle fatigue may result in pain and overuse injuries, placing a financial burden on the family and society (Al-Mulla et al., 2011a; Kumar et al., 2003; O'Sullivan et al., 2018; Qi et al., 2011).

Objectively in the laboratory and clinic, several techniques are used to determine muscle fatigue for a client (Kumar et al., 2003). One of the most reliable methods currently used to detect fatigue in the laboratory is to analyze blood lactate (Cifrek et al., 2009). However, this does not provide any site-specific measure of fatigue but a global one instead and cannot be measured in real-time (Cifrek et al., 2009). The skeletal muscle in the human body is subject to voluntary control. Recordings of the electrical activity of skeletal muscle are referred to as electromyography (EMG) and are used by clinicians to analyze the human body's skeletal muscle activity in the clinic (Kumar et al., 2003). EMG can be recorded invasively using a fine wire electrode inserted through the skin and placed intramuscularly with a needle. Alternatively, EMG can be recorded from the skin surface non-invasively, referred to as surface EMG (sEMG) (Kumar et al., 2003). Needle EMG provides excellent localization of muscle fibres' electrical activity compared to the surface EMG, where signals from nearby co-contracting muscles can complicate the interpretation of the signal.

One of the limitations is that needle electrodes have to be inserted by a qualified clinician and are subject to breaking during intense activity, leaving the wire in the muscle. This is not an acceptable risk other than for physiological research or specific clinical diagnostic procedures. Therefore, needle EMG is not well-suited for everyday use (Qi et al., 2019).

For more than 40 years, surface electromyography (sEMG) signals have been used to detect and analyze muscle fatigue (Lindstrom & Magnusson, 1977). The sEMG records continuous physiological changes in muscle activities during fatigue, and therefore, it is a useful tool for assessing muscular function (Wu et al., 2016; Yang et al., 2014). Using signal processing, it is possible to investigate muscular functions during fatigue, enabling it to draw the relationship between the sEMG signal and the mechanical force produced by the subject. Furthermore, EMG sensors are relatively inexpensive and can be easily placed on various body muscles, making them suitable for wearable real-time applications (Al-Mulla et al., 2011a).

With the advent of readily available signal conditioning technologies, the sEMG sensor can be used straightforwardly to record the EMG signal during activities in daily living, along with exercise and training sessions. Processing the sEMG data in real-time has the potential to automatically alert the individuals as fatigue occurs, perhaps enabling them to titrate their effort to complete the task safely. However, at present, individuals generally have to rely on their own perception of muscle fatigue which does not provide the objective data needed to predict whether the task can be completed successfully (Al-Mulla et al., 2011a; Kumar et al., 2003). Obtaining the balance between enhancing performance and preventing injury can help plan exercise and training programs applicable for a specific task (O'Sullivan et al., 2018). Determination of the dose-response to exercise is usually determined by measuring optimal rest periods. This enables exercise and training sessions to be designed as efficiently and effectively as possible without suffering

diminishing returns or injury (Cifrek et al., 2009; Vigotsky et al., 2018). Exercise participants can be enabled to define their limits during training and exercise sessions to prevent injury (Al-Mulla et al., 2011a; O'Sullivan et al., 2018). To define the limit for optimal test-specific activities and exercises, we propose that a real-time muscle fatigue system would be preferable to current post-processing systems (Enoka & Duchateau, 2008; Ibitoye et al., 2014; Qi, 2009; Toledo-Peral et al., 2018). A real-time system automating the early detection of fatigue has the potential to provide the visual feedback of fatigue conditions to the end-users directly during activities and training sessions (Al-Mulla et al., 2011a). Therefore, a method for real-time modelling of fatigue is needed to facilitate the development of a wearable device for health and rehabilitation research and for consumer applications where clients can be enabled to track their limits during activities.

Numerous strategies have been developed to quantify muscle fatigue comprehensively by processing the sEMG signal. Most of these techniques are have applied post-processing analysis rather than in real-time (Al-Mulla et al., 2011a; Kumar et al., 2003; Qi et al., 2020). In fact, more sophisticated analysis techniques, along with Wavelet and Principal Component Analysis, have been developed by our RRL Lab at the University of Alberta for detecting muscle fatigue using offline analysis (Qi, 2009; Qi et al., 2019, 2020). However, these techniques are highly computationally demanding. In addition, they require laboratory analysis to be conducted post-hoc rather than in real-time. Conjointly, these methods necessitate a more powerful processor and a longer running time than can currently be achieved with microcontrollers. In contrast, fatigue is an instantaneous time-varying non-linear phenomenon. Therefore, these models are not suitable for detecting muscle fatigue in real-time since a faster response model is desired (Clancy et al., 2008; Madeleine et al., 2002; Taylor et al., 1997).

With technological advancement, wearable devices have been extensively used in diverse fields, particularly from the healthcare sector to the rehabilitation area, to monitor patient's health and welfare to prevent injuries (Al-Mulla et al., 2011a).

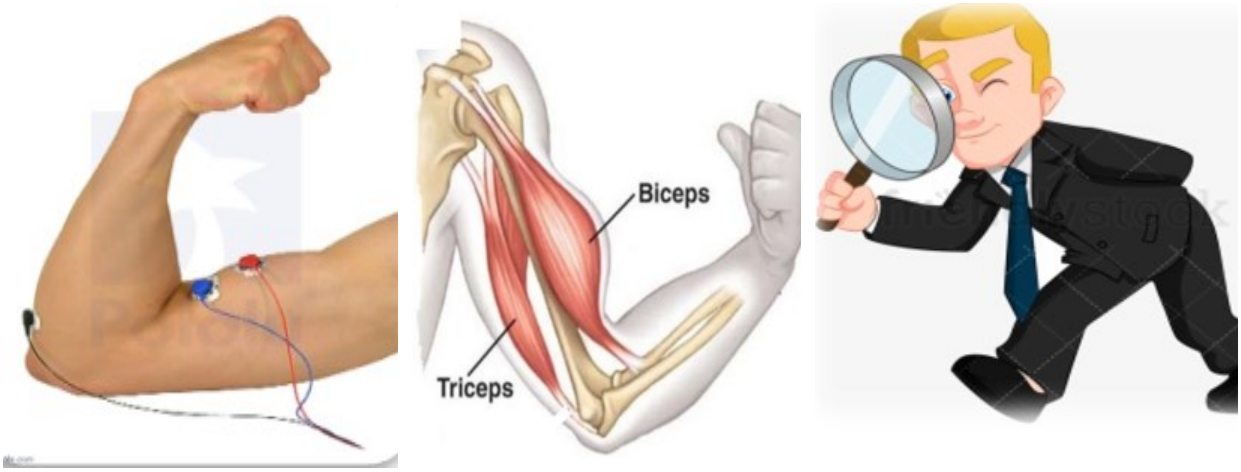

Figure 1.2: A wearable device is adjustable to fit the body (Image: Google)

Recent research demonstrates that people are increasingly inclined to use body-worn devices to monitor the state of their bodies while engaging in physical exercise (Al-Mulla et al., 2011a). Although research on muscle fatigue has been advancing for several decades, the development of a wearable device has been elusive. The demand for a wearable device is highly significant for the disciplines such as ergonomics and prosthetics, human-computer interactions, sports injuries and performance, rehabilitation like spinal-cord injury, paraplegia, cerebral palsy, low back pain, shoulder and neck pain, arthritis, stroke recovery and so on (Al-Mulla et al., 2011a; Koutsos, 2017; O'Sullivan et al., 2018). Furthermore, wearable devices are also used to facilitate Virtual Health assessments where the information on muscle fatigue status could be used to assess patients

in remote settings (Seshadri et al., 2020). These application areas motivate the development of a real-time wearable device to detect fatigue while performing physical activities.

The purpose of this research is to develop a model using a machine learning algorithm to detect muscle fatigue in real-time from the sEMG signal during a sustained single maximum voluntary contraction and to recommend a wearable system using a current embedded device. Significantly this system can be applied in clinical and consumer applications to monitor fatigue in real-time, mainly to prevent work-related injury (Al-Mulla et al., 2011a).

1.2: Research Question

To develop a wearable device, a trained ML model is necessary. However, there is no evidence of an automated model in the literature currently used to detect fatigue in real-time. Therefore, this research problem motivates us to develop an automated model using machine learning embedded in a wearable device. As a result, the following research question has driven the research to overcome the literature gap.

Is it possible to detect muscle fatigue in biceps brachii from sEMG data associated with a sustained single 80% maximum voluntary contraction (MVC) incorporating a machine learning algorithm in real-time?

1.3: Purpose Statement

The purpose statement of this research is to develop a model using machine learning that is intended to be embedded in a wearable device to detect muscle fatigue based on the sEMG data associated with a sustained single 80% maximum voluntary contraction (MVC).

1.4: Objectives

The objectives of this research project are as following:

1) To conduct a scoping review to identify all machine learning algorithms that are potentially capable of detecting muscle fatigue in real-time and computationally adaptable to be embedded in a wearable device.
2) To extract features from the previously recorded sEMG data during a sustained single 80% MVC and select the most promising features that are associated with a pattern of fatigue.
3) To evaluate the performance of the selected algorithms in Objective 1 using the features identified in Objective 2.
4) To select the most promising algorithm based on its classification accuracy on fatigue state.
5) To develop a model using the promising ML algorithm that has the potential to be embedded in a wearable device to detect muscle fatigue based on the sEMG data associated with a sustained single 80% MVC.

1.5: Muscle Contraction

Different skeletal muscle tissue is subjected to voluntary control, which investigates muscle fatigue (Al-Mulla et al., 2011a). Skeletal muscle tissue comprises large cells called muscle fibres (Engel & Warmolts, 2015). A motor unit (MU) comprises a single motor neuron in the spinal cord and all of the muscle fibres it controls (Al-Mulla et al., 2011b). During contraction, the elastic tissue named epimysium covers the muscle and holds upon it for large force generation (Koutsos, 2017). Similarly, the endomysium envelops and strengthens each muscle fibres cell. Myofibrils are the muscle fibres that contain cylinders of muscle proteins to allow the muscle to contract, shown in Figure 1.3. Myofibrils comprise two major protein filaments: actin and myosin (Koutsos, 2017;

Koutsos et al., 2016; Qi et al., 2019). The myosin protein filament is thick compared to the thin protein filaments of actin. Figure 1.3 was taken from (Koutsos, 2017).

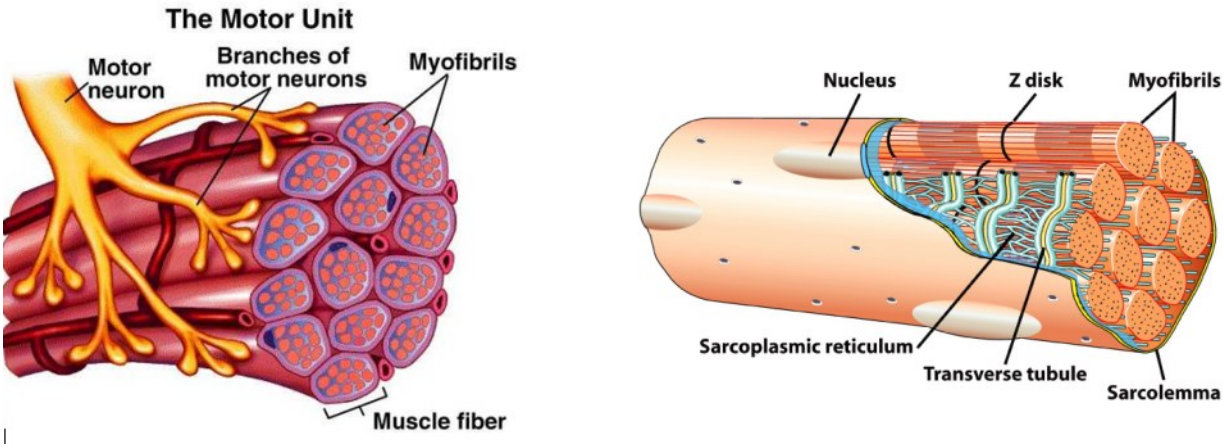

Figure 1.3: Muscle anatomy along with motor neuron, motor unit, muscle fibres, and associated muscles cells

Z-disk shown in Figure 1.3 is the connective structure positioned at the end of the filaments repeating mold. T-tubules are likely to run along the Z-disk (Koutsos, 2017; Koutsos et al., 2016). T-tubules are also part of the cell membrane called the sarcolemma, which expands inside the fibres. A membrane called the sarcoplasmic reticulum runs along the fibre axis and between the T-tubules, storing and freeing the calcium ions ($Ca^{2+)}$ that trigger muscle contraction.

During muscle, relaxed conditions, the protein filaments actin and myosin are blocked by other protein filaments troponin and tropomyosin (Koutsos, 2017; Koutsos et al., 2016). An electrical current is passed through the nerve throughout muscle contractions, known as an action potential (AP) (Al-Mulla et al., 2011b). The AP reaches the muscle cell through the sarcolemma and then through the T-tubules into the myofibrils (Koutsos, 2017). After that, the AP triggers the sarcoplasmic reticulum releasing calcium ions in the cytoplasm protein filaments area. Calcium ions bind to troponin-tropomyosin molecules, changing their shape and causing them to shift away

from actin filaments. As a result, myosin and actin are free to bond with one another, resulting in contraction. Figure 1.4 was taken from Koutsos et al. (Koutsos, 2017).

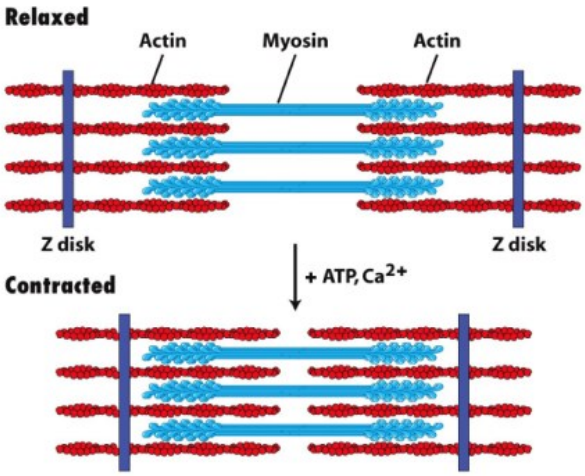

Figure 1.4: Muscle contraction and relaxation

At that time, AP is passed, and the calcium ion closes the gate from the cytoplasm. As a result, tropomyosin-troponin returns to the normal state and holds the myosin-actin proteins, and the muscle relaxes. For muscle contraction and relaxation, energy is required, and adenosine triphosphate (ATP) supplies the energy to muscles. Mitochondria contain inside the muscle fibres cells where ATP is produced. This how ATP is used to contract muscles and relax to a normal state.

1.6: Types of Contraction

There are different types of muscle contractions. Based on changing the muscle length during contractions, they are commonly isotonic and isometric contractions.

1.6.1: Isotonic Contraction

The isotonic contraction can be categorized into eccentric and concentric contraction.

Eccentric Contraction: The eccentric contraction is a muscular contraction in which the muscle length increases (*Medicine LibreTexts*, n.d.). An eccentric contraction results in muscle extension as the muscle continues to generate force. Figure 1.5 and Figure 1.6 were taken from (*Medicine LibreTexts*, n.d.).

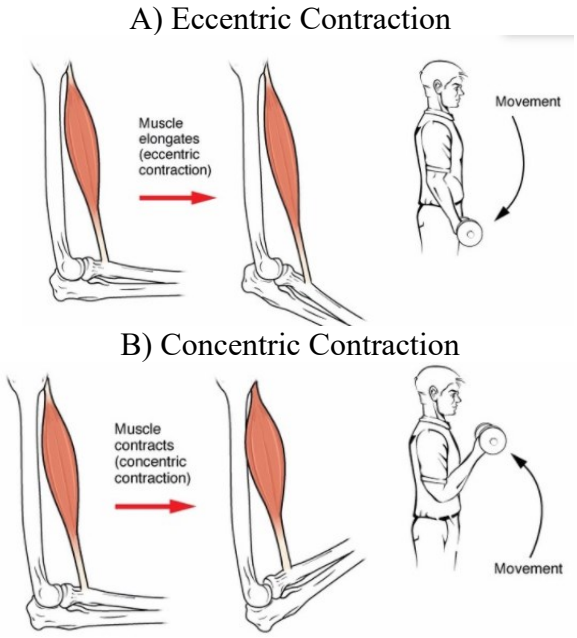

Figure 1.5: Isotonic contraction

Concentric Contraction: In concentric contraction, the length of the muscle shortens while generating force to overcome resistance.

1.6.2: Isometric Contraction

The type of contraction in which the muscle length remains unchanged, but the load on the muscle can be varied. Isometric contractions, unlike isotonic contractions, produce force without increasing the muscle's length (*Medicine LibreTexts*, n.d.). shown in Figure 1.6. The following figure was taken from (*Medicine LibreTexts*, n.d.).

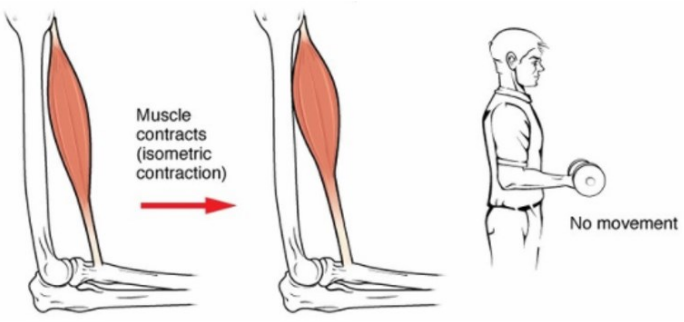

Figure 1.6: Isometric contraction

The sustained single isometric test is a type of test in which participants try to maintain the load during the cycle of exhaustion until it hits its entire state and then releases it. The individuals in the test held weight in their dominant hand, and the sEMG sensor was placed on the biceps brachii muscle to record the EMG signal. The participants were advised to go up to 80% maximum voluntary contraction (MVC). Research has revealed that the biceps brachii muscles have a more comprehensive recruitment range of up to 80% MVC, and force increment is mainly handled by recruiting more motor units till 80% MVC (Esposito et al., 1996).

1.7: What is Muscle Fatigue

The muscle fibres cell membrane named sarcolemma is semi-permeable (Koutsos, 2017). The membrane pumps Na^+ out of the cell and K^+ into the cell while the muscle is relaxed (Koutsos, 2017; Seunggu, 2017). As a result, Na+ and K+ ions concentrations outside and within the fibres cell have risen. Since ions have a voltage, the difference in their concentration creates an AP gradient. Resting potential is formed by an ionic balance between a muscle cell's inner and outer parts (-70 to -90 mV) (Koutsos, 2017; Qi et al., 2011). With neurotransmitters, a chemical stimulus, the membrane's permeability to Na^+ neighbouring rises and rushes into the cell. Due to the increment of Na^+ ions, the membrane potential crossed the threshold level and increased to +30

mV. In the meantime, the shift of the membrane voltage to zero triggers the opening of K+ channels (Barbero et al., 2012), causing the release of potassium ions shown in Figure 1.7 (Koutsos, 2017).

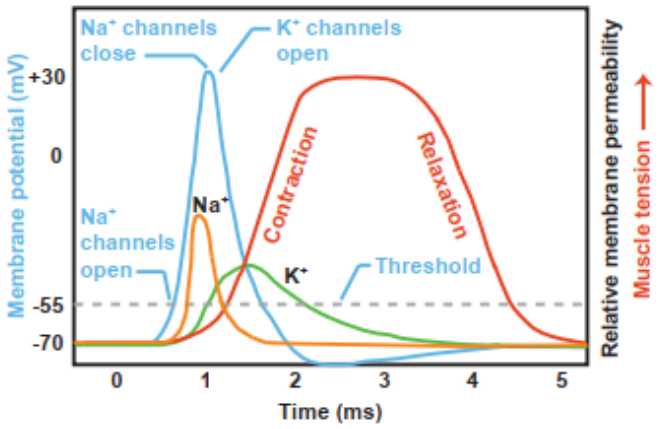

Figure 1.7: Moto unit action potential from Koutsos et al.

Because the outflow of positive charges cancels out the potential increase caused by the entry of sodium ions, the membrane voltage begins to drop toward zero (Barbero et al., 2012; Koutsos, 2017; Qi et al., 2019). As a result, Na^+ channels start to close, and membrane potential drops even further, returning to the resting potential. Therefore, based on the sliding filaments model, the muscle contraction and relaxations cycle begins when the membrane threshold is exceeded.

This depolarization wave propagates along the surface of the muscle fibres (Koutsos et al., 2016; Pilarski et al., 2013). It causes calcium ions to be released into the intracellular space, causing the muscle cell to shorten (Jawadwala, 2012). This impulse excitation is known as AP of muscle fibres. When a MU fires, an AP is sent to the muscle evoked in all of the MU's innervated muscle fibres through a motor neuron. EMG monitors the motor unit action potential (MUAP), which is the outcome of all this electrical activity (Al-Mulla et al., 2011b).

As soon as there is a surge of Na^+ into the cell after a muscle contraction, the cell depolarizes, and when there is a rush of K^+ out, the cell repolarizes (Koutsos, 2017). The exercises or activities that are short with high intensity cause a large amount of K^+ in the extracellular membrane. When AP propagates down the t-tubules, it accumulates more K^+ ions where t-tubules reside. As a result, the propagation of AP to the sarcolemma fails, which causes a decrease of Ca+ ions from the sarcoplasmic reticulum; therefore, no initiation of muscle contraction can happen within the muscle fibres the muscle fatigue. Finally, it is concluded that muscle fatigue has occurred when there is the accumulation of a large amount of K^+ ions in the extracellular membrane.

1.8: Detection of Fatigue

Muscle fatigue has no physically quantitative value. To ascertain fatigue is challenging, as no universal index exists for fatigue. Most of the time, the maximum voluntary contraction force while performing a task is used to detect the intensity level of fatigue. However, it is recommended to detect fatigue in real-time by analyzing the progressive changes in the muscle fibres activation, sEMG amplitude, and sEMG spectral estimation. As a result, the time and frequency domain characteristics of the sEMG signal are considered for real-time fatigue detection. Skeletal muscle tissue consists of large cells called the muscle fibres, categorized depending on the speed of contractile twitch (Al-Mulla et al., 2011b; Al-Mulla & Sepulveda, 2010). Therefore, all muscle tissues are a mixture of both fast-twitch and slow-twitch fibres (*CLA: Pathophysiology*, n.d.). The fast-twitch fibres can generate higher forces, contract faster, and have a higher anaerobic capability (Koutsos, 2017). On the other hand, the slow-twitch fibres produce force slowly and sustain contractions for more extended periods with aerobic capacity. Koutsos et al. depicted the following power spectrum shown in Figure 1.8 during isometric contraction for non-fatigued and fatigue states. Figure 1.8 was taken from Koutsos et al. (Koutsos, 2017).

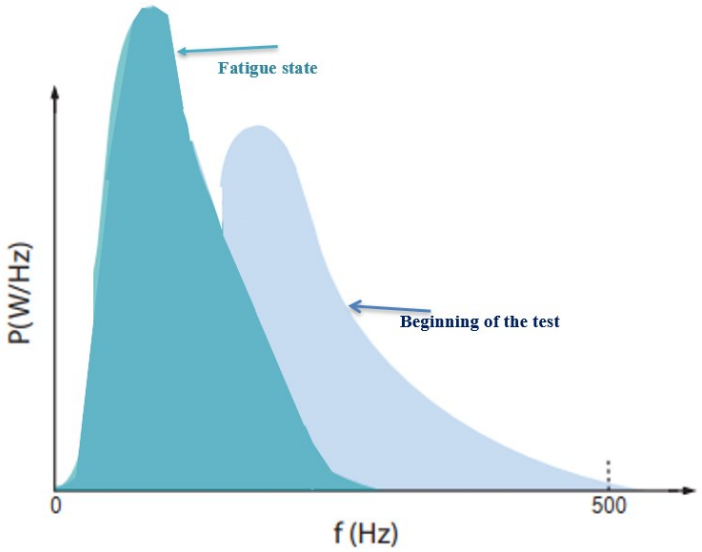

Figure 1.8: The power spectrum of the sEMG signal during static isometric contraction – beginning and fatigue conditions

The recruitment of MUAP increases during fatigue and the fast-twitch fibres fatigue first, while the slow-twitch fibres remain, and tension drops off (O'Sullivan et al., 2018; Qi et al., 2011). From the power spectrum shown in Figure 1.8, it is evident that the sEMG signal has a lower magnitude and higher frequencies at the beginning of the test. In contrast, as the muscle fatigues, the sEMG power spectrum transitions to higher amplitudes and lower frequencies (Georgiou & Koutsos, 2017; Mitra & Cumming, 2017). For isometric contraction, the power spectrum of the sEMG signal moved to lower frequencies during fatigue, and the magnitude of the sEMG signal increased (Al-Mulla et al., 2011b; Koutsos, 2017; Mitra & Cumming, 2017).

1.9: Dissertation Format

The chapters in this thesis are arranged in chronological order, and each section builds on the research that has been done to address each of these specific goals.

A general overview of the thesis was presented in Chapter 1, where the introduction of the thesis, research question, the purpose of the research, research objectives were mentioned. In addition,

muscle contraction, the definition of muscle fatigue, how fatigue occurs and can be detected, all of the related terminologies about muscle fatigue were described in this section briefly.

To fulfill Objective 1, a scoping review was conducted and described in Chapter 2. The methodology of the scoping review, result analysis of the review, the number of selected papers, list of promising algorithms, literature review on wearable devices, and direction to real-time muscle fatigue research mechanism were discussed in Chapter 2.

Chapter 3 illustrates how Objectives 2 to 4 were accomplished. Likewise, Chapter 3 reports on the performance of the algorithms identified in the Scoping Review when applied to a database of sustained contractions for 100 healthy participants. An ML model was also trained on the database of sEMG signals demonstrating its potential for use in a real-time system and comparing it to those from the Scoping Review. Chapter 3 also explains the feature extraction and selection process from the sEMG signal, the trend of the features, results, the performance of the selected machine learning algorithms, evaluation metrics, and identifies the most promising algorithm for real-time fatigue detection and training for embedding in a wearable device.

Chapter 4 summarizes the findings from the Scoping Review and the ML model, demonstrating the potential of the model that was developed in this study for use in a wearable device. It highlights the contributions of the novel approach proposed in this master's thesis and finally provides future directions for this work.

CHAPTER 2: **CAN AN ALGORITHM BE APPLIED TO IDENTIFY MUSCLE FATIGUE FROM SURFACE EMG SIGNALS IN REAL-TIME? — A SCOPING REVIEW**

Abstract

Background: Wearable devices have been used widely in the healthcare sector to monitor patient health and avoid injury. A wearable device that can provide an indication of muscle fatigue in real-time would not only improve health and reduce injury, but it is also highly desirable for both biomedical research and consumer applications. To develop a wearable device detecting muscle fatigue, an algorithm able to process non-linear EMG signals in real-time is required

Objectives: The objectives of this scoping review included: 1) To review the literature and identify the existing algorithms that have been used for detecting muscle fatigue based on sEMG signals obtained from dynamic, repetitive, or single voluntary muscle contractions, 2) To determine if algorithms exist that are capable of detecting muscle fatigue and their accuracy in detecting fatigue in real-time, and 3) To assess is these algorithms are adaptable for integration into a wearable device.

Methods: Six electronic databases were systematically searched (Scopus, Web of Science, PubMed, IEEE Xplore, IET Digital Library, and Google Scholar). Our search terms included titles and keywords relevant to muscle fatigue, algorithm, method, ML, DL, sEMG, real-time, wearable, detection. Inclusion criteria for selected studies included that they were published in English, that the described algorithms be used for detecting muscle fatigue from surface EMG signals during different contractions and that the papers were published between January 2005 to February 2021.

Results: The search identified a total of 1213 articles. After applying the inclusion criteria, 67 papers were included in the study and their data were extracted. From these papers, 4 algorithms met the pre-defined criteria for potential inclusion in a wearable device. Further, 4 studies of the included studies attempted to develop a wearable device; however, no wearable device reported in the literature is currently able to detect muscle fatigue in real-time in a clinical setting.

Conclusion: This review has suggested four ML algorithms that have the potential to be included in wearable devices. As a result, we recommend that further research be performed to assess these algorithms for their ability to classify fatigue states within the boundaries of a wearable device.

Keywords: Muscle fatigue, Surface EMG, Wearable device, Algorithm, Real-time.

2.1: Introduction

Muscle fatigue occurs when muscles can no longer contract or exert force effectively even while the work in progress endures (Al-Mulla et al., 2011a; Kumar et al., 2003). Fatigue eventually prevents sustained work from being completed (Al-Mulla et al., 2011b). During exercise and training programs, it is crucial to balance improving performance and preventing injury (Cifrek et al., 2009).

Surface Electromyography (sEMG) is a method of measuring the electrical activity of muscle fibres during contractions (Lindstrom & Magnusson, 1977; Moniri et al., 2021) and can be used to investigate muscle fatigue. The sEMG sensors are easy to place on various muscles and relatively inexpensive, making them ideal for wearable real-time tracking (Al-Mulla et al., 2011a).

However, muscle fatigue is a complex physiological phenomenon. To detect muscle fatigue using the sEMG method, an algorithm is required to process the sEMG signal and provide an indicator of fatigue. An algorithm is a set of instructions programmed to accomplish a particular task to generate precise outputs, without human intervention, within a defined computing time limit (Moschovakis, 2001). Efforts to develop standalone algorithms for real-time monitoring are increasing (Cifrek et al., 2009); however, their adaptiveness and potential to accurately detect fatigue and use in wearable technology have not yet been well established. This apparent knowledge gap inspired this scoping review to investigate the current effectiveness of existing algorithms to detect muscle fatigue during various contractions and activities.

This scoping review aims to provide a comprehensive literature review identifying the state of the art of algorithms methods used to detect muscle fatigue during activities or physical exercise. In

the literature, this review's results could help to develop a wearable device capable of detecting muscle fatigue while exercising in real-time in the coming days.

2.2: Methods

2.2.1: Overview

A scoping review is an acceptable methodology for broadly exploring the contemporary literature on a specific research problem (Daudt et al., 2013). Specifically, a scoping review is a literature synthesis architecture that maps available literature on a selected topic (Arksey & O'Malley, 2005; Daudt et al., 2013; Jun et al., 2020). The review's significance is identifying key concepts and accessible evidence, searching for, and analyzing the research gaps on a particular problem (Munn et al., 2018). Subsequently, a scoping review was undertaken to identify the available algorithms used for detecting muscle fatigue processing surface EMG (sEMG) signals during different activities. The methodological procedure for the scoping review was followed according to Arksey et al. (Arksey & O'Malley, 2005). The primary goal was to discover what has been achieved to assess muscle fatigue and identify potential algorithms for a real-time wearable system.

2.2.2: Research Question

The well-known and established scoping review methodology (Arksey & O'Malley, 2005) was applied to list and coordinate the essential information to guide the current body of the literature. To undertake the scoping review, the following research question was developed: "Can an algorithm be applied to identify muscle fatigue from sEMG signals in real-time?"

2.2.3: Scoping Review Objectives

1. To review the literature and identify the existing algorithms that have been used for detecting muscle fatigue based on sEMG signals obtained from dynamic, repetitive, or single voluntary muscle contractions.

2. To determine if there are algorithms capable of detecting muscle fatigue in real-time and whether these algorithms are accurate at detecting fatigue.

3. To assess the suitability of these algorithms for wearable devices.

2.2.4: Reviewed Literature

The methodology of Arksey & O'Malley (2005) was used to conduct an extensive literature search strategy based on the research question. In its continuity, the PRISMA (Preferred Reporting Items for Systematic Reviews and Meta-analyses) and, in particular, the expansion for Scoping Reviews (PRISMA-ScR) protocol was consistently followed throughout the review (Arksey & O'Malley, 2005). With the growing number of articles being published on this topic, we considered it more appropriate to examine the various databases' studies. As a result, six (6) different electronic databases were selected for systematically recognized specific published articles about the subject. The electronic databases were Scopus, Web of Science, PubMed, IEEE Xplore, IET Digital Library, and Google Scholar. The literature search lasted from September 2020 to February 2021.

2.2.5: Search Parameters

For the exploration of the update to date algorithms currently used in the literature for detecting muscle fatigue processing surface EMG signals during different types of activities, including sports and rehabilitation, Search words using combinations of logical operators "AND" and "OR" were used to pull published papers from electronic databases. Different subject headings, MeSH

terms particular to each database, and a mixture of keywords and associated key phrases pertaining to the detection of muscular tiredness were included in the search string. The search terms were described broadly in the Appendix A section. The search period was restricted to January 2005 to February 2020, so as not to consider obsolete algorithms. The search string was reviewed by the librarian (Liz Dennett) of the University of Alberta.

2.2.6: Studies Selection Process

The study selection procedures of Arksey (2005) were used to select the specific studies: firstly, the research questions were created, and then the search string was formulated based on the research question. One researcher (MMI) performed the database search and the initial duplicate elimination. After that, two independent researchers (MMI and HA) read the nominated abstracts of all articles for evaluating with the Inclusion and Exclusion criteria. In case of any dissatisfaction, the paper was reviewed by the third senior researcher (GK). When the senior researcher agreed to include the paper, the paper was accepted for the data extraction step.

Inclusion Criteria:

1. Studies included at least one algorithm that has used for:
    a. Detecting muscle fatigue during dynamic, repetitive, single voluntary contraction or related activities based on the surface EMG signal.
    b. The activities are rehabilitation activities or sports activities related.
    c. The algorithm was used, at least in a laboratory environment.
2. The real-time muscle fatigue detection system used surface EMG signals.

3. Studies were published in peer-reviewed journals or conference proceedings and made available in complete form through electronic abstract database systems.

4. Research articles published in the English language.

5. Published between January 2005 to February 2021.

Exclusion Criteria:

1. Studies that did not use any types of algorithms for detecting muscle fatigue

2. Studies that included systems for detecting mental fatigue, or muscle fatigue in animals.

3. The studies that used other non-invasive techniques i.e., image processing, photonics, plasma optics, and etc. other than surface EMG based biosignals methods.

4. Studies that included algorithm for detecting fatigue using needle EMG (fine wire), blood lactate or other invasive techniques.

5. Abstracts or journal articles and papers that were not available to access in full.

6. Research and studies published in review articles and journals, book chapters, published books, news reports, magazines, newspapers and discussion articles, Masters or Ph.D. dissertations.

7. Abstracts or journal articles and papers that were published before 2005.

8. If the studies did not mention enough information about methodology and result section regarding detection of muscle fatigue.

Scoping Review Prisma Flow Diagram:

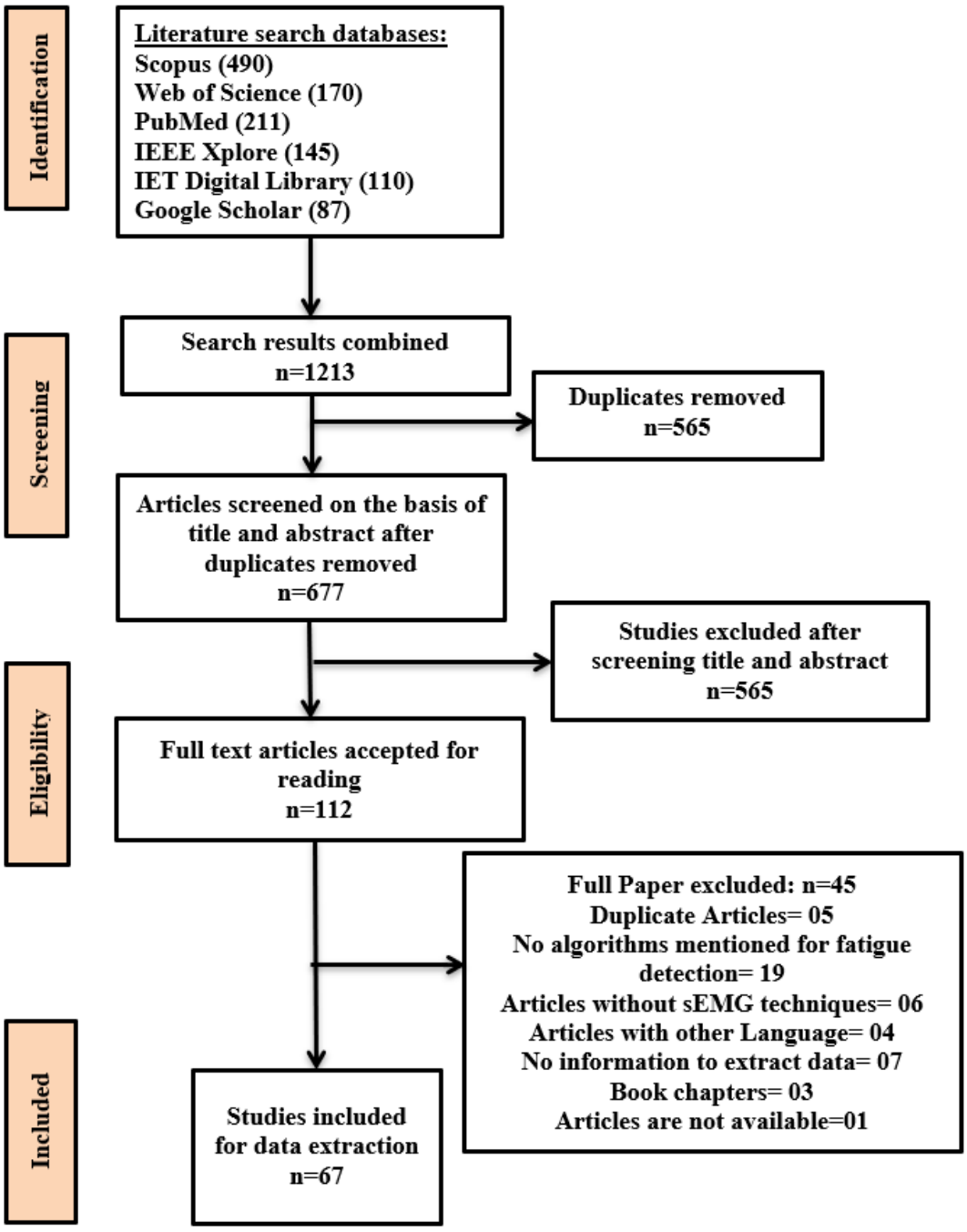

Figure 2.1: PRISMA flow chart of the Scoping review.

2.2.7: Study Selection Reliability & Bias Control

Selection using a combination of engineering and health science electronic databases was expected to improve reliability and reduce source publication bias in this scoping review. The first consistency filter to ensure a certain level of methodological rigour included papers in abstract digital systems at the scientific level. Any non-English language papers were excluded from our study. We included two researchers for the title, and abstract evaluation eliminates bias. If there were any disagreements, our third senior researcher reviewed and analyzed the entire report, reducing bias.

2.2.8: Data Extraction and Bibliometric Indicators

At the outset of data extraction, the senior researchers (GK & MFP) notified the other researcher (MMI) how to retrieve data from the paper in a scoping review. The senior researchers (GK & MFP) resolved any disagreement concerning data extraction and advised which information should be stored in the Excel file. After completing the data extraction of the selected papers by the researcher (MMI), the data extraction master file was thoroughly checked by the other researcher (HA) independently. The extracted data from each included studies contained: i) Authors name and publication year, ii) Types of published articles (whether Journal or Conference papers) and quartile, iii) Objectives of the study, iv) Name of the algorithm used and goals of the algorithm, v) indicators of fatigue mentioned, vii) Types of contractions or activities and its environment, viii) Name of the surface EMG sensor used and protocol of the sensor, ix) EMG signal pre-processing data (Filter, Amplifier, and Sampling frequency), x) Name of the software and hardware tools used, xi) Sample Size and gender with weight, xii) The medical condition of the participants, xiii) Ground truth, and xiv) System accuracy along with sensitivity, specificity, precision, and resolution.

2.3: Results Analysis

2.3.1: Data Overview

This scoping review literature search strategy identified overall 1213 articles in six different databases. A total of 565 duplicated abstracts were removed, whereas 677 studies were selected for abstract reading. After reading the detailed abstract and applying the Inclusion & Exclusion criteria, 112 papers were screened for a full reading. After applying the Inclusion & Exclusion criteria to the 112 articles, a total of 67 papers were selected for data extraction. Among the 45 excluded studies, there were 5 repeated studies, 19 studies did not mention any algorithm, a total of 6 studies indicated altered mechanism rather than sEMG, there was no information to extract in 7 studies, 4 articles were published in other languages, total 4 studies are book chapters, and 1 study was unavailable in online. The PRISMA flow diagram in Fig. 2.1 depicts the detailed overall study overview of included studies. Later, 67 papers' data was extracted in an Excel file in a tabular format.

2.3.2: Research Trend and Quartile of studies

This scoping review clearly shows the yearly research advancement on muscle fatigue. As the included studies were considered before 2005, the bar chart demonstrated the development of the research through each year among the extracted studies. Figure 2.2 shows the performance stattics of included studies.

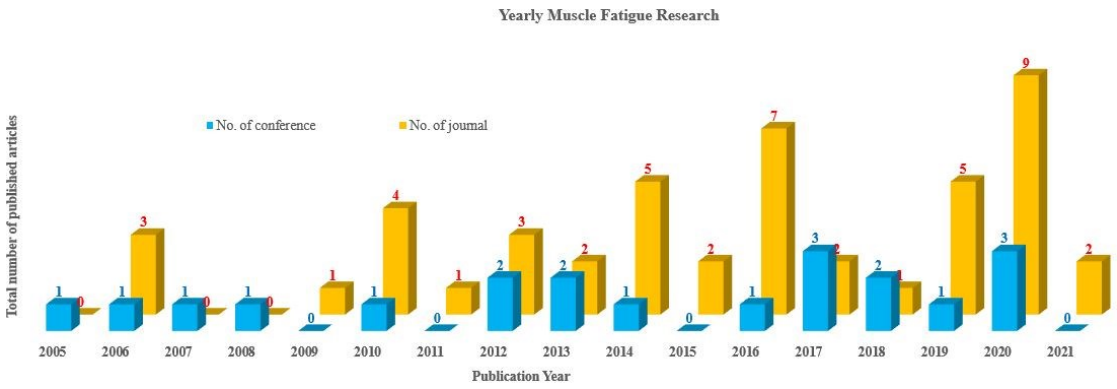

Figure 2.2: Research trend of muscle fatigue yearly based on the included studies.

The result shows that as technology has advanced, research in this area has increased. The total number of journal articles (47) is greater than the conference proceedings (20). Statistics indicate that the majority of journals were published in high-impact factor journals. Among the included journal articles, 24 (51.06%) studies were published in the Q1 quartile journals. Total 18 (38.19%) articles were published in the Q2 quartile journals. Only 3 studies were published in the Q3 quartile journal, whereas 2 studies reported the Q4 quartile journal. The quality of muscle fatigue publications is high and increasing yearly.

2.3.3: EMG Sensor

In total, 61 out of 67 of the included studies mentioned the details of the sensors used. Six studies did not report any sensor details for recording the EMG signal. Most of the sensors used were electrodes. Analyzing the statistical data from the sensors used, the scoping review shows that about 37% use Ag/Cl electrodes (S. H. Liu et al., 2019; Moniri et al., 2021; Phinyomark et al., 2018; Zhao et al., 2020), 20% Bagnoli Delsys sensors (Pilarski et al., 2013; Qi, 2009; Qi et al., 2011, 2012, 2019) and the rest of the studies reported other sensors like bipolar surface EMG, strain gauge, Myogrip dynamometer and Myon. Very recent studies mentioned Trigno Hybrid

Sensors (Q. Liu et al., 2021; Wu et al., 2016; Yang et al., 2014) for the data acquisition. The reported sensors are mainly bipolar sensors, and very few are monopolar electrodes (Hotta & Ito, 2013; G. Zhang et al., 2018).

2.3.4: sEMG Signal Conditioning (Filter, Sampling Frequency, Amplifier)

Among the total 67 included studies, about 51 studies referenced the use of filters for signal conditioning. Most of the filters used in the included studies were bandpass filters. A total of 37 (55.22%) studies reported a bandpass filter, either Butterworth or Bessel filter and 14.82% of studies reported notch filter. Five studies also mentioned the use of low-pass filters (Kahl & Hofmann, 2016; Moniri et al., 2021; Nagai, 2017; Rong et al., 2013; Yochum et al., 2012), and total 3 studies reported high pass filters (Hegedus et al., 2020; Q. Liu et al., 2021; Moniri et al., 2021). The passband frequency of the filters varies for different criteria; for example, the lower pass frequency varies between 1-20 Hz, and the high pass frequency varies between 450-500Hz. The most common format of using bandpass filters based on their passband is 1-500Hz, 5-500Hz and 20-500Hz. In 2 studies, the passband frequency was used to 20-100Hz (Jordanic & Magjarevic, 2012; G. Zhang et al., 2018). Kumar et al. (2003) used the passband frequency to 5Hz-2kHz, and Dayan et al. (2012) reported 10Hz-10kHz as the passband used band-rejection range for the notch filter 10-50Hz.

Another essential task in signal conditioning is signal amplification. Among 67 papers, a total of 51 papers mentioned the use of signal amplification features. Two studies reported AD620 Instrumentation Amplifiers (Jamaluddin et al., 2019; S. H. Liu et al., 2020), whereas 6 studies used sensors built-in sEMG amplifiers. Dayan et al. (2012) reported the use of a bio-potential amplifier. The commonly used amplification factor for amplifying the sEMG signal is 1000; Also the study

(Al-Mulla et al., 2011a) reported an amplification factor of 330 for sEMG and 270 for goniometer, and the differential gain is 2500 (Moniri et al., 2021).

For sampling frequency, a total of 27 studies reported sampling frequency 1000 Hz. In 2 studies, the EMG signal was sampled at 2048 Hz (De Rocha et al., 2018; G. Zhang et al., 2018). The range of the sampling frequency varies from 1000 Hz to 4000 Hz among the included studies.

2.3.5: Sensor Placement

The EMG sensor is placed on various parts of the body to capture surface EMG signals from different skeletal muscles. A total of 38 studies (which is 56.71% of included studies) reported that the sensor was placed on the biceps brachii muscles to record the sEMG signal. Four studies reported combining hand and shoulder muscles shown in Table 2.3 for recording EMG signals. Seven studies mentioned different finger and hand muscles for EMG recording. On the other hand, 17 studies used various lower extremities especially leg muscles, for recording the EMG signal.

Table 2.1: Placement of EMG sensor on the human body

Muscle Type	Total Included Studies
Biceps Brachii (BB)	38
AD, PM, BB, TB, UT, MD, and PD	04
Carpi Ulnaris, Flexor carpi Radialis (FCR), Extensor Carpi Radialis Longus (ECRL), Extensor Digitorum (ED), and Extensor Carpi Radialis Brevis (ECRB)	07
Gastrocnemius	03
Rectus Femoris (RF), Vastus Lateralis (VL)	03
RF, Biceps Femoris (BF), Tibialis Anterior (TA), Vastus Medialis (VM), and Gastrocnemius	07
Tibialis Anterior (TA), Lateral Gastrocnemius (LG), Medial Gastrocnemius (MG) and Soleus (SO)	02
Trunk Muscle: Latissimus Dorsi (LD), Longissimus, Iliocostalis, Multifidus, Rectus Abdominis (RA), Internal and External Obliques (IEO)	01
Gluteus Maximus (GLTMAX), Gluteus Medius (GLTMED), Tensor Fascia Lattae (TFL), Rectus Femoris (RFEM), Vastus Medius (VMED), Vastus Lateralis (VL), Long Head of Biceps Femoris (BFEM), Semitendinosus (STEN), Tibialis Anterior (TA), Medial Gastrocnemius (MGAS), Lateral Gastrocnemius (LGAS), and the soleus (SOL)	01

2.3.6: Types of Muscle Contraction and Environments

Table 2.2 shows the summary of different contractions along with the activity characteristics mentioned in the included studies. In addition, Table 2.3 demonstrates the detailed contractions characteristics with the specific studies. Among the included studies, 25 (37.31%) reported isometric contraction. The isometric contraction was performed through various activities, including biceps curl on the Preacher machine, dumbbell movement and lifting, and a new type of environment notified about the Biodex system (Al-Mulla et al., 2011a; Smale et al., 2016; Wu et al., 2016). The maximum isometric voluntary contraction varies from 5% to 90% MVC in the included studies.

Alternatively, 15 studies reported performing dynamic contractions mentioning futsal activities, factory work, wheelchair propulsion and bicycling with 80% MVC. For isotonic contractions, 3 studies stated bicycle exercise, grip strength movement activities. Alongside, 1 study reported static contraction, and 1 study mentioned static & dynamic contraction describing seated dumbbell lifting and cycling. A total of 8 (10.11%) studies articulated repetitive activities (running, cycling, and wheelchair propulsion). Finally, 6 (8.90%) studies described voluntary contractions, including finger movement, sitting in a neutral position, and gripping the hand activities.

Table 2.2: Different types of muscle contractions and activities

Types of Contractions	Isometric 5% to 90% MIVC	Isotonic Isokinetic	Dynamic 80% MVC	Isometric & Dynamic	Static	Static & Dynamic	Repetitive	Voluntary
Different Activities	Biceps curl on Preacher Machine	Bicycle Trainer, Giant Taiwan	Futsal	Weightlifting	Dumbbell in seated position	Static: Held a load with elbow fixed position Dynamic: Cycling	Running	Finger movement
	Dumbbell lifting	Bicycle Trainer, Giant Taiwan	Factory work	Curl exercise on Preacher Machine			Wheelchair	sitting on a comfortable
	Wrist attached to rope & belt of weight	Grip strength	Curl Machine	Dumbbell			Bicycle	sitting position
	Biodex system		Wheelchair Propulsion and Bicycling	Pulling loadcell-80%MIVC			Pedaling	Hand gripping

2.3.7: Fatigue Feature Vector

In the total included studies, there were reports of different fatigue features. Remarkably, 27 studies reported a combination of time and frequency domain fatigue indicators. Time-domain fatigue features were included in the 15 studies, whereas frequency domain only features were reported in 20 studies. Five studies followed the time-frequency characteristics of the EMG signal to detect fatigue. The most promising research for the detection of muscular fatigue was the study of (Wu et al., 2016) where three different classes of fatigue were defined: static fatigue, local fatigue, and dynamic fatigue. Static fatigue was recognized using three feature vectors (RMS, IEMG), (RMS, IEMG, Wavelet Energy (WE)), and (RMS, IEMG, WE, and ERHL). The local fatigue was identified using a sample set of feature vectors (MPF, MDF). Five kinds of feature combination (RMS, IEMG, MIF, WE, and ERHL) was used to detect dynamic fatigue. Therefore, it is apparent that a range of features is required for identifying static fatigue accurately. Table 2.3 demonstrated most of the features of the EMG signal that are used for detecting muscle fatigue in the included studies.

Table 2.3: A list of features used for forecasting muscle fatigue

Time domain feature	Frequency domain feature	Time-Frequency domain feature
Average Power, Simple square integral (SSI), ARV, MAV, RMS, IEMG, ZC (Peak & Spike counting), Waveform length, Slop Sign change, Sample Entropy, Mean absolute value, Mean absolute value slope, Variance, Mean variance, Willison amplitude, Amplitude of the first burst, Log detector,	MF, MPF, MDF, SMR, Mean Power, Standard deviation, Maximum-to-minimum drop in power density ratio, Frequency ratio, Peak to Peak frequency, Power Spectrum, Power spectrum ratio, Spectral moment, Signal to noise ratio, Variance of Central frequency, Energy ratio of all high frequency and low frequency (ERHL), EMG Intensity, Frequency decomposition, Spectral Correlation Density (SCD), Increased Average Ratio (IAR),	ISE (Inst. Spectral Entropy), IMF, IMDF, IMFB, AIF, WIRM1551*, MIF, IE, IMF1, Total power (TTP), WCZ (Weighted cumulative Zero crossing estimator), WCM (Weighted cumulative Median Frequency estimator), WCR, (Weighted cumulative Root Mean Square estimator)
ARV=Average rectified value, RMS=Root mean square, IEMG=Integrated EMG, ZC=Zero Crossing, MF=Mean Frequency, MPF=Mean Power Frequency, MDF=Median frequency, IMF=Instantaneous mean frequency, IMDF=Instantaneous median frequency, IE= Instantaneous energy, IMFB= Instantaneous mean frequency band, MIF=Mean instantaneous frequency, IMF1= Intrinsic component of EMG signal, AIF= Average instantaneous value, *WIRM1551 means the wavelet ratio between moment 1 at scale 5 and moment 5 at scale 1 based on the discrete wavelet transform.		

2.3.8: Index of Muscle Fatigue

Fatigue index is the degree of fatigue intensity to real-world fashion where common people can surely be able to perceive and define their limit during training or exercise. Among 67 included

studies, 64 papers reported either non-fatigue or fatigue state. On the other hand, Al-Mulla et al. (2011a) presented three categories of fatigue labelled as non-fatigued, transition-to-fatigue, and fatigue state (Al-Mulla et al., 2011a). The study (Chen et al., 2014) mentioned the Borg scale to quantify the intensity of exercise where each subject was asked to rate the perceived exertion during exercise and translate the perception into a numeric value. To translate fatigue index, the study (S. H. Liu et al., 2019) reported a fatigue index formula mentioned in the Appendix C

2.3.9: Sample Size, Age, and Medical Condition of Participants in included Studies

A total of 66 selected studies reported participant information from experimentation. Only 1 study did not report any information about the participants. Among the included studies, 833 participants (male-668 and female-165) volunteered for the muscle fatigue research. However, no research has been done to see how fatigue levels differ between men and women. Qi et al. (2020) reported the participants' medical condition where people with spinal cord injury (SCI) participated in the experiment. A total of 10 participants (Male-7, Female-3) with SCI took part in the test. The overall age of the participant with SCI was under 18 and over 50 years. Approximately every aged population took part in the test except children. So, there is a gap in the literature of the participants' muscle fatigue research with different neuromuscular disorders and how fatigue affects them early enough.

2.3.10: Algorithms based Method used for Detection of Fatigue in Literature

Table 2.4 shows that a total of 13 (19.40%) studies reported Wavelet Transform (WT) directly for the identification of muscle fatigue. WT supports a wide range of standardized mother wavelet functions. Four different types of WTs were reported in the included 13 studies. Continuous Wavelet Transform (CWT) was reported in the 4 studies (Smale et al., 2016; Soo et al., 2008;

Yochum et al., 2010, 2012). Regular WT was used for the 6 studies (Beck et al., 2014; Duan et al., 2020; Fidalgo-Herrera et al., 2021; Kahl & Hofmann, 2016; Nagai, 2017). Also, Discrete Wavelet Transform (DWT) was applied in 1 study (G. Zhang et al., 2018). Both CWT and DWT were also deployed in 1 study (Hari et al., 2020). Another type of WT, named Tunable Q-Wavelet Transform (TQWT), was also reported in the study (Hari et al., 2021).

Maximum 22 (32.83%) studies reported the combination of FT, WT, ML and DL method (listed in Table 2.4) to detect muscle fatigue. The combination of FT, WT with ML or DL method is the automated approach for the detection of muscle fatigue. Either Fourier Transform (Fast Fourier Transform) or Wavelet Transform were used to extract frequency domain features. Based on the features, ML and DL algorithms were trained to detect fatigue. Among different ML algorithms, fuzzy-LDA with FFT was reports in 2 studies (Al-Mulla et al., 2011a; Al-Mulla & Sepulveda, 2010) and presented 90.7% maximum fatigue classification. These studies reported that a real-time wearable system was developed using the LDA with FFT for the detection of fatigue.

Correspondingly total of 7 studies reported the Support vector machine (SVM) algorithm (Table 2.4). However, they used different optimizers for SVM. Two study fuzzy optimizer for SVM (Karthick et al., 2018; Wu et al., 2016). The bacteria foraging base high computational optimizer was also reported in the study (Wu et al., 2016) . Q. liu et al. (2021a) reported an improved whale optimization algorithm (WOA) for optimizing the SVM technique. The WOA-SVM and BF-SVM require high processing memory; therefore, they could be used to develop a laboratory based automated system using a parallel processor. However, they are computationally challenging for integration into a wearable device. Besides, the regular SVM with a simpler optimizer can be used to be embedded in a wearable device.

Karthick et al. (2018) applied Logistic Regression (LR) and Ensemble method with the FFT. Two methods were found to have real-time implications, according to the study.

The combination of WT and PCA reported 5 studies (Chowdhury & Reaz, 2015; Moniri et al., 2021; Qi, 2009; Qi et al., 2011, 2020). Besides, more robust but high computational demanding algorithms like the ANN and CNN were reported in four studies (Fu et al., 2019; Kumar et al., 2003; MacIsaac et al., 2006; Rogers & MacIsaac, 2013).

Only Fast Fourier Transform (FFT) is used in 7 studies detecting fatigue based on frequency domain features of EMG signal. FFT and WT were also used in 4 studies for analyzing the frequency spectrum of EMG signal (Cao et al., 2007; Chowdhury et al., 2015; De Rocha et al., 2018; Rezki et al., 2017). Jero and Ramakrishnan (2019) proposed Hilbert Huang Transform (HHT) algorithm that extracts frequency domain features vector from EMG signal.

In 2 studies, Empirical Mode Decomposition (EMD) was used (S. H. Liu et al., 2019, 2020), and 4 studies reported HHT-EMD based hybrid algorithm. However, real-time implementation of WT, HHT, EMD into a wearable device is still challenging due to the small processing memory.

Table 2.4: Detailed scenario of the algorithm's method in the included studies

List of Algorithms		Type of Muscle Contraction	Indicators of Fatigue	Accuracy	Software/Hardware	Ground Truth
Wavelet Transform (WT)	CWT (Continuous Wavelet Transform) (Rogers & MacIsaac, 2013; Soo et al., 2008; Yochum et al., 2010, 2012)	Dynamic, Isometric	IMF, RMS, MDF, M-wave	NR	MATLAB, Visual-3D, LabView NIDaq Module (NI)	NR
	DWT (Discrete Wavelet Transform) (G. Zhang et al., 2018)	Isometric, 50% MVC	Power Spectrum, Increased Average Ratio (IAR), Trigger Pattern Index (TPI)	NR	NR	NR
	Wavelet (WT) (Beck et al., 2014; Duan et al., 2020; Fidalgo-Herrera et al., 2021; Kahl & Hofmann, 2016; Nagai, 2017)	Isometric, Repetitive, Dynamic	MF, MDF, Scalet wavelet, Center frequency, wavelet intensity pattern (WIP), Ratio of normalized intensities.	0.95	MATLAB	ANOVA Analysis
		Isometric 60%MVC	MF, Spectral moments ratio (SMR), Fuzzy approximate entropy (fApEn) and Recurrence quantification analysis (RQADET), Fuzzy approximate entropy (fApEn)	NR	R-Studio	NR
		Dynamic	Wavelet Spectrum, Borg Rating of Perceived Exertion Scale	NR	MATLAB	Statistical Analysis
	CWT, SWT (Hari et al., 2020)	Isometric	Mean and Standard Deviation (SD) and CV, SVD maximum singular value, SVD entropy	NR	NR	NR
	TQWT (Tunable Q-Wavelet Transform) (Hari et al., 2021)	Isometric	RMS, Mean Absolute Value (MAV), Variance (VAR), and Integrated EMG (IEMG)	NR	NR	NR
FT + WT + Machine & Deep learning	Fuzzy, Linear Discriminant Analysis (LDA) (Al-Mulla et al., 2011a; Al-Mulla & Sepulveda, 2010)	Isometric 30% MVC	IMDF, Total EMG band power, Elbow Angle, Arm Oscillation	LDA=90.3% sensitivity= overall delay 7.4 s	MATLAB SunSpot Microcontroller	Offline Computer-based measurement LR=84.8% NN=80.4% Fuzzy KNN=82.6% OCAT Approach=89.1

List of Algorithms		Type of Muscle Contraction	Indicators of Fatigue	Accuracy	Software/Hardware	Ground Truth
	OGD (Online Gradient Descent), Discrete Fourier Transform (DFT) (Gokcesu et al., 2018)	Dynamic	MDF, MNF, ZCR	NR	SPSS	NR
	Naïve Bayes (Jamaluddin et al., 2019)	Repetitive	MAV, MNF, MDF, RMS	0.98	NR	NR
	Predictive Machine learning (Pilarski et al., 2013)	Dynamic	Smart wheel data, Time-to-Fatigue (TTF), Absolute prediction error	NR	MATLAB	Smart Wheel data self-reported fatigue
	FFT PCA (Moniri et al., 2021)	Dynamic	RMS, MF, MDF	NR	MATLAB	NR
	Support Vector Machine (SVM), WOA (improved whale optimization algorithm) DE (Differential evolution) (Q. Liu et al., 2021)	Isometric	Average rectified value (ARV), IEMG, IMF, IMDB, SMR, Band spectral entropy (BE), Lempel-Ziv complexity (LZC)	average accuracy of 85.50% in ankle dorsiflexion (DF) and 84.75% in ankle plantarflexion (PF)	Statistical Analysis tools	NR
	FFT, PCA, SVM (Chowdhury et al., 2019)	Isometric	MAV, SSC, IEMG), Simple square integral (SSI), VAR, RMS, WL, Log detector (LOG), ZC, V-order 2 (V2), sample entropy (SampEn), MDF, MF, Average instantaneous value (AIF), Total power (TTP) and Mean Power	FD set: 86.76%, error: 13.24%, TD set: 92.65%, error:7.35, Compound feature set: 92.65%, error: 7.35%, Time-frequency domain feature set: 94.12%, error: 5.88%	MATLAB	NR
	LMS (Least Mean Square), NLMS (Normalized LMS), GNGD (Generalized Normalized Gradient Descent), AP (Affine Projection), CNN, (Moniri et al., 2021)	Isometric	RMS, IEMG, ZC, MF, MDF	NR	NR	Significance Wilcoxon signed-rank test with Bonferroni correction ($p < 0:01$).
	KNN (Bukhari et al., 2020)	Isometric & Dynamic	NR	40% for ISO 73% for ECC and 80% for CON	MATLAB	NR

List of Algorithms		Type of Muscle Contraction	Indicators of Fatigue	Accuracy	Software/Hardware	Ground Truth
	BF (Bacterial Foraging), PBSO, FSVCM (Fuzzy support vector classification machine), DWT, FFT, EEMD-HT (Ensemble Empirical Mode Decomposition Hilbert transform (Wu et al., 2016)	Isometric 60% MVC	RMS, IEMG, MPF, MDF, MIF, Wavelet Entropy (WE), Energy ratio of all high frequency and low frequency (ERHL)	***Static Fatigue*** SVCM= 86.36% PSO-SVCM=91.91% FSVCM = 91.91% BF-FSVCM= 91.91% BF-PSO-FSVCM=95.45% ***Local Fatigue*** SVCM= 75% PSO-SVCM=85.77% FSVCM = 80.65% BF-FSVCM= 88.64% BF-PSO-FSVCM=93.18% ***Dynamic Fatigue*** SVCM= 86.36% PSO-SVCM=90.91% FSVCM = 89.66% BF-FSVCM= 93.1% BF-PSO-FSVCM=96.55%	MATLAB	Statistical analysis
	FFT, GA (Genetic algorithm), BPSO (Binary particle swarm optimization, Naïve Bayes, LR, Ensemble, SVM, Random Forest, Rotation Forest (Karthick et al., 2018)	Dynamic	MDF, MF, NSM, Concentration measure, Spectral entropy, Renyi entropy, SVD based entropy, Mean,Variance,Skewness, Kurtosis, Cofficient of Variannce (CoV)	Overall, 91.39% LR = 85% Ensemble=90%	NR	Statistical analysis
	Welch Method, ANN, Backpropagation, Logistic Regression, Ensemble, (Rogers & MacIsaac, 2013)	Isometric, Repetitive Dynamic	Generalized mapping index (GMI), PCA Theta (Q) Score, MDF	NR	MATLAB, NI-DAQ	Off-line. (mean ± std.dev.): PCA: (12.6 ± 5.6), GMI: (11.5 ± 5.4), NSM: (10.3 ± 5.4), WI: (8.9 ± 4.6), HE: (8.0 ± 3.3)

List of Algorithms		Type of Muscle Contraction	Indicators of Fatigue	Accuracy	Software/Hardware	Ground Truth
	PCA, Wavelet (Qi et al., 2011, 2012, 2020)	Isometric, Isotonic	EMG Total Intensity, MF, Wavelet Center Frequency, PCI and PCII loading scores Theta (θ), MU	NR	Mathematica 6.0	ANOVA, ANCOVA
	Wavelet, ANN (Kumar et al., 2003)	Dynamic	MUAP, Frequency decomposition	NR	MATLAB	NR
	CWT, Transfer Learning (AlexNet, and ResNet-18) CNN-LSTM (Nahid et al., 2020)	Voluntary	Time-Frequency representation	CNN-LSTM for UCI Dataset 99.72% For Khusaba dataset 99.83%	MATLAB	NR
	GA, Pseudo-wavelet function (R. et al., 2012)	Isometric and dynamic	Wavelet decomposition	87.90 %	Computer, Data logger	NR
	DWT, Pbest (Personal best), PBPSO (Particle binary particle swarm optimization), BPSO (Binary particle swarm optimization), GA, MBTGA (modified binary tree growth algorithm), BDE (Binary differential evolution) (Too et al., 2019)	Voluntary	MAV, WL, RMS, Maximum fractal length, and Average power	85.20%	MATLAB	NR
	Wavelet, Backpropagation, NN, SVM, GA-SVM (Rong et al., 2013)	Voluntary	EMG Spectral intensity, Energy Analysis, High and low frequency power, and MDF, MF	97.3% with seven-fold cross-validation	NR	NR
	Wavelet, CNN, SVM, PBSO, (Wang et al., 2020)	Repetitive	RMS, IEMG, MPF, MDF, and Band Spectral Entropy	CNN 80.33% SVM 86.69%	Portable gas analyzer (K4b2 Cosmed, Rome, Italy)	NR
Standalone ML	ANN (Artificial Neural Network), RBN (Radial Basis Network), GRN (General Regression network) (MacIsaac et al., 2006)	Static & Dynamic	MAV, Zero Crossings (ZC), Slope sign changes (SSC), and Wavelength (WL).	ANN=70%	MATLAB, Microsystems	NR
EMD	Empirical Mode Decomposition (EMD) (S. H. Liu et al., 2019, 2020)	Isotonic & Isokinetic	IMF1 (Intrinsic component of EMG signal), MDF	NR	MATLAB, Microcontroller	MCU computed MDF (IMF1) was compared with offline computer system

List of Algorithms		Type of Muscle Contraction	Indicators of Fatigue	Accuracy	Software/Hardware	Ground Truth
	EMD, FFT (Yang et al., 2014)	Isometric	RMS, IEMG, MF, MDF, IMF, EMG Power	NR	MATLAB	FFT & ANOVA
EMD & WT	EMD, WT (Chowdhury et al., 2014; Chowdhury & Reaz, 2015)	Repetitive	RMS, IAV and AIF	NR	MATLAB	NR
	EMD, HT, LR (Xie & Wang, 2006)	isometric	MF	NR	MATLAB	Statistical analysis
HHT	Hilbert Huang Transform (HHT) (Jero & Ramakrishnan, 2019)	Isometric & Dynamic	IF, IA, HMS, Shannon entropy (ShEn), Renyi entropy (ReEn), Tsallis entropy (TsEn), Approximate entropy (ApEn), Sample entropy (SamEn) and Conditional entropy (CndEn)	NR	Statistical analysis BIOPAC system	t-test
HHT & EMD	HHT EMD (K. Li et al., 2012; Peng et al., 2006; Srhoj-Egekher et al., 2011; Xie & Wang, 2006)	Isometric, Dynamic, 80% MVC	MF, Initial force proportion (IFP), Force output (FO), Relative force output (RFO), IE, IF, MDF	NR	MATLAB, SPSS, ME3000P2	CoV HHT 0.0061 AR 0.0407 WT 0.1190 24 Anova, t-test, Kolmogorov-smirov test. 26
Polynomial Chirplet Transform	Polynomial Chirplet Transform (Ghosh & Swaminathan, 2017)	Isometric	IMF, IMDF, ISE (Inst. Spectral Entropy)	NR	MATLAB Biopac MP36 data acquisition system	NR
FFT	FFT (Fu et al., 2019; Han, 2017; Hotta & Ito, 2013; Nagai, 2017)	Static Concentric Isometric 90% MVC Dynamic 5% MVC	MPF, MF, MDF	Error of MATLAB processing result and DSP processing result is 0 0.000002 Hz	MATLAB, DSP Kit TMS320C6748	Regression MPF compared MATLAB Pearson correlation coefficient
	SCD (Cyclostationarity), FFT (Karthick et al., 2016)	Isometric	Spectral Correlation Density (SCD), Cyclostationarity property of sEMG	NR	MATLAB	NR
	Short Term Fourier Transform (STFT) (Ming et al., 2014; Subasi & Kiymik, 2010)	Isometric	MDF, MF	MLPNN=90% STFT = 87.5% SPWVD = 89% CWT = 89% 69	MATLAB	NR
	FFT (Dayan et al., 2012)	Isometric	MDF, Peak and Spike Counting of EMG signal	RF: r2 for PC and SC 0.9275 and 0.9235	MATLAB, Digital Comparator Asynchronous Counter	NR

List of Algorithms		Type of Muscle Contraction	Indicators of Fatigue	Accuracy	Software/Hardware	Ground Truth
				VL: r2 for PC and SC 0.9567 and 0.9581		
	FFT (Chang et al., 2016)	Isometric 90% MVC	Mean Amplitude of EMG, RMS, MDF	NR	MATLAB SPSS	Pearson correlation coefficient, r=0.74: p<0.001
FFT & Wavelet	FFT, DWT (Chowdhury et al., 2015)	Dynamic	Spectral analysis, power of different frequency bands (mean power values, grand mean power)	NR	MATLAB, Channels portable SEMG system (Noraxon Inc., Arizona, USA),	NR
	FFT, Wavelet (De Rocha et al., 2018)	Isometric & Dynamic	ZCR, MDF, WCZ (Weighted cumulative Zero crossing estimator), WCM (Weighted cumulative Median Frequency estimator), WCR, (Weighted cumulative Root Mean Square estimator)	NR	NR	Statistical analysis
	FT, CWT, Cyclostationarity (Cao et al., 2007)	Isometric & Dynamic	MF, Energy (En), IE, IMF, SC (Spectral coherence).	NR	Statistical software	NR
	STFT, Wavelet (Rezki et al., 2017)	Voluntary	Amplitude, Mexican hat and Haar scale.	NR	Arduino Card	NR
Hybrid Algorithm	OCEEMD (optimized complementary ensemble empirical mode decomposition), LSMI (least-squares mutual information), CQPSO (chaotic quantum particle swarm optimization), (Z. Li et al., 2020)	Repetitive	multi-scale envelope spectral entropy (MSESEn), root mean square error (RMSE), the number of IMF components, and the standard deviation of the amplitude ratio	NR	NR	fast Fourier transform (FFT)
	FES (Functional Electrical Simulation, selective interpolated CEEMDAN with logistic regression (SICEEMDAN-LR) (Zhou et al., 2020)	Isometric	IMF, M-wave	NR	MATLAB	NR

2.3.11: Performance Qualities and Ground Truth

Table 2.4 represents the detailed summary of performance qualities with the ground truth of the listed algorithm reported in the included studies.

Overall, the standalone use of FT, WT, EMD, and HHT methods does not offer an automated fatigue detection approach. As a result, fatigue detection, in this case, is determined by expert clinicians or trained researchers who can interpret the results from analyzing the sEMG signal using these algorithms.

To validate the WT, FFT, EMD, and HHT frequency-based analysis performance, a couple of statistical techniques along with t-test, Chi-square test, ANOVA, ANCOVA, F-max, Wilcoxon test, Pearson coefficient test, regression analysis was reported shown in Table 2.4.

The automated fatigue detection approach requires the combined use of FT, WT, HHT, and ICA with the ML and DL algorithm. Different approaches based on ML showed satisfactory classification accuracy. Among the ML techniques listed, LDA showed maximum classification accuracy and was close to 90.3% (Al-Mulla et al., 2011a; Al-Mulla & Sepulveda, 2010) when implemented in real-time. LDA was therefore identified as one of the promising algorithms for the real-time detection of muscle fatigue.

The standard SVM algorithm with FFT achieved a maximum average accuracy of 85.50% in ankle dorsiflexion (DF) and 84.75% in ankle plantarflexion (PF) (Q. Liu et al., 2021), where adding other algorithms or optimization techniques improves the classification accuracy. For example, PCA with SVM attains a classification accuracy of 86.76% when using the frequency domain features set and 92.65% for the combination of time and frequency features set (Chowdhury et al., 2019). The Fuzzy SVM shows the maximum classification accuracy is 91.91% with the time

and frequency domain features (Wu et al., 2016). An algorithm like the KNN attains 73% for eccentric and 80% for concentric contractions. In parallel, genetic algorithms with binary particle swarm optimization and naive bias achieve 91.39% of overall classification accuracy.

In addition, two other real-time algorithms showed promise. The LR achieved an accuracy rate of up to 85%, and the Ensemble showed maximum accuracy of 90%.

Considering only time domain features, the ANN achieved maximum accuracy of 70%, and the CNN attained 80.33% accuracy. However, the ANN and CNN are very unlikely to be embedded in a wearable device due to their sizeable computational requirement.

The performance of the ML algorithms was validated mainly by either the confusion matrix or cross-validation techniques. In addition, a single ML algorithm's performance was checked by other ML algorithms and statistical analysis. For instance, the LDA performance was compared with the LR, NN, Fuzzy KNN, and OCAT approach (Al-Mulla et al., 2011a), where the LDA shows superior performance.

2.3.12: Wearable System in the Literature

Currently, 4 studies among 67 included studies attempted to model real-time wearable muscle fatigue detection systems.

The study (Dayan et al., 2012) conducted a feasibility study of monitoring muscle fatigue using peak counting (PC) and spike counting (SC) of EMG signal instead of median frequency. However, with only one feature (MDF or PC/SC, or IMDF), the fatigue detection model failed to achieve acceptable clinical accuracy.

An FFT based real-time monitoring of muscle activity during cycling was reported (Chen et al., 2014). The study demonstrated graphical results in real-time in the LabView. However, an expert clinician or therapist is required to interpret the results to detect fatigue. Moreover, the study recommended using FFT to detect muscle fatigue in a wearable device but did report any mechanism for implementation in real-time.

An EMG Patch was developed for the real-time monitoring of muscle fatigue during cyclic exercise using a microcontroller unit applying an EMD algorithm (S. H. Liu et al., 2019). However, the device was designed to forecast muscle fatigue based on only IMDF features. The study did not report any classification or validation performance. Single feature IMDF generates oscillatory output and goes beyond the fatigue spectral frequency region. As a result, it is not very likely to forecast consistent results with satisfactory accuracy using only IMDF features.

Correspondingly, a microcontroller based autonomous system using fuzzy-LDA was built to predict muscle fatigue in BB muscles for 30% MVC (Al-Mulla et al., 2011a). the classification accuracy was reported at 90.7%. Red LED light was turned on when the transition-to-fatigue occurred, and blue light turned on meant non-fatigue. The elbow angle, arm oscillation, power, and IMDF were used as features. The elbow angle and hand oscillation are entirely subjective measures and remain error bias. However, the elbow angle and hand oscillation vary drastically from contraction to contraction and are not appropriate for all contractions.

There is a very likely gap in the literature that can be filled by developing a wearable device that can detect muscle fatigue in real-time and apply it.

2.4: Discussion

This scoping review aimed to search comprehensively in the current literature to uncover state of the art for algorithms used to train models to detect muscle fatigue from the sEMG signal during exercise or physical activities. The scoping review suggested 4 algorithms that have the potential to train models to be embedded in a wearable device. Wearable devices have had a significant impact in the fields of rehabilitation research, health science and sports research. However, based on the result of the scoping review, we did not find any wearable devices in the literature that are currently being used for detecting muscle fatigue in real-time.

One of the outcomes of this scoping review is that before constructing any automated real-time system, it is critical to train algorithms utilizing fatigue features from large enough datasets to avoid overtraining. Most of the studies reported extracting both time and frequency domain features from the sEMG signal. Algorithms that trained models using both time and frequency domain features simultaneously had greater accuracy than models that were simply trained on only time, or frequency domain features alone, as shown in Table 2.4.

A promising algorithm method is recommended based on the adaptability to deploy in an embedded device and the performance of the algorithm's methods portrayed in Table 2.4.

The scoping review determined that the FFT, HHT, WT, ICA, and EMD are currently used algorithms to analyze the frequency spectrum of the sEMG signal. However, these algorithms are not readily implemented in a wearable device since they require the trained eye of a specialist to predict fatigue using these techniques (Wu et al., 2016).

Al-Mulla et al. (Al-Mulla et al., 2011a) developed an autonomous system for detecting muscular fatigue with a combination of fuzzy and LDA algorithms embedded into a microcontroller. The

LDA showed a maximum of 90.3% accuracy. LDA is computationally light and compatible with embedding in a wearable device. Therefore, LDA is considered one of the potential algorithms to train models that could be embedded into a wearable device.

The study (Karthick et al., 2018) suggests that the LR and Ensemble algorithm could be embedded in a wearable device. The study reported the performance accuracy of two algorithms (LR=85% and Ensemble = 90%) that results are acceptable to use in practice. The LR is light and low-computational demanding model included in the list of algorithms that may be used with wearable devices. The Ensemble ML algorithm requires a medium processing compared with LDA, LR and SVM. However, Ensemble shows superior performance most often in the complex classification problem. Therefore, Ensemble can be used to justify its performance in detecting fatigue in real-time.

A fuzzy support vector classifier machine algorithm (FSVCM) combined with FT and WT, was proposed and showed 89.66% classification accuracy (Wu et al., 2016). The study was conducted to classify muscle fatigue, but not in a real-time fashion. However, the study suggested that the SVM model together with FT is potentially feasible to be embedded in a wearable device. It is also concluded that the SVM would be one of the promising algorithms to develop a real-time model that can be embedded into a wearable device.

The CNN, WOA, and Naïve Bayes also demonstrated superior training and testing accuracy described in (Q. Liu et al., 2021). However, these algorithms have a multi-layer network and required high computational time. These algorithms could be suitable to develop for fatigue detection models but require a high processing laboratory setup and are therefore not feasible to embed into a wearable device.

Although muscle fatigue research has been conducted for a couple of decades, there is no evidence from the literature of an automated real-time fatigue model embedded in a wearable device. Accordingly, the recommendation of this scoping review, it is that the LDA, LR, SVM, and Ensemble have the potential to be embedded in a wearable device.

2.4.1: Research Approach for Real-Time Wearable Device

The sEMG signal is a time-varying and non-linear signal. Without time and frequency-domain analysis to extract features as input to models, it is unlikely to detect muscle fatigue precisely (Wu et al., 2016). In addition, the review revealed that algorithms that were trained on both time and frequency domain features simultaneously were more accurate. As a result, it is clear that muscle fatigue models require both time and frequency domain feature vectors to provide adequate accuracy.

The outcome of this scoping review recommends considering three steps to develop a model that can detect muscle fatigue in real-time which is compatible with and embedded in a wearable device:

i) To decompose EMG signal using various signal processing techniques.

ii) To extract features from the decomposed EMG signal.

iii) To train ML algorithm classifier using the extracted features, then validated and tested with new EMG data.

To Decompose EMG Signal: It has already been established that the EMG signal contains both time and frequency domain features. The result of this review suggested that Wavelet Transform (WT), Hilbert Huang transforms (HHT-EMD), Fourier transform (FT), and Independent

Component Analysis (ICA) are the most widely used tools for extracting frequency domain features from EMG signals. However, except for the FFT, all three methods are highly computationally complex systems. No wearable devices can handle these methods due to low memory size, power consumption, number of iterations, clock frequency and limited parallel processing capability. Therefore, one of the significant challenges of this research is to extract time and frequency domain features from the EMG signal and to process them simultaneously.

To extract frequency domain features, the sEMG signal needs to be converted into the frequency domain. FFT typically requires 16 KB (S. H. Liu et al., 2019) while processing which is feasible for deployment in the flash memory of embedded devices. Fourier Transform based techniques can undoubtedly convert the sEMG signal into the frequency domain and estimate the power spectrum. Contrarily, less processing is required for extracting time domain features compared to the frequency domain.

To Extract Features from the Decomposed EMG signal: After decomposition, the features of the EMG signal will be extracted. The time domain features can be extracted directly with less processing of the EMG signal. Therefore, the process to calculate time domain features is a little faster than frequency domain calculation.

However, the extraction of frequency domain features takes some time. The power spectrum can be estimated to extract the features. Chapter 3 discusses which features were selected in this research.

Adding so many features creates a computation burden for the processor. The challenge is to achieve the smallest number of features that will capture the required patterns in the data. The feature selection approach was undertaken to select the most relevant features describing fatigue

patterns and remove unneeded or redundant features. As this is a trial-and-error approach, some features will be added or subtracted during the experimental analysis.

Train the Classifier and Extract Unknown Signal: The ML classifier is trained based on the extracted features to classify muscle fatigue on the unknown EMG signal in this stage.

This review suggested some algorithms that are suitable to use a real-time wearable device. The anticipating algorithms are: i) LDA, iii) SVM, iii) LR and iv) Ensemble.

Recent research shows that these algorithms have the potential to be embedded in a wearable device. As a result, these algorithms must be optimized to reduce dimension, making light and compatible models for the deployment in a wearable device.

It is a strong belief that this approach will help to develop a robust wearable system that can detect muscular fatigue for a large group of people in real-time.

2.4.2: Study Limitations

We must keep in mind that this scoping review has some limitations because we have only been able to collect studies that employ algorithms to determine muscle fatigue, not other types of indicators. The papers were extracted based on the six databases ,as a result, it may create bias. The selection of the databases did not follow any scientific methodology rather the researcher's empirical knowledge. Studies included in this review were only published in the English language. The studies were included that have been published between January 1, 2005, to January 1, 2020. On the contrary, within the literature search interval, the earliest articles are likely outdated because of technological advancement.

2.5: Conclusion

The purpose of this scoping review was to identify algorithms that could be applied to detect muscle fatigue in real-time and compatible with deploying it in a wearable device. However, despite the inclusion of 67 studies, it was still found that the limitations in the algorithms reported would not meet our pre-defined criteria. We conclude that the technology readiness level of an automated system using ML algorithms is still low. However, this review has suggested four ML algorithms that have the potential to be used to train models that can be embedded to create a wearable device. Primary research with adequate size datasets to avoid overtraining is required to assess these algorithms and select the optimal model for muscle fatigue studies. It is concluded that there is no wearable device in the current literature that can detect muscle fatigue in real-time as well as be acceptable to the clinical setting. In addition, the challenge of integrating these selected algorithms into wearable devices remains unclear. Therefore, this review advocated to alleviate the research to develop a wearable device using the potential algorithms for detecting muscle fatigue in real-time.

CHAPTER 3: **DEVELOPMENT AND VALIDATION OF A MODEL TO DETECT MUSCLE FATIGUE BASED ON sEMG DATA ASSOCIATED WITH A SUSTAINED SINGLE 80% MVC**

Abstract

Background: Muscle fatigue impairs the muscle's ability to contract and exert force and eventually leads to complete loss of function, preventing a task from being finished. A balance between optimizing performance and preventing injury is critical in designing fitness programs to improve strength and endurance. To define the maximum limit for optimal test-specific activities and exercises, it is desirable to develop a wearable system to detect muscle fatigue in real-time.

Objectives: The objectives of this research were: 1) To extract features from the previously recorded sEMG data during a sustained single 80% MVC and select the most promising features associated with fatigue, 2) Utilizing the features identified in Objective 1 to evaluate the performance of the algorithms identified in the scoping review, 3) To select the most promising machine learning algorithm based on the classification performance of fatigue state and 4) To develop a model that has the potential to be embedded in a wearable device.

Methods: Different features were extracted from the sEMG signal in the time and frequency domains during sustained single 80% maximum voluntary contraction (MVC). To extract frequency domain features, power spectrum of the sEMG signal was estimated using the Fast Fourier Transform. Then, to eliminate the unnecessary features, the NCA feature reduction tool was used. Next, each algorithm (recommendation of the scoping review) was tested to evaluate its performance with the selected features. Finally, based on the performance of fatigue classification and adaptiveness to a wearable device, the most promising algorithm was selected for developing the proposed model.

Result: The NCA selected 14 significant features from 35 features extracted from the sEMG signals. Using 14 features, the OSVM algorithm outperformed other algorithms with respect to fatigue classification accuracy. The proposed OSVM algorithm achieved 99.2% overall classification accuracy with a sensitivity of 99% and a specificity of 99.2%. Testing with a new dataset, the model showed 100% fatigue classification accuracy and is excellent performance among the existing muscle fatigue research. With a reduced feature set of the 5 most prominent features, the OSVM model achieved a maximum of 92% fatigue classification accuracy.

Conclusion: The specifications for a suitable microcontroller capable of implementing the model are summarized and indicated that a wearable device using our model is feasible.

Keywords: Surface EMG, MVC, Muscle fatigue, Feature extraction, Feature selection, Model, Wearable device, Real-time.

3.1: Introduction

Wearable devices have been extensively used in diverse fields, particularly the healthcare sector to the rehabilitation area and the Olympic event, to monitor patients' health and welfare and to prevent injuries (Al-Mulla et al., 2011a; S. H. Liu et al., 2019). Recent research demonstrates that people are increasingly willing to use body-worn devices to monitor their health status while engaging in physical exercise (S. H. Liu et al., 2019). Although research on muscle fatigue has been advancing for several decades, an accurate wearable device has not been reduced to practice. A wearable device is highly desirable for use in ergonomics and prosthetics, human-computer interactions, sports injuries and performance, rehabilitation like spinal-cord injury, paraplegia, cerebral palsy, low back pain, shoulder and neck pain, arthritis, stroke recovery and so on (Al-Mulla et al., 2011a; Koutsos, 2017; Koutsos et al., 2016; O'Sullivan et al., 2018; Qi et al., 2011).

Muscle fatigue reduces muscles' ability to contract and exert force overtime during a sustained task (Wan et al., 2017). If muscle fatigue is not managed carefully, there is a risk of injury (Al-Mulla et al., 2011b). Currently, individuals generally have to rely on their perception of muscle fatigue during exercise (Al-Mulla et al., 2011a). A quantitative approach has the potential to manage available muscle capacity to complete a task safely and to an optimal level of performance. In addition, clients can use the information to define their limits using the wearable device during training and exercise sessions to prevent injury.

Wearable devices are widely used to predict health statuses, such as monitoring respiration, blood pressure, pulse rate, and body temperature. In these examples, the data sampling rates required are relatively slow (10-20 Hz) (Dias & Cunha, 2018) compared to sEMG signals which are typically 1000 Hz per muscle (Qi et al., 2011). In addition, the models needed to detect muscle fatigue are

computationally more complex that most other physiological signals. These two factors in combination create a significant technological challenge when designing a wearable muscle fatigue sensor. This necessitates the development of efficient models to match the available lean computational resources of modern wearable devices.

3.1.1: Relevant Literature

There are a few literatures that attempts to develop a wearable device sEMG-based fatigue sensor. Chen et al. (2014) developed an FFT-based real-time method for detecting muscle fatigue while cycling and displayed graphical findings in LabView (a desktop application). Fatigue was detected by trained-eye observation based on the displayed spectrum in LabVIEW (Chen et al., 2014). The study suggested the use of FFT to detect muscle fatigue in a wearable device but did not reduce it to practice.

The study (S. H. Liu et al., 2019) reported an EMG Patch that was developed for real-time monitoring of muscle fatigue during cyclic exercise using a microcontroller unit. The empirical mode decomposition (EMD) algorithm was applied to measure the instantaneous median frequency (IMDF) as fatigue indicator. The EMD is a very complex algorithm to embed in controller. Instead, only a small portion of the EMD algorithm called the first intrinsic mode function (IMF1) was embedded in a microcontroller to measure IMDF. No validation or accuracy was reported in the study. This study only reported the difference between the calculated IMDF in the microcontroller and measured in a computer system (post-processing or offline approach). Wu et al. (2016) stated that single feature IMDF does not have the capability to detect the occurrence of fatigue that is clinically acceptable. The authors in study (Wu et al., 2016) argued that IMDF becomes very high and even assumes negative values that bear no relationship to the real the real world data collected. Very often IMDF is oscillatory and extends beyond spectral range of the

sEMG signal. To overcome the limitation of IMDF frequency, it is essential to utilize multiple features while developing a wearable device for fatigue pattern.

Al-Mulla et al. (2011a) developed a microcontroller based wearable device to detect muscle fatigue in BB muscles for the 30% MVC. Only five participants volunteered in the experiment. A fuzzy classifier is used to set the boundaries for labelling the sEMG signals based on manual input two main kinematic criteria: elbow angle and hand oscillation obtained by a goniometer. The elbow angle, hand oscillation, total EMG power, and IMDF were used for fatigue features. However, from contraction to contraction, the elbow angle and hand oscillation differ dramatically and not applicable for every contraction. The study reported two states of EMG signal: non-fatigue and transition-to-fatigue state. The fuzzy-LDA based system was capable of predicting the onset of fatigue with an average error of 7.4 seconds of five participants. The overall classification accuracy of the LDA algorithm was reported as 90.3%. The system was capable of alerting the user in a simple way by turning on the LED light as a fatigue indicator. The elbow angle and hand oscillation which is entirely subjective measures and remains error bias.

Finally, there are sufficient gaps in the current literature for developing a wearable device that can be used to detect muscle fatigue in real-time as well as acceptable to the clinical setting. This research gap identified an opportunity for developing a real-time wearable device to detect fatigue. The main objective of this research is to develop a model using machine learning that can be used to deploy in a wearable device to detect muscle fatigue in real-time from the sEMG signal during a sustained single 80% MVC. An accurate, well-designed wearable device could be applied in clinical and consumer applications to monitor fatigue in real-time helping to prevent work-related injuries.

3.2: Methodology

3.2.1: General Overview: The Process of Developing a Model using Machine Learning Algorithm.

The block diagram presented in Figure 3.1 shows the overall process of developing a model using an ML algorithm. The early phase is known as the data collection step, where raw EMG signal was recorded from biceps brachii muscle during static isometric voluntary contraction.

The raw data was processed and conditioned in the signal grooming stage. In the grooming stage, the dataset of brief period and did not represent any fatigue were removed. After that, the sEMG signal was conditioned in the same stage.

After grooming the captured raw sEMG signal, the next stage was the feature extraction. Feature extraction was a crucial part of the workflow (Wu et al., 2016). Subsequently, the feature selection technique was applied to select the most prominent features that follow the fatigue pattern. Feature selection is essential to avoid irrelevant features reducing the computational burden to the system.

Following that, ML algorithms (selected in Chapter 2) were trained using a database of sEMG signals to evaluate their performance and select the most promising algorithm for modelling sEMG to detect fatigue in real-time. The most promising algorithm was required to demonstrate excellent performance accuracy and suitability for embedding in a wearable device. The rest of the section of this chapter provides detailed information about each stage.

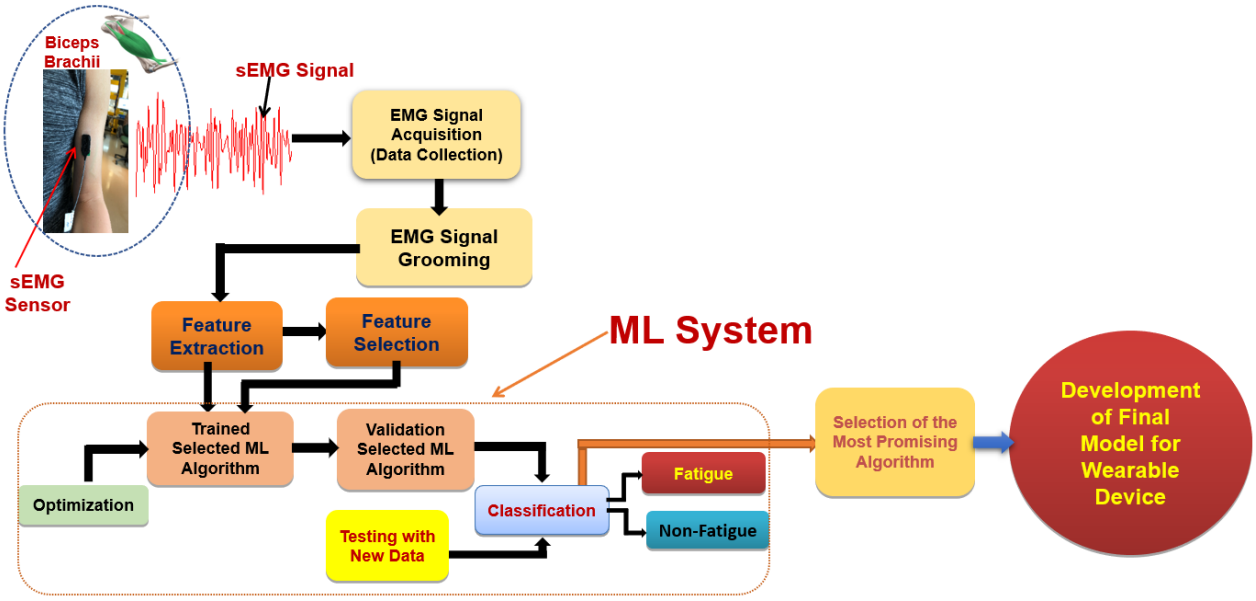

Figure 3.1:Architectural framework for developing a Model using ML algorithm to detect fatigue.

3.2.2: Participants' Information

The participants' data were previously collected as part of an sEMG data bank at the Rehabilitation Robotics Laboratory (RRL), Edmonton Clinic Health Academy at the University of Alberta. The study that collected the data and its use for the development of models for fatigue detection was approved by the University of Alberta Research and Ethics Management Committee (Pro00063851, 2016). A total of 100 participants participated in the test. Each participant was informed about the study and took written consent before the trial. All participants were asked to complete the PARQ+ before testing (Cifrek et al., 2009; O'Sullivan et al., 2018). A total of 100 healthy participants volunteered in this study (the number of male n = 50, female n = 50, age 18-75). The sEMG data included equal numbers of males and females, thus guaranteeing gender equality. The participants were free of neuromuscular disease and any upper extremity injury within the past year (O'Sullivan et al., 2018).

3.2.3: sEMG Recording and Data Collection

Each participant performed a single thirty-minute session in the RRL Lab using the Delsys Bagnoli EMG system (Massachusetts, USA). A single session consisted of a maximum voluntary contraction test followed by a single sustained isometric contraction at 80% of the participant's MVC, held until fatigue. The study (Cifrek et al., 2009) report recommended procedures for measuring fatigue systematically. Participants were provided with a visual analogue feedback of the force they were generating using a force-transducer that was integrated into the data acquisition system. They were asked to exert a maximum force to define the MVC.

Figure 3.2: Isometric single sustained maximum voluntary contraction test (Photo: RRL Lab).

Figure 3.3:Bagnoli™ Surface EMG Sensor (Photo: BagnoliTM website)

Then for the sEMG data collection to fatigue test, they were asked to maintain the force as close to 80% of their MVC as possible. Participants used their dominant arm for the contractions. EMG recordings were collected using DE 3.1 Bagnoli Double Differential surface electrodes placed on the skin overlying the belly of the biceps brachii (BB) muscle (O'Sullivan et al., 2018; Qi et al., 2020) parallel with the direction of the BB muscle fibres. Superior to the antecubital fossa, a reference electrode was placed on the anterior side of the non-dominant arm (O'Sullivan et al., 2018). The bandwidth of the EMG sensor is specified as 20-460/Hz while being sampled at 1000 Hz. The following information is considered as a recommended configuration for obtaining muscle activity information.

3.2.4: Data Grooming

Removal of Outliers from the Dataset: All 100 participants were asked to sustain the 80% MVC force until they could no longer do so, and this was defined as the point of fatigue. Four participants stopped the test after a very short time and were not considered to have fatigued but very likely stopped due to discomfort in applying the 80% force. Consequently, we applied statistical analysis to exclude the lower test duration subjects from the entire dataset. The Stem-and-Leaf method was used to choose the outliers with the lowest value. A total of 4 participants' data were omitted from the study since their test length was less than 19 seconds.

```
Test_Length Stem-and-Leaf Plot

 Frequency     Stem &  Leaf

    15.00 Extremes    (=<19)
    25.00        4 .  0000033333666666666666666
     5.00        5 .  99999
    30.00        6 .  333334444455555777777777777
    45.00        7 .  22222333335555566666666667777788888888888999999
    75.00        8 .
000000000000000111122222444444444466666666667777777777777777888889999999999
    70.00        9 .
111111111122222222233333444444444455555777777777777777888889999999999
    55.00       10 .  000000000011111111122222444445555566666777778888899999
    65.00       11 .
000001111122222222233333444445555566666666667777788888999999999
    15.00       12 .  111112222244444
    25.00       13 .  1111111111333339999999999
    20.00       14 .  333335555577777888888
    20.00       15 .  555556666677777888888
      .00       16 .
    15.00       17 .  000004444466666
    20.00 Extremes    (>=192)

 Stem width:  10.00000
 Each leaf:        1 case(s)
```

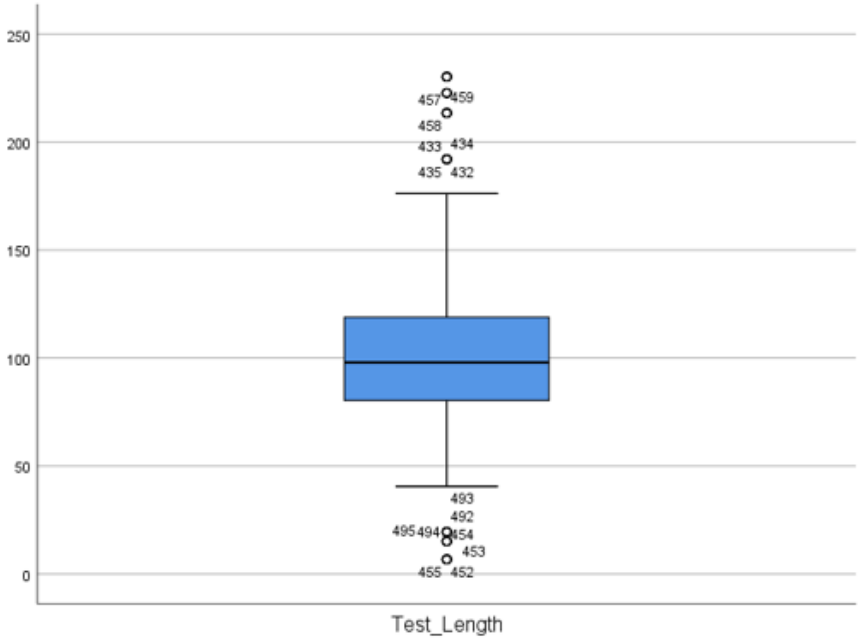

Figure 3.4: Steam-and-Leaf plot for removing lower value outlier data from the 100 participants data.

Movement Artifacts and Noise Removal: The sEMG signal captured from human muscle is unavoidably contaminated by the noise that originates in the amplification circuit (known as thermal noise), at the electrode-skin interface, due to crosstalk between neighbouring muscles and other peripheral sources (De Luca et al., 2010; Qi et al., 2011). These noise sources interact when

a sensor is attached to the skin and form the baseline noise detected while capturing EMG signal from the muscle. The crosstalk can be reduced by careful sensor positioning and managing the contraction task to reduce co-contractions. Movement artifacts originate at the electrode-skin interface. They occur when the muscle beneath the skin moves, and the force impulse passes causes relative movement between the electrode-skin-muscle interface. Movement artifacts tend to contaminate the low-frequency part of EMG spectra and can be removed by applying a high pass filter only transmitting signal frequencies greater than 20 Hz.

Given the goal of developing a wearable real-time sensor, complex-filter circuits would add to the system's complexity and computational demand. All electronic circuits that employ AD converters must employ a low pass antialiasing filter to remove signals above the sampling frequency. This can be implemented in hardware. To remove the low frequency movement artifacts however we chose not to use a 20 Hz high pass filter preferring to test how the real-time system operates with the raw sEMG signal and allowing the ML model to eliminate the movement artifacts. We used a completely new method to eliminate movement artifacts and high-frequency harmonic elements, adding novelty to this study.

In the first step of signal conditioning, we cleaned all data by statistically removing artifact spikes and outliers using the filling outlier's technique. This technique was implemented in the MATLAB environment to find and fill the outliers. A value that is more than three scaled median absolute deviations (MAD) from the median is considered an outlier. The outliers were filled with the nearest median of the time-series EMG data. The MATLAB function used can be readily deployed in a microcontroller environment if necessary.

Detrending was used to remove the low frequency power contribution in the frequency domain (Elipot & Gille, 2009). Detrending produces straightforward spectra that focusing on the physiological components in the signal. For our study, we used the 2^{nd} order detrend function to remove the quadratic trend of the EMG signal so that it could maintain original physiological information.

As an afterthought, we applied a different strategy to remove the low-frequency components due to the motion artifacts and high-frequency harmonic components in the spectrum. The study (Qi, 2009) suggested that the low-frequency components added to the EMG spectrum are less than 20 Hz due to movement artifacts. Furthermore, the authors in (Naeije & Zorn, 1982) stated no fatigue information in the EMG spectrum beyond the 150 Hz frequencies for isometric contraction. Based on the previous literature recommendation, we used a sorting function that captures frequencies between the ranges from 20 to 150 Hz and eliminated the rest of the frequencies. For the remainder of our research, frequencies in the range of 20 Hz to 150 Hz were used to remove artifacts and harmonic components.

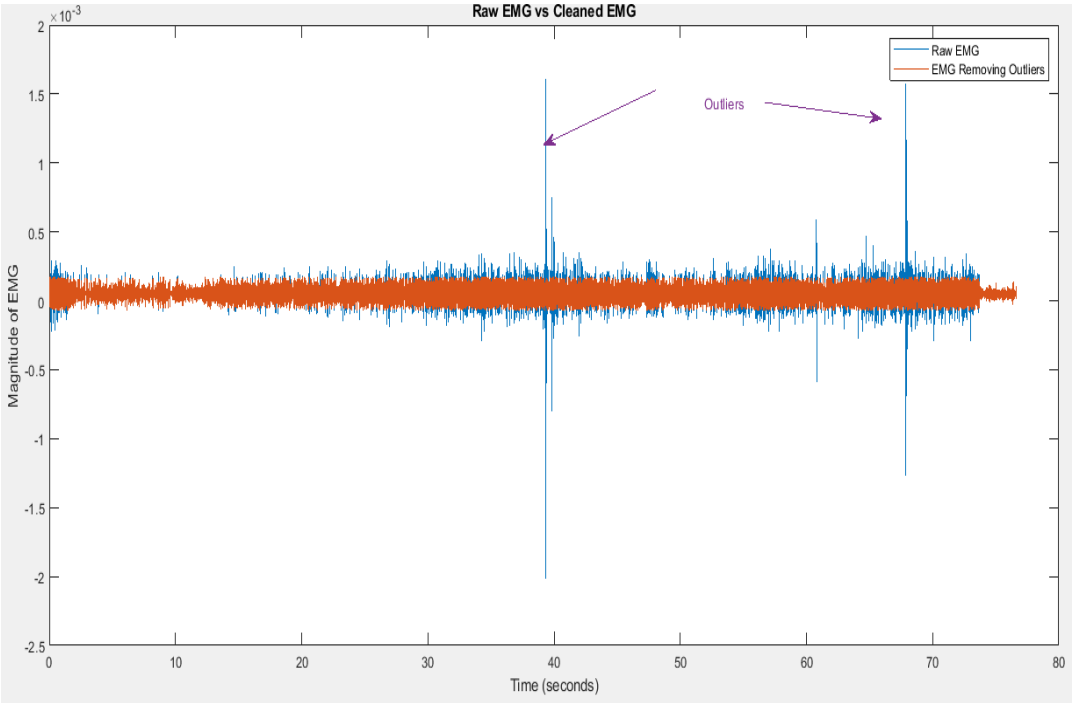

Figure 3.5: The sEMG signal before and after clearing the outliers.

3.2.5: Extraction of Features to be Used by Algorithm

The extraction of features is a crucial step in the study of muscle fatigue. Extracted features are used to train ML algorithms to depict and classify muscle fatigue effectively and intuitively. The muscle activity during fatigue is reflected by various features in the sEMG signal, as indicated in previous studies. The feature characteristics of an EMG signal are divided into two categories include: time and frequency domain characteristics. To detect fatigue accurately for the acceptance of clinical setting, it is essential to extract both time and frequency domain features simultaneously, as suggested by the coping review in chapter 2.

To extract features from a captured sEMG signal, we divided the entire signal into different epochs, with some epochs containing the non-fatigued portion of the EMG signal and other epochs covering the EMG signal with the fatigue portion. The concept of epoch analyzing EMG signal for fatigue shows superior performance than the time window technique because our participants

sustained their contractions for widely varying lengths of time to reach the fatigue state. Research has shown that window size significantly affects characteristic frequencies of the power spectrum (Waly et al., 1996). The study (Luebke et al., 2010) reported that the size of the time window used to extract features from EMG signals caused errors in the calculated power spectrum parameters (Waly et al., 1996). The authors in the study (Waly et al., 1996) investigated that by using window size to analyze EMG signal, the frequencies are overestimated, especially in the mid-range of the power spectrum. The mid-range frequencies in the spectrum carry the fatigue information of the EMG signal. This effect is evident in calculating median frequency, which is one of the critical parameters for indicating fatigue. Unlike the time window technique, the epoch technique solves the frequency overestimation dilemma and inconsistency assumptions for fatigue forecasting. The effectiveness of two different numbers of epochs (5 and 10) for detecting muscular fatigue using the ML method was also investigated in this study. In this study the entire EMG signal was divided into epochs, with the first epoch representing the EMG signal at the start of the test.

Features Extraction in Time Domain: Time-domain (TD) features often characterize fluctuations in EMG magnitude over the entire duration of contractions. TD features of EMG amplitude during isometric voluntary contractions are critical for carrying fatigue information. TD features can be derived and extracted directly from the raw EMG signal (Phinyomark et al., 2013). As a result, extracting and implementing the TD features require low computational requirements.

IEMG: The IEMG (Integrated EMG) considers time-domain attributes of the sEMG signal as a fatigue indicator. The mathematical definition of IEMG is the integral of the absolute value of the raw EMG signal (Yang et al., 2014). To extract the IEMG function, divide the EMG signal into different epochs and measure the region under the curve of the rectified EMG signal. The mathematical expression of the IEMG signal is denoted as

$$IEMG = \frac{1}{N}\sum_{i=1}^{N}|E_i| \tag{3.1}$$

Where E_i represents the sEMG sequence of each epoch within the length of N.

Normalized IEMG: Normalized IEMG depicts the variation of EMG signal from the beginning of the test to the fatigue state. The IEMG of the first epoch reflects the progression of the MVC test's beginning state hence $IEMG_{Epoch\ First}$ is used to normalize the IEMG of every updated epoch.

$$Normalized\ IEMG = \frac{IEMG_{Epoch\ new} - IEMG_{Epoch\ First}}{IEMG_{Epoch\ First}} \tag{3.2}$$

IEMG Trend: The IEMG trend indicates how the EMG trend varies from the start of the test to the progression of fatigue.

$$IEMG\ Trend = IEMG_{Epoch\ New} - IEMG_{Epoch\ Old} \tag{3.3}$$

RMS: The root mean square (RMS) amplitude is related to motor unit recruitment and muscle contraction. The magnitude of RMS changes with the recruitment of muscle fibres. RMS is calculated in each epoch with the following formula

$$RMS = \sqrt{\frac{1}{N}\sum_{i=1}^{N}{E_i}^2} \tag{3.4}$$

Where E_i represents the sEMG sequence of each epoch within the length of N

Normalized RMS: The RMS of the first epoch reflects the progression of the MVC test's beginning state hence $RMS_{Epoch\ First}$ is used to normalize the RMS of every updated epoch. The normalized RMS is calculated as follows.

$$Normalized\ RMS = \frac{RMS_{Epoch\ new} - RMS_{Epoch\ First}}{RMS_{Epoch\ First}} \quad (3.5)$$

RMS Trend: The RMS trend indicates variation of RMS value from the start of the test to the progression of fatigue.

$$RMS\ Trend = RMS_{Epoch\ New} - RMS_{Epoch\ Old} \quad (3.6)$$

Average Force: sEMG sensor also provides force data during the whole contraction periods. The average force magnitude of each epoch is a way to observe the changes of force magnitude during non-fatigue and fatigue states.

$$Average\ Force = \frac{1}{N}\sum_{i=1}^{N} E_{force} \quad (3.7)$$

the symbol E_{force} represents the force signal within the length of N in each epoch.

Features Extraction in Frequency Domain: The frequency domain (FD) feature extraction technique is an exceptionally attractive tool for muscle fatigue research. FD features are often derived from the statistical properties of the power spectrum of the EMG signal (Moniri et al., 2021).

Power Spectrum: Because of the nonlinearity and time-variability of the EMG signal, a power spectrum in the frequency domain is a popular method for obtaining detailed information about muscle activity during fatigue. A Fourier transform-based approach is used to generate the power spectrum of an EMG signal. The power spectrum was estimated by considering the real-part of the Fast Fourier Transform. The power spectrum can be used to extract a large number of features that exhibit a nominal relationship to the onset of fatigue

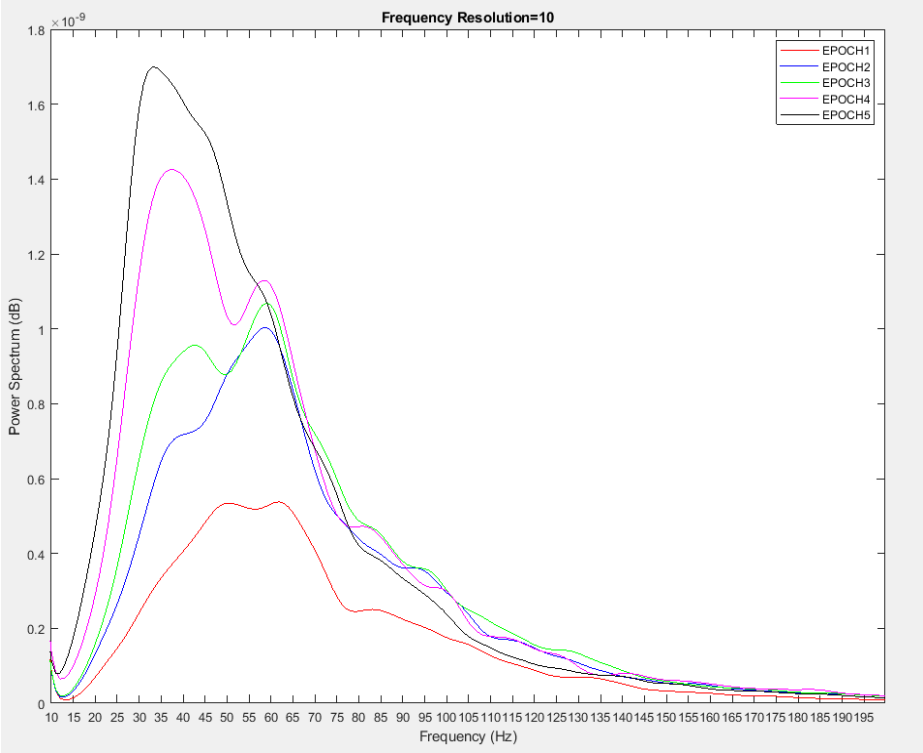

Figure 3.6: EMG power spectrum for five epochs technique during static isometric MVC.

Mean Frequency: Mean frequency (MF) is calculated from the power spectrum analysis of the sEMG signal. The mean frequency in the frequency domain is the frequency at which the average power in the spectrum was reached for each epoch or time interval.

$$MF = \frac{\sum_{m=1}^{N_f} Fm.\ P(Fm)}{\sum_{m=1}^{N_f} P(Fm)} \tag{3.8}$$

Where $P(F_m)$ is the power spectrum calculated using Fourier Transform with signal frequency F_m, and N_f is the Nyquist range in the power spectrum.

Median Frequency: The Frequency at which total power reaches a maximum of 50% is called the median frequency (MDF) (Yang et al., 2014). The MDF divides the power spectrum into two equal halves of the total spectrum.

$$MDF = \sum_{m=1}^{MDF} P(Fm) = \sum_{m=MDF}^{N_f} P(F_{MDF}) = \frac{1}{2}\sum_{m=1}^{N_f} P(F_m) \tag{3.9}$$

Median frequency can be calculated from the time-series signal using sampling frequency. The MDF can also be measured from the power spectrum analysis. We used both techniques to calculated MDF.

Instantaneous Frequency: The instantaneous frequency (IF) represents each frequency component added to the EMG signal at each period. The instantaneous frequency is calculated through the following equation

$$IF = \sum_{0}^{N_f} P(F_m) \tag{3.10}$$

The idea of instantaneous frequency shows which frequency components are added to the EMG power spectrum at each time in the frequency domain. Frequency components added due to movement artifacts and surrounding noise can be differentiated using the IF technique. For instance, when the frequency pattern of a specific application and muscle fatigue research is established, IF is very powerful to trace that previously identified pattern.

Instantaneous Mean and Median Frequency: Based on the protocols widely reported in the literature, the instantaneous mean and median frequencies were measured within the ranges from 20 to 150 Hz.

Peak's Prominence: The definition and concepts of the peak's prominence were taken from the MATLAB library. The prominence of a peak refers to how noticeable a peak's amplitude is relative to other neighboring peaks. A low, isolated peak may be more conspicuous than a higher peak surrounded by other large peaks.

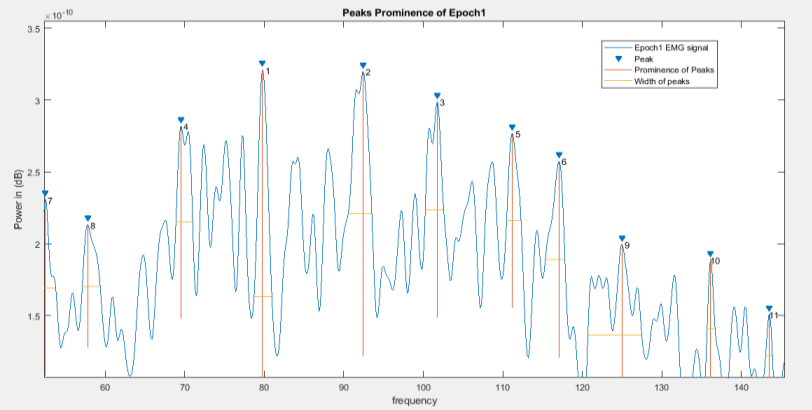

Figure 3.7: Prominence and width of peaks for epoch 1

Based on the prominence measure, the top five peaks were selected as extracted features. The top five most prominent peaks were measured for each epoch and tabulated in the feature dataset

Peak's Width: The width of the peaks is thought to play a crucial role as a fatigue feature. The half-power width of the sEMG signals associated with fast-twitch and slow-twitch fibres are more may differ from peaks arising in the spectrum that are associated with artifacts or unwanted noise. Recent research has shown that during fatigue, the width of the slow-twitch fibres peaks is considerably larger (65 to 70 %) than the width of the non-fatigue state. In brief, the greater the width peaks are associated with contributions from both fast-twitch or slow-twitch fibres peaks whereas narrower width peaks are more likely to be associated with the fatigue state where the fast twitch fibers are no longer active.

Peak's Frequency: At the beginning of the contraction, the EMG power spectrum exhibits two dominant peaks in the frequency domain associated with the activity of both the fast-twitch and slow-twitch fibres activation. But when fatigue occurs, only slow-twitch fibres peak remains in the spectrum.

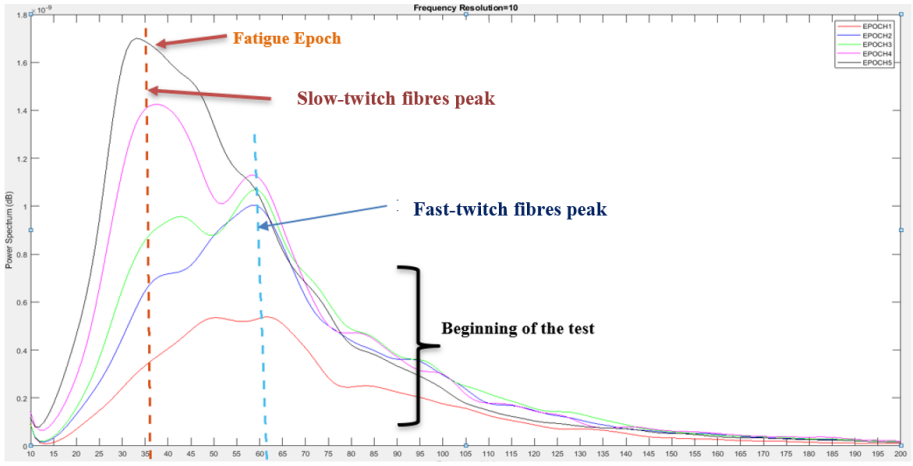

Figure 3.8: Illustration of slow-twitch and fast-twitch fibres peaks.

Peak's Power: The prominence of the five highest peaks were sorted for each epoch of the EMG signal. Following that, the power of five peaks was determined for each epoch and stored in the feature table for training the machine learning model.

3.2.6: Selection of Algorithm to Generate a Model

We conducted a comprehensive scoping review described in Chapter 2 to find the potential ML algorithms developing our proposed model. Based on the scoping review, four potential machine learning algorithms were selected that have ultimately potential to be deployed into a wearable device to detect muscle fatigue in real-time. These ML algorithms selected were:

A. Linear Discriminant Analysis (LDA)
B. Logistics Regression (LR)
C. Optimized Ensemble
D. Support Vector Machines (SVMs)

In order to select the most promising algorithm for the development of the model to detect muscle fatigue, each ML algorithm were applied to the sEMG dataset to train a model incorporating the features defined above. Their performance was then evaluated by applying the model to test data selected randomly from sEMG signals produced by the 96 participants. The following describes the functioning of each algorithm when integrated into the MATLAB Machine Learning development system.

LDA: LDA is a supervised-based ML algorithm that shows superior performance over principal component analysis (PCA) (Nugent et al., 2020). LDA is very light-resource and compact ML algorithm. The following linear transformation function manifests the classification where the LDA maps the data feature vector X (Al-Mulla et al., 2011a):

$$Y = W_0 + W^T X = \sum_{i=1}^{N} W_i{}^T X_i + W_0 \tag{3.11}$$

here, W_0 and W^T are determined by maximizing the ratio of between-class variance to within-class variance guarantee maximal separability (Al-Mulla & Sepulveda, 2010; Fisher, 1936). Using the formula, at least two or more classes of features can be extracted. We presented two classes here non-fatigue and fatigue. After classifying two classes correctly, we will add the fatigue class in our final documentation.

$$X = \begin{cases} Non - Fatigue & if \quad Y < 0 \\ Fatigue & if \quad Y > 0 \end{cases} \tag{3.12}$$

The signal will be classified based on the above logic (Al-Mulla et al., 2011a).

LR: Unlike linear regression (that requires a numerical dependent variable or output), logistic regression produces a binary output. A logistic function can map any value to an 'S' shaped curve whose extreme points are either 0 or 1. The following equation represents a logistic function,

$$Logistic\ function = \frac{1}{(1 + e^{-X})} \tag{3.13}$$

where X is a numeric value.

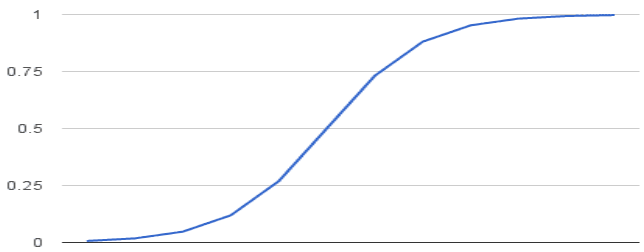

Figure 3.9: Logistic function for LR model.

Below is an example of a logistic regression equation,

$$Y = \frac{e^{(W_0 + W_1 * X)}}{1 + e^{(W_0 + W_1 * X)}} \tag{3.14}$$

or

$$P(X) = \frac{e^{(W_0 + W_1 * X)}}{1 + e^{(W_0 + W_1 * X)}} \tag{3.15}$$

Where, y is predicted output, W_0 is bias or intercept term and W_1 is coefficient for a single input value. The coefficients W_0 and W_1 are learnt from training data. Nonetheless, Logistic regression is a linear method where predictions are transformed using a logistic function.

For the classification of fatigue and non-fatigue from the new sample dataset, a threshold is required by the LR algorithm. The default threshold is 0.5 probability, but it can be adjusted based on if necessary. If a threshold or predicted probability is established such that P(X) > 0.5 or some other threshold, y = 1 and y=0 otherwise, then a classification algorithm can be established. For instance, in classifying an EMG signal as non-fatigue or fatigue, it can be established from LR that if x represents the input feature of a cell, then.

for P(fatigue) > threshold, y = 1, Hence the EMG signal is fatigue

and

for, P(fatigue| X) < threshold , y = 0, Hence the EMG signal is non-fatigue.

Optimized Ensemble: Ensemble learning is a particular type of machine learning paradigm where multiple models are trained to solve the same problem and combined to get better results (Anwar et al., 2014; Rocca, 2021; L. Zhang et al., 2019). In the optimized ensemble, there are four different algorithms commonly used: Bagging, GentleBoost, LogitBoost, Adaboost, RusBoost. We used the Bagging model for the optimized ensemble as other studies have shown comparatively better performance for datasets similar to sEMG.

Bagging is the homogeneous learner, learns independently from each other in parallel and combine. The model is defined by Lévesque et al. (Lévesque et al., 2016) for classification samples.

$$s_L(.) = \arg\max_k [card(l|w_l(.) = k)] \tag{3.16}$$

$$f(\gamma|E) = L(E \cup A(\gamma, \mathcal{X}_T)|\mathcal{X}_V), \tag{3.17}$$

The advantages of bagging are that they demonstrate parallelization capabilities. Since the various versions are fitted separately, extensive parallelization techniques may be used if required. The procedure for ensemble method is followed by the Lévesque et al. (Lévesque et al., 2016)

Optimized Ensemble procedure

Input: $\mathcal{X}_T, \mathcal{X}_V, B, m, A, \Gamma, L$
Output: H, history of models; E, the final ensemble

$H, G, E \leftarrow \varnothing$
for $i \in 1, \ldots, B$ **do**
  $j \leftarrow i \mod m$
  $E \leftarrow E \setminus \{h_j\}$
  $\mathbf{L}_i \leftarrow \{L(E \cup h|\mathcal{X}_V)\}_{h \in H}$
  $f(\gamma|E) \leftarrow \mathrm{BO}(G, \mathbf{L}_i)$ // Fit model
  $\gamma_i \leftarrow \arg\max_{\gamma \in \Gamma} a(\gamma|f(\gamma|E))$ // Next hypers
  $h_i \leftarrow \mathrm{A}(\mathcal{X}_T, \gamma_i)$ // Train model
  $G \leftarrow G \cup \{\gamma_i\}$
  $H \leftarrow H \cup \{h_i\}$
  $h_j \leftarrow \arg\min_{h \in H} L(E \cup \{h\})$ // New model at j
  $E \leftarrow E \cup \{h_j\}$ // Update ensemble
end for

There are a few options for aggregating the bagging models that were fitted in parallel (Lévesque et al., 2016; Qi et al., 2011; Rocca, 2021). For specific classification problems, the class outputted by each model can be thought of as a selection vote, and the ensemble model returns the class that receives the bulk of the selection votes, also known as hard voting (Lévesque et al., 2016). It is also possible to average the percentages of each class returned by all the models and hold the class with the highest average likelihood (this is known as soft voting) (Rocca, 2021; L. Zhang et al., 2019).

SVM: Support vector machine (SVM) is the most popular and widely used machine learning Algorithm (Patel, 2017). SVM is a set of supervised learning techniques used extensively for classification problems. SVM is one of Vapnik's most robust prediction methods (Boser et al., 1992; Cortes & Vapnik, 1995). The definition and mathematical illustrations of the SVM model were acquired from Brownlee's book of machine learning (Brownlee, 2019). The numeric input variables (*X*) data features or vectors (all columns) form an n-dimensional space. A hyperplane splits the input variable space (Brownlee, 2019). In SVM, a hyperplane is selected to best separate

the points in the input variable space by their class, either non-fatigue or fatigue class. These classes are also known as class 0 or class 1.

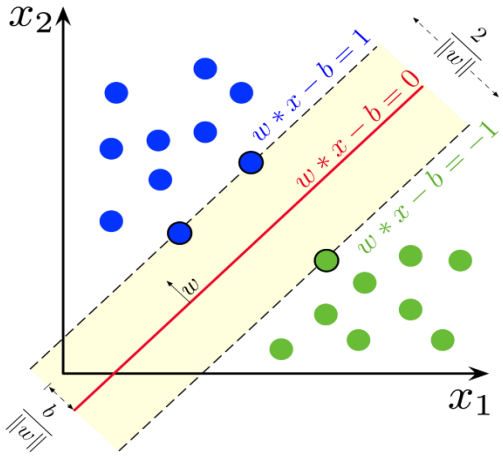

Figure 3.10: Maximum-margin hyperplane for an SVM trained with samples from two classes. Samples on the margin are called the support vectors (Image: Wikipedia).

It can be visualized as a line in two dimensions, and it is speculated that all the input points are separated by the line (Brownlee, 2019). For instances:

$$W_0 + (W_1 \times X_1) + (W_2 \times X_2) = 0 \tag{3.18}$$

Where the coefficients ((W_1 and W_2) that determine the slope of the line and the intercept (W_0) are found by the learning algorithm, and X_1 and X_2 are assumed to be the two input variables for illustration purposes (Brownlee, 2019). Based on the outcomes returned by the formula, the point belongs to either fatigue or non-fatigue class.

SVM Kernels: In practice, the SVM method is implemented using a kernel function. It is mandatory to define kernel function before initialization and to train the model. The inner products of the vectors equation for predicting a new input using the dot product between the input X_1, and each support vector (X_i) is measured as follows (Brownlee, 2019):

$$F(X) = W_0 + \sum_{i=1}^{n} a_i \times (X \times X_i) \tag{3.19}$$

This equation is used to measure the inner products of a new input vector (X) with all support vectors in training data. The coefficients $W_0$and a_i (for each input) can be predicted from the training data by the learning algorithm.

Three different types of kernel functions are commonly used for the SVM classification problem. The kernel defines the similarity or a distance measure between new data and the support vectors.

$$Linear\ kernel, \quad K(X, X_i) = \sum (X \times X_i) \tag{3.20}$$

$$Polynomial\ kernel, \quad K(X, X_i) = 1 + \sum (X \times X_i)^d \tag{3.21}$$

For the polynomial kernel, the degree, *d*, must be defined to the learning algorithm during the training session. This kernel also allows curved lines in the input space.

$$Gaussian\ or\ Radial\ kernel, \quad K(X, X_i) = e^{-gamma \times \sum (X - X_i^2)} \tag{3.22}$$

Like the polynomial kernel degree function, the gamma is needed to be defined during the training session. The gamma parameter lies between $0 < \text{gamma} < 1$ (Brownlee, 2019).

The kernel functions along with the polynomial and radial kernel transform the input vector or feature vector space into higher dimensions based on the nature of the sample problem is called the kernel trick.

Optimized SVM: The optimized SVM searches for the coefficients of the hyperplane, preparing best fitting the SVM model. The most suitable coefficients for fitting the SVM are searched through the iteration process in the optimized SVM classifier. After several iterations, the

algorithm automatically settles down to stabilize the coefficients by altering linear, polynomial, or radial kernel function (Brownlee, 2019). The whole process is continued by iteratively predicting the output and updating weights, slightly adjusting the desired classification results.

$$Output = Y \times (W_1 \times X_1) + (W_2 \times X_2) \tag{3.23}$$

Depending on the output result, two distinct updating techniques are applied. If the output value is more than 1, the training pattern was probably not a support vector. This indicates that the instance was not directly engaged in the output calculation, in which case the weights are reduced slightly:

$$B = (1 - \frac{1}{n}) \times B \tag{3.24}$$

Where B is the weight that is being updated (such as (W_1 or (W_2), on the other hand, n is the current updated iteration step. When an output is less than 1, then it is anticipated that the training sample is a support vector and must be updated to explain the data better.

$$B = \left(1 - \frac{1}{n}\right) \times B + \frac{1}{lambda \times n} \times (Y \times X) \tag{3.25}$$

Similarly, B is the weight that is being updated, n is the current iteration, and lambda is a parameter to the learning algorithm. The lambda is a learning parameter that is often set to small values such as 0.0001 or less. The procedure is continued until the error rate reaches a desired level, or until a large, defined number of iterations have been completed. Learning rates that are lower frequently need significantly longer training periods. The number of iterations in this learning process is a disadvantage.

Based on the MATLAB suggestion, the Bayesian optimizer applies this optimization classification to the positions of points from a Gaussian mixture model. In the optimization, an SVM classifier classifies data by finding the best hyperplane that separates data points of one class from those of

the other class based on the kernel trick (linear, polynomial, or radial kernel). The best hyperplane for an SVM means the one with the most significant margin between the two classes (Hastie et al., 2009). Margin means the maximal width of the slab parallel to the hyperplane that has no interior data points. The model will pick the best model by several iterations based on the best output fitting. In this research, the performance of the SVM with each three-kernel function tested and evaluated.

3.2.7: Training, Validation and Testing of Selected Algorithms

To develop a model that can be embedded in a wearable device to detect fatigue during a sustained single 80% MVC, the most promising algorithm needs to be selected based on its performance accuracy using the values obtained for the features (inputs to the model).

To evaluate performance accuracy, all of the selected algorithms were trained using features-extracted from the dataset. No single machine learning algorithm performs better for every problem. The challenge is to identify the best algorithm for the specific problem by trial-and-error comparing the performance of each algorithm.

We developed and implemented the training paradigm of all algorithms in both MATLAB and Python environments. Before training, we randomized the entire dataset into training, validation, and testing sets. The optimal ratio for dividing the dataset into training, validation, and testing is as follows.

Training=70%

Validation=15%

Testing=15%

Validation of Each Algorithm: Validation accuracy is one of the most significant performance metrics for selecting a promising algorithm (Suhm, 2021). To check the performance metrics, each algorithm was trained on the entire dataset, including the training and validation data. We used k-fold cross-validation for validating the training accuracy of each algorithm on the training and validation dataset. The k-fold cross-validation is a popular technique for investigating ML algorithms' performance in such kind of moderate-size dataset (Total 480 observations). In k-fold cross-validation, we tested the validation performance of each algorithm on different value of K. However, the k=5 technique has been fitted well among other folds. As a result, a 5-folds cross-validation technique was applied to evaluate the validation accuracy of all selected ML algorithms on the classification of fatigue.

Firstly, we represented a single algorithm's validation and testing performance in detail in the result section. Therefore, the performance was illustrated comprehensively of the algorithms that obtained the highest validation and testing accuracy for classifying fatigue from the sEMG signal. The total number of observation tables, confusion matrix, ROC curve, classification error plot, overall accuracy were shown thoroughly in the result section. Finally, we added an evaluation Table 3.2 showing the validation and testing performance of each algorithm.

Testing of Each Algorithm: After training each algorithm on the dataset for classification of muscle fatigue and validating the performance of each, it is time to test how each algorithm performs on the utterly new dataset. To test the performance of each algorithm, we inputted a new testing dataset. The dataset is entirely unknown to the algorithms and was not used for training purposes. A total of 15% of the data was used as a testing dataset. Similar to the validation stage, the detailed performance of a single algorithm was represented in the result section. The model acquired high testing accuracy was shown in detail. The testing performance of that algorithm,

including the total observations table, confusion matrix, ROC curve for fatigue and non-fatigue conditions, were shown in the result section. After that, the testing performance of each algorithm was listed in Table 3.2.

Based on the validation and testing accuracy of each algorithm as well as its adaptiveness in the embedded devices, are the significant consideration to select a most promising algorithm. The proposed model will be developed using the most promising algorithm. Therefore, the developed model can be embedded in a wearable device to detect in real-time during isometric voluntary contraction.

3.2.8: Selection Procedure of the Most Promising Algorithm and Development of the Model: Firstly, we trained each algorithm using all of the 35 features extracted from the sEMG signal. However, in practice it is challenging to process 35 features using current embedded devices.

At the same time, not all features are equally important for determining fatigue. Furthermore, having too many features increases the computing complexity of wearable devices and leads to overfitting (Suhm, 2021). The feature selection approach was undertaken to select the most relevant features describing fatigue patterns and remove unnecessary or redundant features. As a result, it is essential to select the most relevant features that shape a fatigue pattern.

Currently, stepwise regression, PCA, are decision trees, are primarily used to select features. But these models are too computationally large for deployment in an embedded device. So instead, we applied Neighbourhood Component Analysis (NCA) technique to select the most relevant features that contributed to following the fatigue pattern. NCA is an automated method for selecting a small subset of features that hold the most crucial information for fatigue classification while reducing redundancy among the features chosen. The principle of the NCA algorithm was described in

(Kavya et al., 2020). Because of the suitability of NCA to the embedded devices, it is called the embedded feature selection model.

NCA picked total 14 features out of 35 features. Using the 14 features, each algorithm trained and tested. After training, the performance of each algorithm was validated. The classification performance of each algorithm depends on the validation and testing accuracy of fatigue classification.

To select the most promising algorithm based on the fatigue classification performance and adaptability to a wearable device, a criteria table was created. Table 3.4 shows the selection criteria for a promising algorithm. The selection criteria includes fatigue prediction speed, training speed, memory usage, general assessment to the application problems, and fatigue classification performance. Based on Table 3.3, the OSVM is the most promising algorithm for developing our proposed model embedding in a wearable device to detect fatigue during a sustained isometric contraction.

In addition, the 14 features also create computation complexity to most of the embedded device for processing and detecting fatigue in real-time. Therefore, the performance of the OSVM based model again tested with most 5, 3, and 1 feature. Table 3.4 described the performance of the current model with reduced numbers of features.

3.3: Results

3.3.1: Identifying the Primary Feature Set

Hypothesis about IEMG and RMS Magnitude during Fatigue: After close observations of the magnitude of IEMG and RMS on all participants' data, we investigated the magnitude changes of these two features during fatigue.

Changes of IEMG during Fatigue: We investigated how the magnitude of IEMG changes from non-fatigue state to fatigue state. The IEMG variation during non-fatigue and fatigue state was hypothesized after thoroughly observing the 100 participants' data.

A)

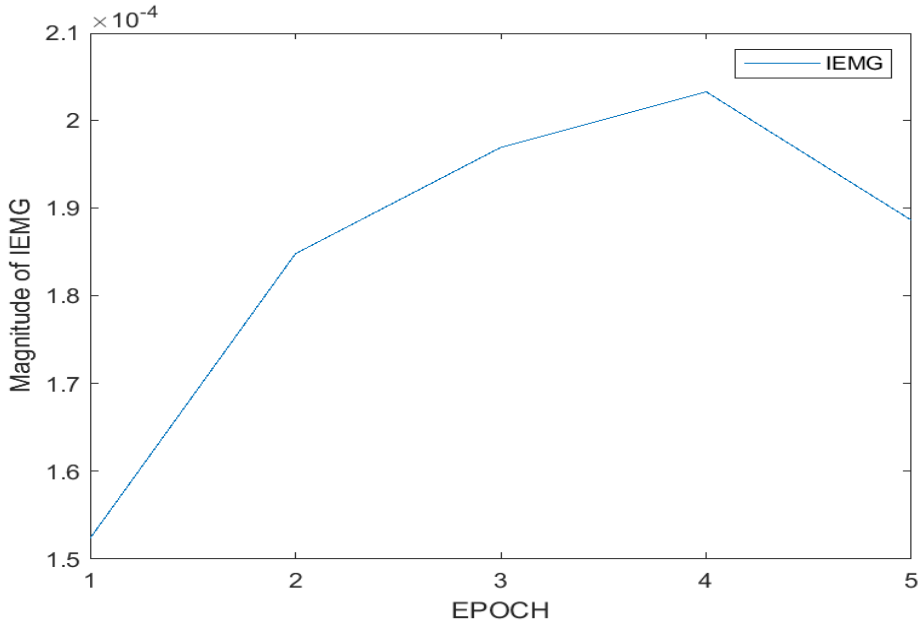

B)

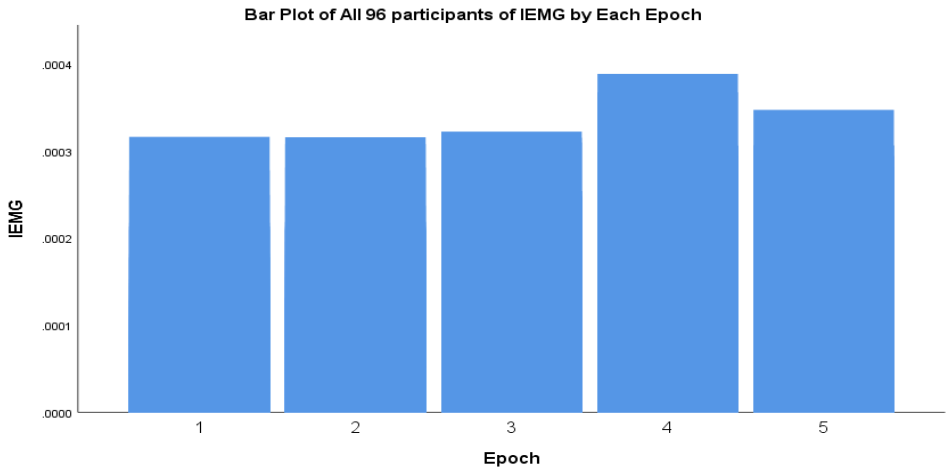

C)

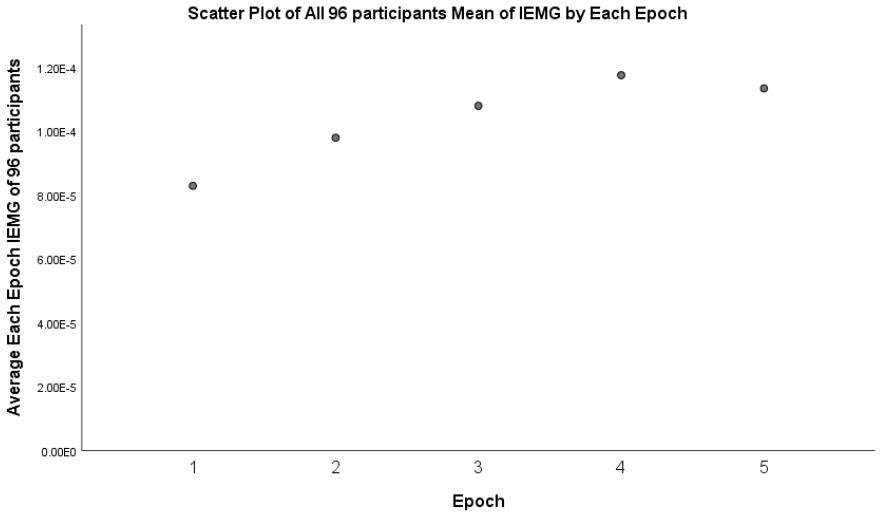

Figure 3.11: A) showed how the magnitude of IEMG changes on each Epoch for one participant data, B) Bar plot of all 96 participants IEMG on each Epoch, C) Scatter plot of all 96 participants Average IEMG by each Epoch.

Figure 3.11 shows the changes of magnitude of IEMG vs epoch for three different maps. The IEMG variation demonstrates the increment of EMG magnitude from epoch 1 to epoch 5. For each case, epoch 5 contains the fatigue signal. Obviously, the magnitude of IEMG is increment during the progression of the test and in the fatigue state. Figure 3.11 (A) is the individual IEMG plot concerning the epoch. Figure 3.11 (B) is the bar plot of each of the participants' IEMG on each epoch and depicts the increasing trend of IEMG magnitude during the progression of the fatigue. The average IEMG on each epoch of all 96 participants was shown in Figure 3.11 (C) as a scatter plot. The scatter plot also shows the increasing trend of IEMG for sustained isometric maximum voluntary contraction. We conducted a paired-sample t-test shown in Figure 3.12 to validate our hypothesis of increment of IEMG magnitude during fatigue.

Paired Samples Statistics

		Mean	N	Std. Deviation	Std. Error Mean
Pair 1	IEMG_5	.0001133430	96	.0000781318	.0000079743
	IEMG_1	.0003160348	96	.0000000000	.0000000000
Pair 2	IEMG_5	.0001133430	96	.0000781318	.0000079743
	IEMG_2	.0000978989	96	.0000664476	.0000067818
Pair 3	IEMG_5	.0001133430	96	.0000781318	.0000079743
	IEMG_3	.0001078875	96	.0000743002	.0000075832
Pair 4	IEMG_5	.0001133430	96	.0000781318	.0000079743
	IEMG_4	.0001174660	96	.0000837496	.0000085477

Paired Samples Test

		Paired Differences					t	df	Sig. (2-tailed)
		Mean	Std. Deviation	Std. Error Mean	95% Confidence Interval of the Difference Lower	Upper			
Pair 1	IEMG_5 - IEMG_1	-.000202692	.0000781318	.0000079743	-.000218523	-.000186861	-25.418	95	.0000000000
Pair 2	IEMG_5 - IEMG_2	.0000154441	.0000326358	.0000033309	.0000088314	.0000220567	4.637	95	.0000112876
Pair 3	IEMG_5 - IEMG_3	.0000054555	.0000257700	.0000026301	.0000002340	.0000106770	2.074	95	.041
Pair 4	IEMG_5 - IEMG_4	-.000004123	.0000228876	.0000023360	-.000008760	.0000005145	-1.765	95	.081

Figure 3.12: Paired-Sample t-test for observing the significant incremental of IEMG magnitude during fatigue state.

In the paired-sample test, IEMG_5 is the magnitude of IEMG for epoch 5, which is also the fatigue epoch. And the rest of the symbols denote accordingly. The significance level of the test statistics for IEMG_5 and IEMG_2, alongside the difference of IEMG_5 and IEMG_3, is extreme for both cases compared to the critical value (p=0.05). As a result, the null hypothesis is rejected, and there is a significant difference in the IEMG magnitude between epoch 2 and epoch 3. The result concluded that the magnitude of IEMG is increasing in the progression of the test. Epoch 1 indicates the beginning of the test where movement artifacts affect the magnitude, so we are not interested in epoch 1 IEMG. Further, the statistical significance level of the IEMG difference between epoch 5 and epoch 4 is less than the critical value; hence there is no significant difference between these two epochs' IEMG magnitude. Consequently, the IEMG magnitudes of epochs 4 and 5 are nearly equal and greater than the IEMG magnitude of epoch 3. Finally, the following hypothesis is concluded for IEMG magnitude while fatigued.

"For a single sustained static isometric maximum voluntary contraction, the magnitude of the IEMG increases in the progression of the test until fatigue state before the participants give up the test".

Changes of the RMS during Fatigue: The root means square (RMS) magnitude of the EMG signal is also a significant feature in the time domain. As the RMS magnitude is carefully observed at each epoch of all 96 participants' data, it is apparent that the RMS magnitude increases when the test progresses and up to the fatigue state.

A)

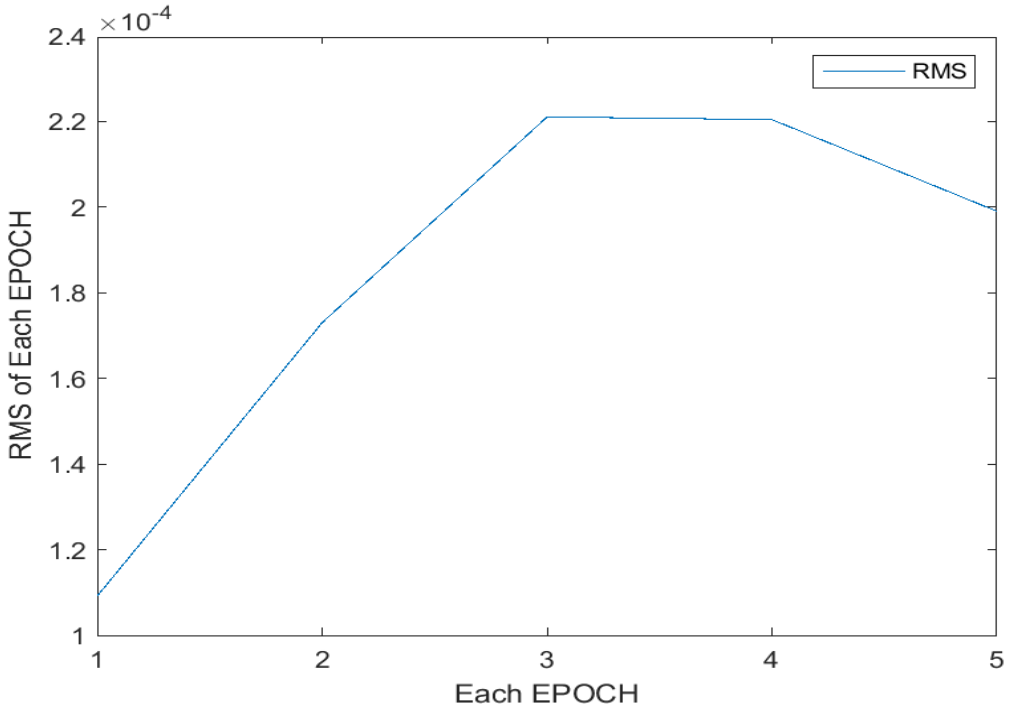

B)

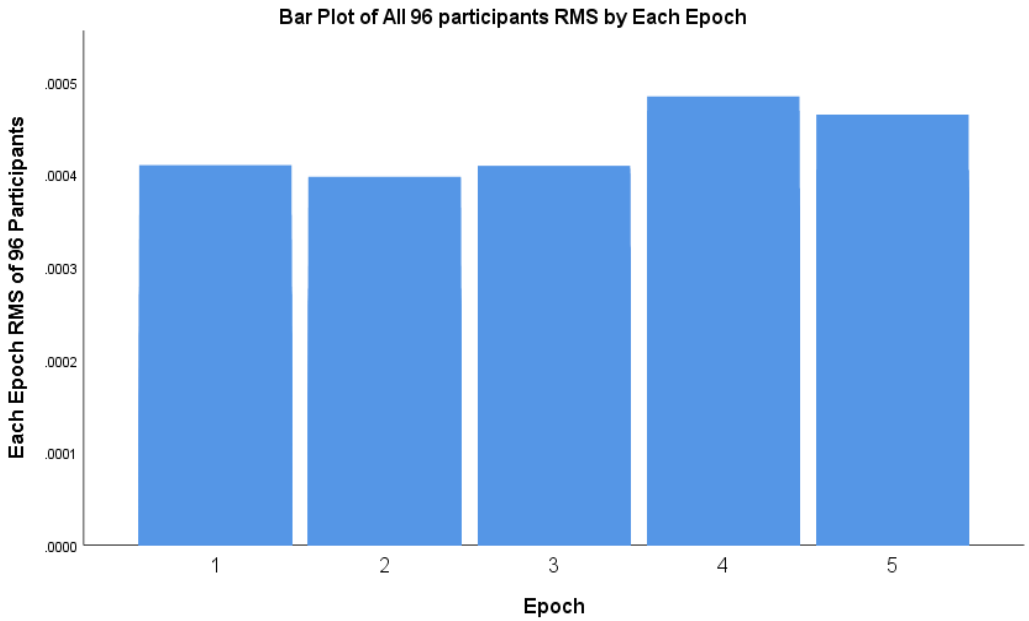

C)

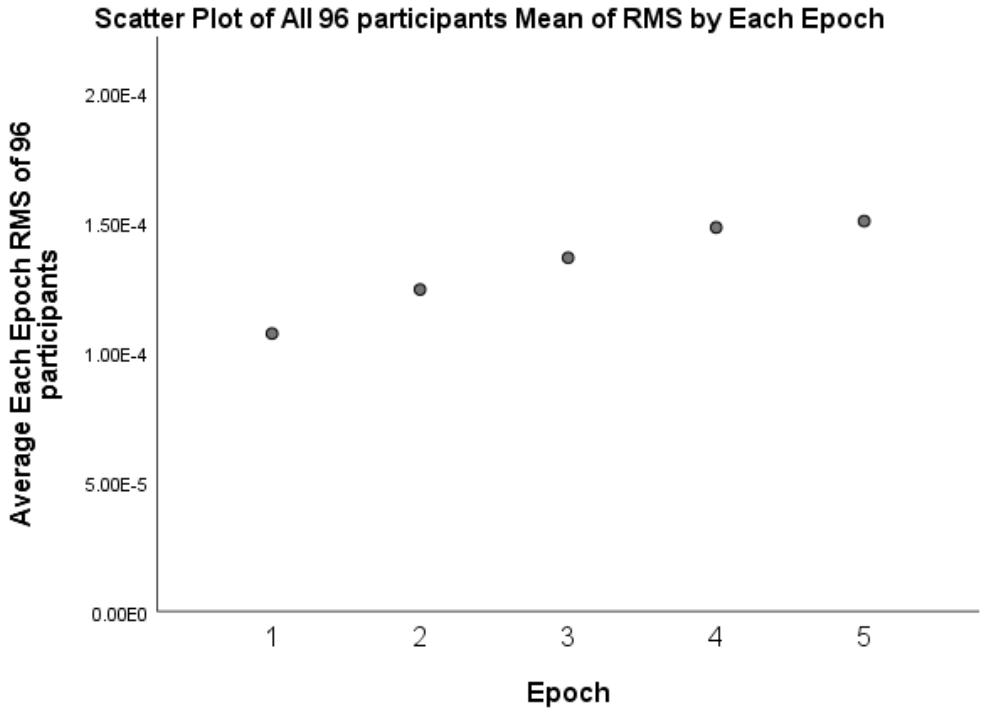

Figure 3.13: A) showed how the magnitude of RMS changes on each Epoch for one participant data, B) Bar plot of all 96 participants RMS on each Epoch, C) Scatter plot of all 96 participants Average RMS by each Epoch.

Paired Samples Statistics

		Mean	N	Std. Deviation	Std. Error Mean
Pair 1	RMS_5	.0001508484	96	.0001065678	.0000108765
	RMS_1	.0001073470	96	.0000790801	.0000080711
Pair 2	RMS_5	.0001508484	96	.0001065678	.0000108765
	RMS_2	.0001244067	96	.0000850585	.0000086813
Pair 3	RMS_5	.0001508484	96	.0001065678	.0000108765
	RMS_3	.0001366807	96	.0000947806	.0000096735
Pair 4	RMS_5	.0001508484	96	.0001065678	.0000108765
	RMS_4	.0001483608	96	.0001061278	.0000108316

Paired Samples Test

		Paired Differences					t	df	Sig. (2-tailed)
		Mean	Std. Deviation	Std. Error Mean	95% Confidence Interval of the Difference Lower	Upper			
Pair 1	RMS_5 - RMS_1	.0000435014	.0000498206	.0000050848	.0000334068	.0000535960	8.555	95	.0000000000
Pair 2	RMS_5 - RMS_2	.0000264417	.0000395993	.0000040416	.0000184182	.0000344653	6.542	95	.0000000030
Pair 3	RMS_5 - RMS_3	.0000141677	.0000295078	.0000030116	.0000081889	.0000201466	4.704	95	.0000086357
Pair 4	RMS_5 - RMS_4	.0000024876	.0000207800	.0000021208	-.000001723	.0000066980	1.173	95	.244

Figure 3.14: Paired-Sample t-test for observing the significant incremental of RMS magnitude during fatigue state.

The significance difference level between epoch RMS_5 and the other four epochs RMS was measured using a paired-sample t-test. The statistical significance of the difference between RMS_5 with RMS_1, RMS_2, RMS_3 is extreme for every three cases compared to the critical value (p=0.05). As a result, the null hypothesis is rejected, and there is a significant difference in the RMS_5 magnitude with RMS_1, RMS_2, and RMS_3. It is determined that the magnitude of RMS is increasing in the progression of the test. We did not find any statistically significant difference between RMS_5 and RMS_4. Epoch 5 is the fatigue signal, and the participant did not carry the test any longer in this epoch where EMG fell zero levels. As a consequence, the RMS magnitudes of epochs 5 and 4 are nearly equal and are greater than the RMS magnitude of epoch 3. Finally, the following hypothesis is concluded for the RMS magnitude while fatigued.

"For a single sustained static isometric maximum voluntary contraction, the magnitude of the RMS increases in the progression of the test until fatigue state before the participants give up the test".

Pattern of Time Domain Features During Fatigue: We paid more attention to all possible time and frequency domain features that could aid muscle fatigue research in developing a robust real-time wearable device. Owing to the larger dataset, the population samples for the sEMG-based muscle fatigue study will be followed by our experimental findings.

Analogous to the IEMG and RMS features, the changes of the normalized IEMG and RMS as well as the trend of IEMG and RMS demonstrated in Figure 3.15, are valuable characteristics and highly correlated. The magnitude of the EMG changes in the fatigue state; hence, RMS and IEMG also change. As a consequence, these characteristics measurements can be used to describe the fatigue state in detail. Figure 3.15 shows the rising and falling nature of the EMG magnitude during the whole test session. The average force signal likewise displays the alternating behaviour and the magnitude of the EMG and the force signal, increasing

at the beginning of the test, the rate of the motor unit recruitment increases to maintain the required force, similarly, as a result the EMG amplitude rises abruptly. However, the motor unit recruitment continues up to 80% MVC for biceps brachii muscle. Subsequently, there is no recruitment of motor unit after 80% MVC, and fatigue occurs, which declines the EMG signal and force magnitude immediately. the individual can be no longer able to sustain the task and quickly abandons.

Despite exerting maximum effort, the person could not sustain the test. It is concluded that the magnitude trend of the IEMG and RMS increases up to the cession of the test by the individuals.

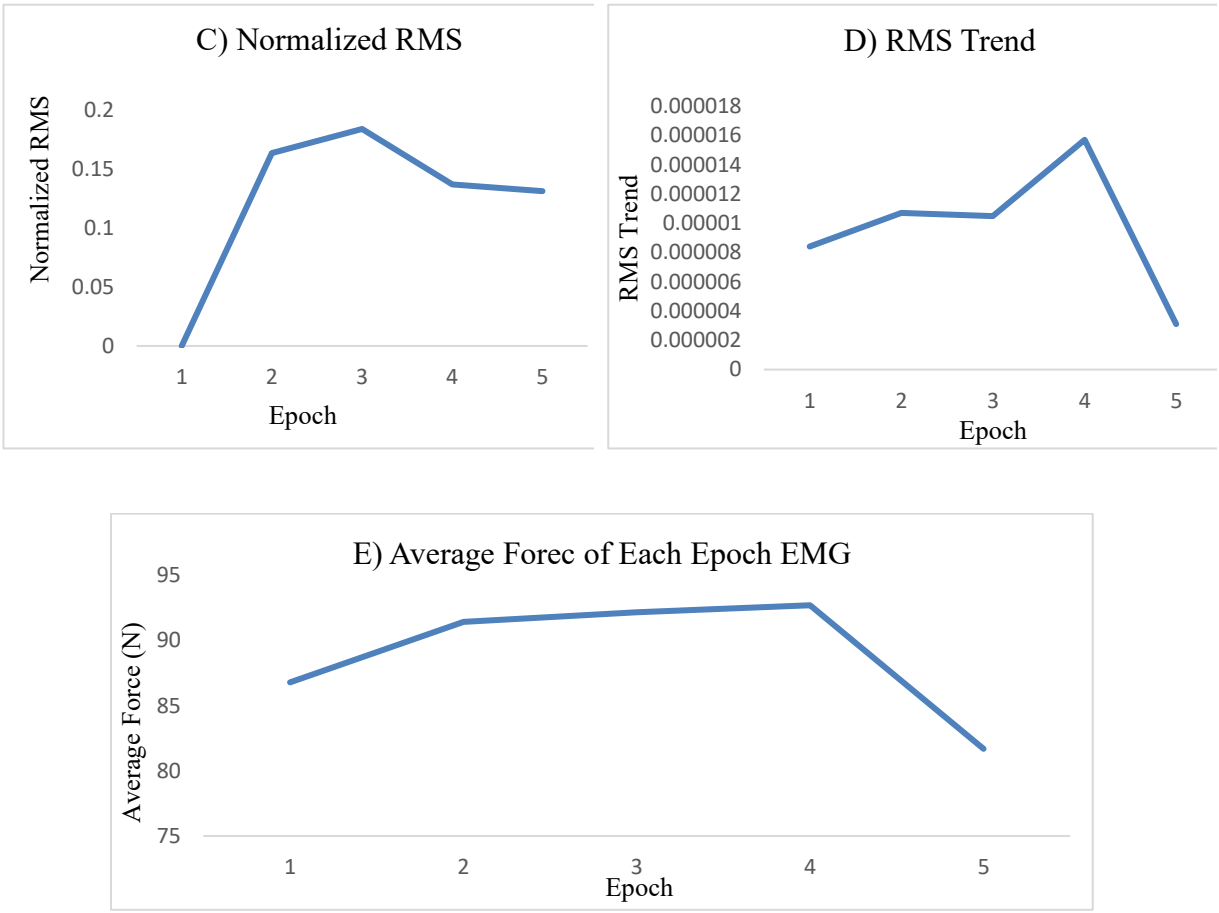

Figure 3.15: TD features for fatigue indicators and represented the changes of the pattern from beginning of the test to the fatigue state.

Pattern of Frequency Domain Features During Fatigue

Instantaneous frequency: Instantaneous frequency (IF) can be observed in the time domain. For each time interval, it displays the frequency components that add to the signal. A specialist can diagnose fatigue conditions by observing IF frequencies using current knowledge. IF aids in the rapid modelling of an individual's non-fatigue range and MVC amount that the user can lift. In addition, it can facilitate measuring the instantaneous mean and median frequency. Besides, the average of the IF depicts the fatiguing nature as the mean and median frequency does.

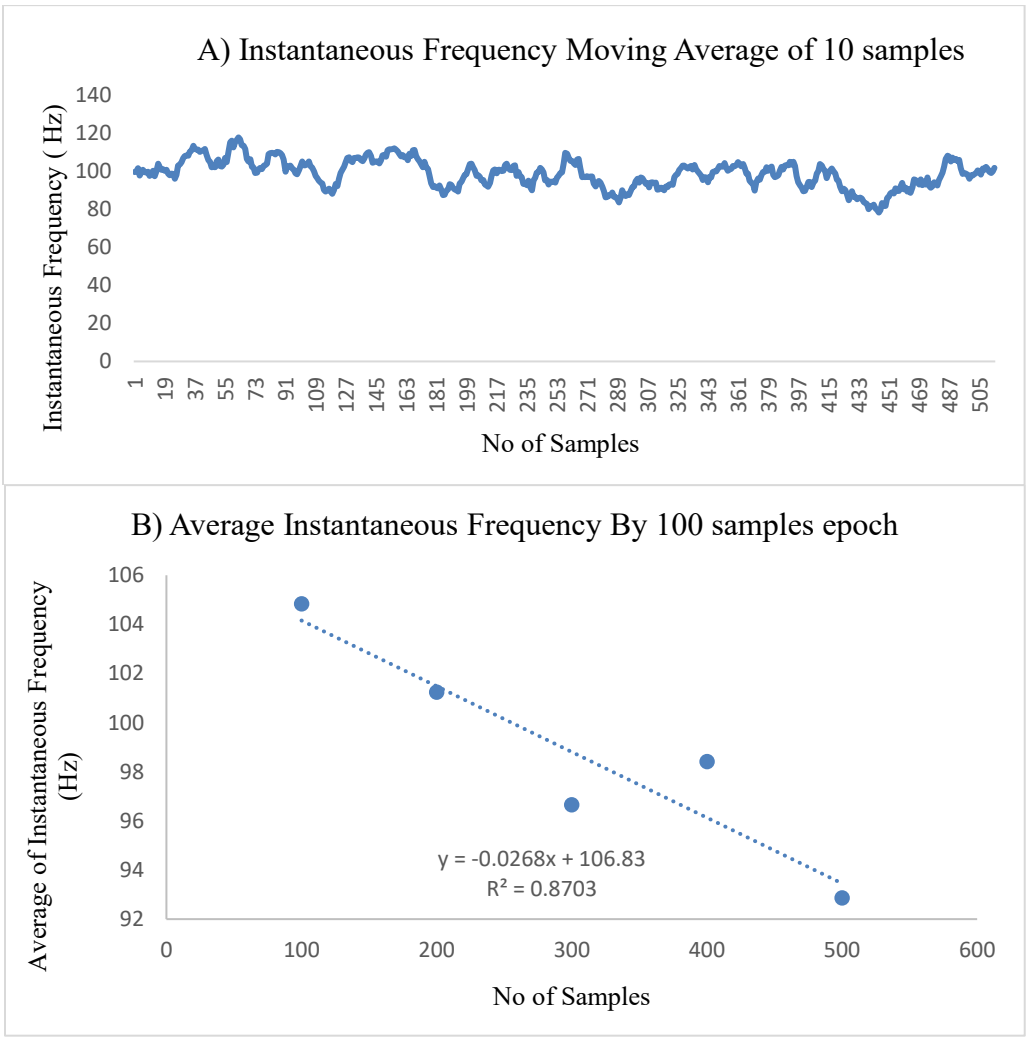

Figure 3.16: A) Moving Average of instantaneous frequency, B) Average of 100 samples instantaneous frequency

Mean frequency: The mean frequency is one of the dominant features of fatigue forecasting in the frequency domain. The plot of the instantaneous mean frequency (IMF) and epoch mean frequency (MF) reveals the shift of the power spectrum to the lower frequency components during fatigue. Epoch 5 is the fatigue state of the EMG signal. Both IMF and MF decline in the epoch 5 positions. During contraction, the slow-twitch fibres contribute to low-frequency components that range from 20 to 60 Hz. In contrast, the fast-twitch fibres are the high-frequency components and range from 60 to 120 Hz. Throughout the beginning of the test, both fibres remain hences increase

the mean frequency, but only slow-twitch fibres sustain the test and decreses the mean frequency at the fatigue state.

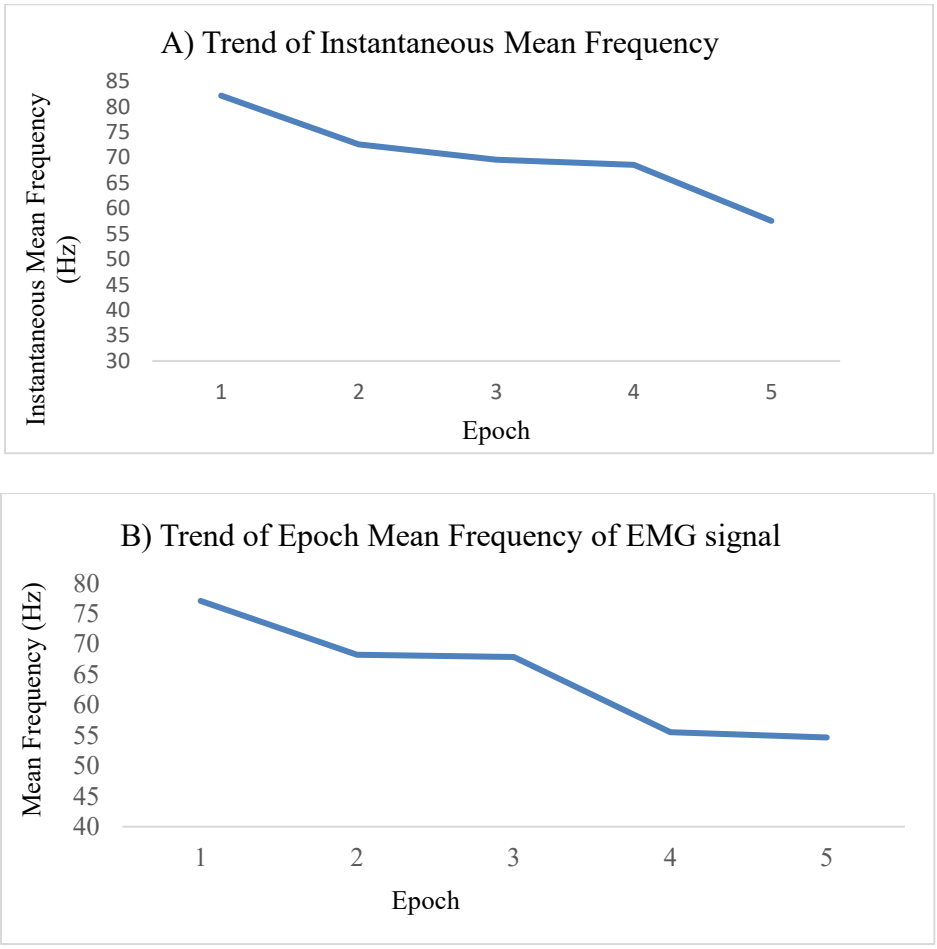

Figure 3.17: A) Trend of instantaneous mean frequency, B) Trend of epoch mean frequency

Median Frequency: Resembling the mean frequency, median frequency is the most used feature in the literature as an indicator of fatigue. The instantaneous median frequency (IMDF) and epoch median frequency (MDF) simultaneously shows the declining trend in the fatigue condition shown in Figure 3.20 A) and B). it is well-established that biceps brachii muscles have a wide range of motor unit recruitment up to 80% MVC (Orizio et al., 2003; Qi et al., 2011). Slow fibres in the biceps brachii are mainly recruited below 25% MVC, and they contribute low-frequency

components to the power spectrum. The fast fibres motor units are rapidly recruited up to 60% - 80% MVC and increases the frequency in the spectrum for isometric contraction. On the contrary, increasing the firing rate of active motor units is commonly believed to be responsible for a forced rise above this stage (Orizio et al., 2003; Qi et al., 2011). As fast-twitch fibres fatigue first, while the slow-twitch fibres remain, the power spectrum shifted to the lower frequency components. As a result, the IMDF and MDF both reduce fatigue conditions.

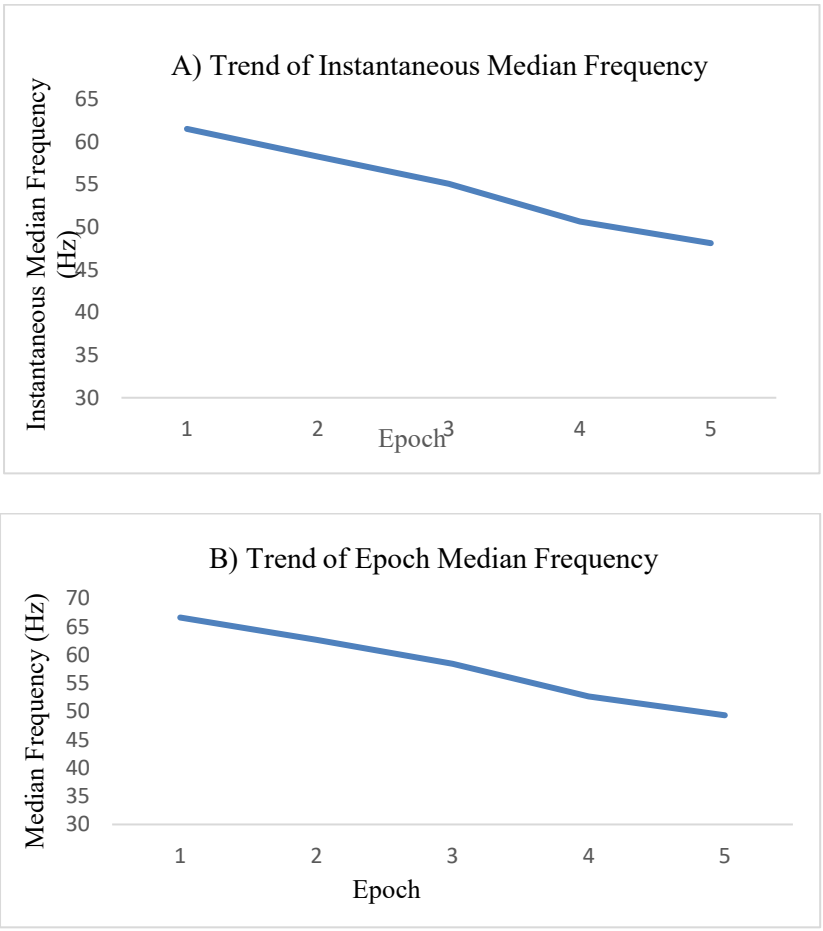

Figure 3.18: A) Trend of instantaneous median frequency, B) Trend of epoch median frequency

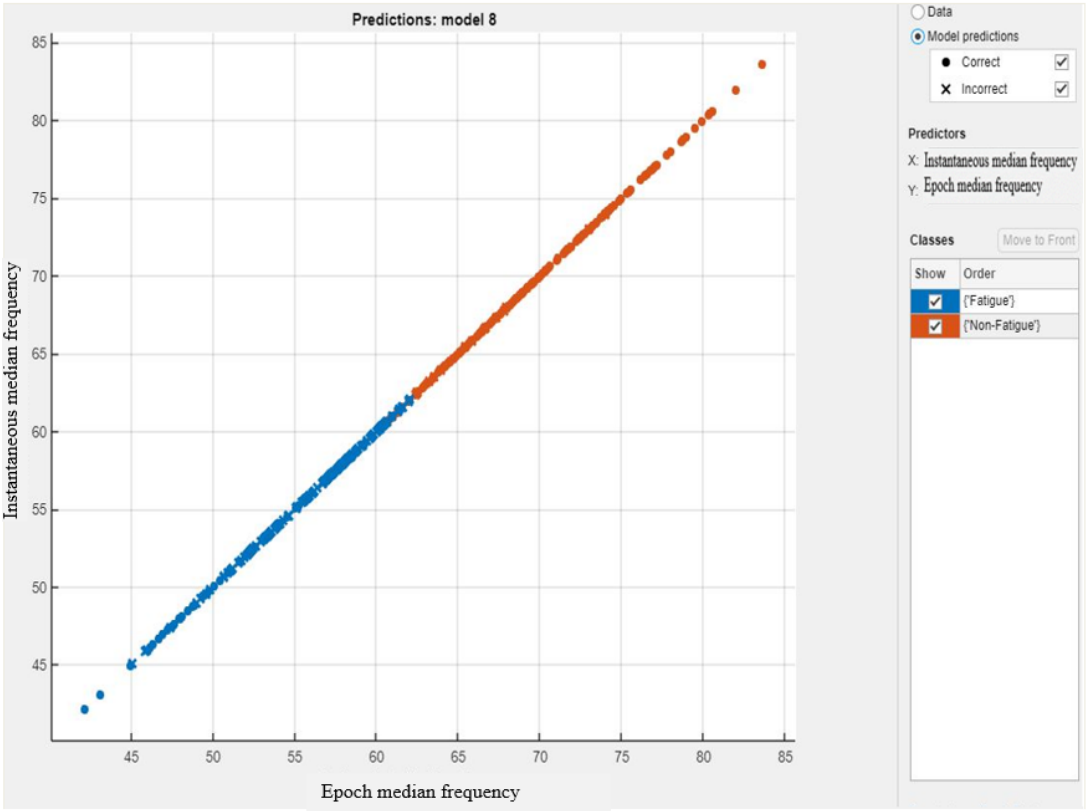

Figure 3.19: Instantaneous median frequencies of all 96 participants and clear indicated the ranges of the instantaneous median frequencies for fatigue and non-fatigue state.

Figure 3.19 depicts a clear demonstration of how the IMDF characteristics change as a result of fatigue. The scatter plot of instantaneous median frequencies for fatigue and non-fatigue conditions for 96 participants is seen below. Both frequency components transferred to lower components during fatigue, while higher frequencies suggest a non-fatigue state. In the fatigue state, the IMDF varies from 35 to 63 Hz, which is the slow fibres recruitment range, and in the no-fatigue state, it ranges from 65 to 90 Hz. At the beginning of the test, all together, fast, and slow fibres contribute to sustaining the task or load and the power spectrum shifts to a higher frequency region. However, only slow fibres remain to sustain the task when fatigue occurs, and the power spectrum steps down to the lower region. The scatter plot shows that the median frequency decline in the fatigue condition and power spectrum changes to lower frequency components.

Peak frequencies vs mean & median frequencies

A)

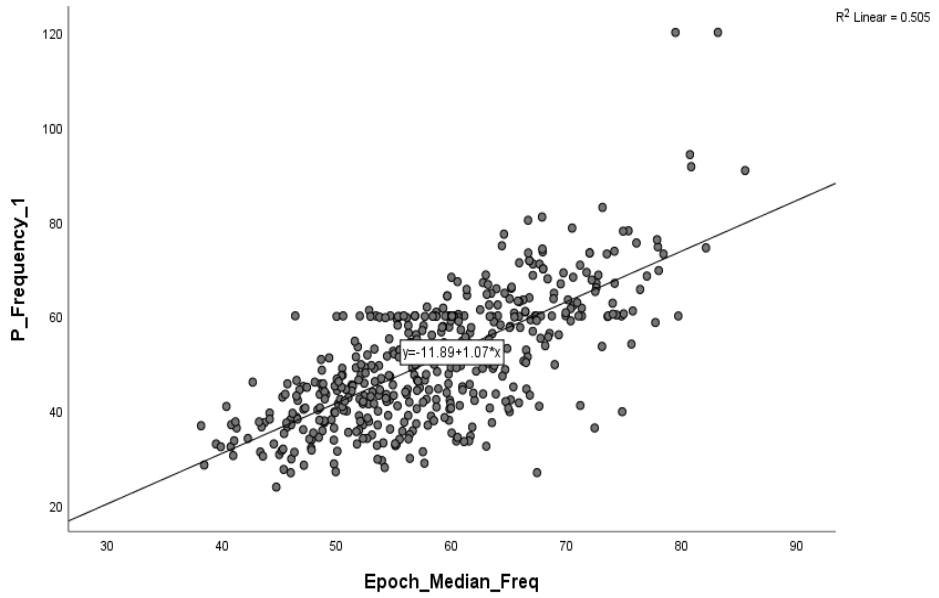

B)

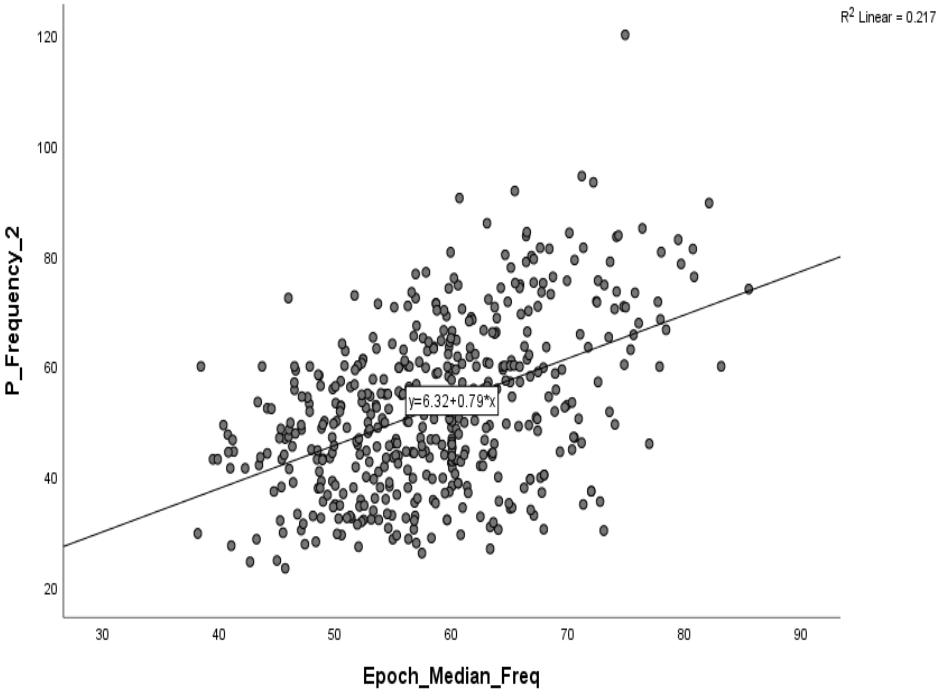

C)

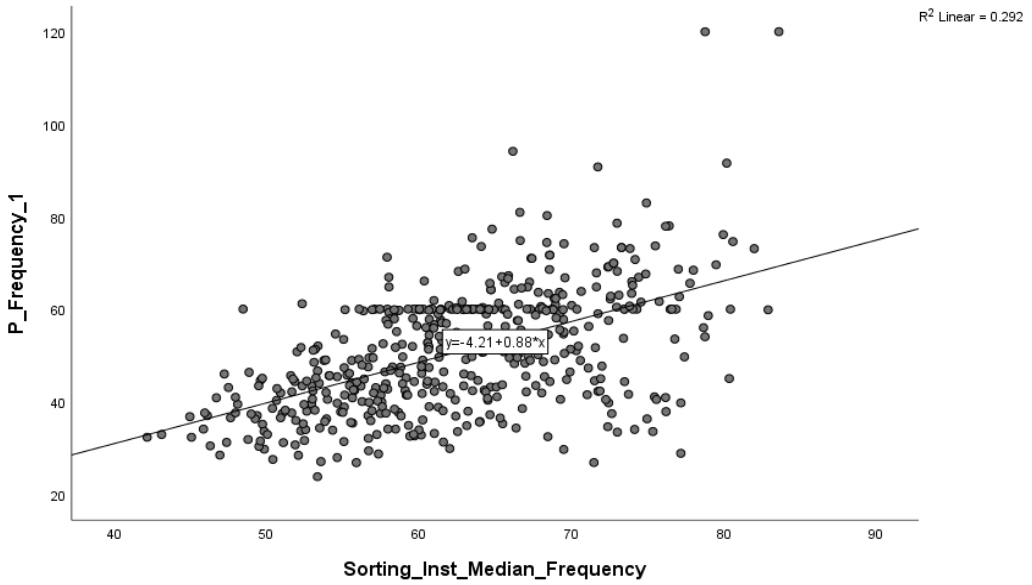

D)

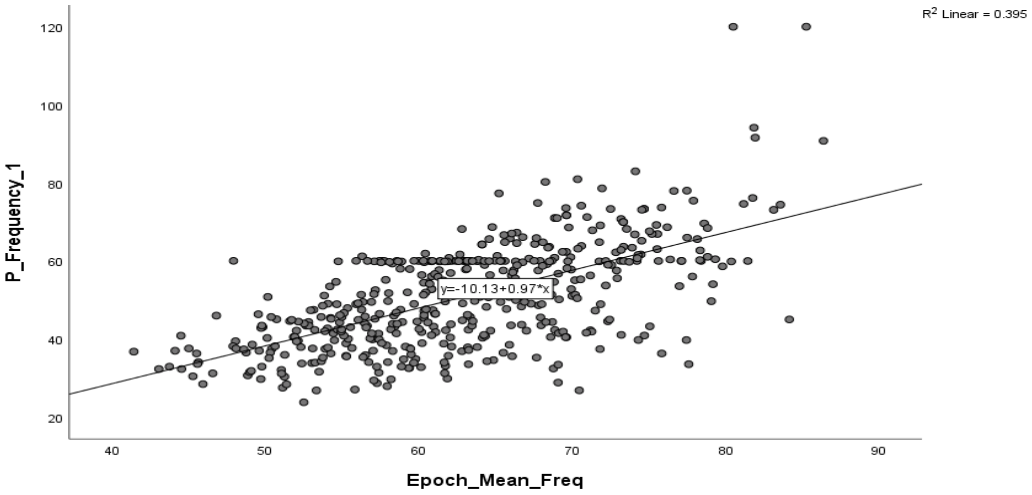

Figure 3.20: Correlation between A) Peak_frequency_1 vs Epoch median frequency, B) Peak_frequency_2 vs Epoch median frequency, C) Peak_frequency_1 vs Instantaneous median frequency, and D) Peak_frequency_1 vs Epoch mean frequency for all 96 participants.

We sorted five peaks' frequencies for each epoch according to the peak's prominence as a fatigue function of the EMG signal in our experiment. There is almost certainly a connection between each peak frequency and the mean and median frequency. Among others, peak_frequency_1 has the strongest association with the mean and median frequency. The correlation coefficient between peak_frequency_1 and median frequency is nearly 50%, indicating that peak_frequency_1 matches median frequency in at least 50% of cases. Furthermore, there is an approximately 40%

correlation coefficient with the mean frequency. Definitively, among the other peaks' frequencies, peak_frequency_1 is suggested as the most prevalent attribute as a measure of fatigue.

Aggregated Power Spectrum from the Date of All 96 Participants: After classifying the fatigue samples using the current model, we plotted the power of all 96 participants from the recorded sEMG signals during non-fatigue and fatigue conditions. The motion of this analysis is to observe what happens in power inserted by individuals during non-fatigue and fatigue conditions. The orange curve shows the aggregated power for all 96 participants during fatigue state; in contrast, blue depicts the aggregated power for non-fatigue conditions.

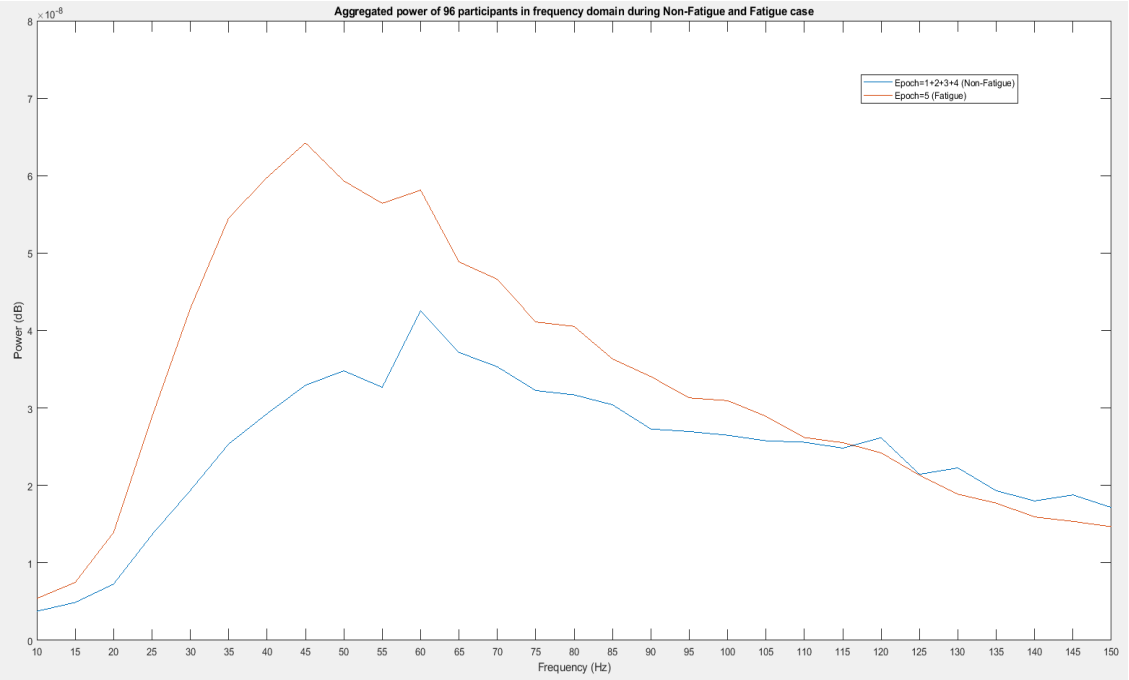

Figure 3.21: Aggregated power spectrum plot for 96 participants during non-fatigue and fatigue condition

Figure 3.21 indicates that the total power during the fatigue is more compared to the non-fatigue power, but there is no work done in the fatigue state. As a result, individuals exert more energy

during fatigue than the amount of power required to complete the job. However, the same task can be completed by exerting less energy in the non-fatigue state.

3.3.2: Relative Contributions of Inputs from Training Data and Features Selection

NCA technique shows the most relevant features describing the fatigue. Only 14 features out of 35 features contributed mostly to the output. These features were used to train the selected ML algorithms. Among the selected features, the IEMG, RMS, median and mean frequency, instantaneous median frequency, peak frequency 1 contribute significant weight for forecasting fatigue.

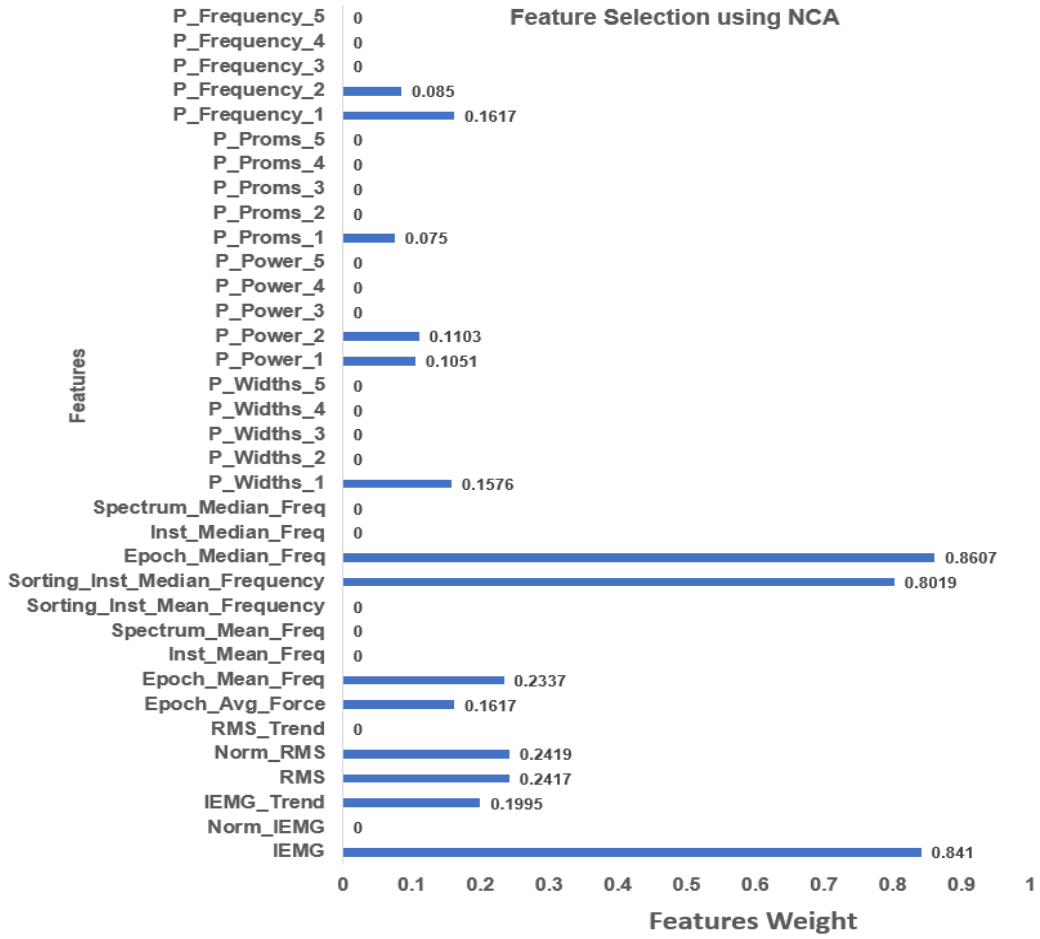

Figure 3.22: Importance matrix plot of the NCA model and portrayed the weight importance of the selected features in the development of the final predictive classification model.

3.3.3: Validation and Testing Performance of Algorithm

We evaluated the performance of each algorithm for the classification of muscle fatigue in real-time on our dataset. An example of the information provided by the classifier is given in Table 3.1.

Table 3.1: Optimized SVM (OSVM) Classifier

Model Type
Model name: **Optimized SVM**
Optimization hyperparameters
Kernel function: **Linear**
Box constraint level: **90.8455**
Standardized data: true
Kernel scale: **1**
Iteration: **30**

Validation Performance of OSVM:

The validation results suggest that the classifier's training accuracy is 99.2% for the OSVM classifier, which is an outstanding performance.

Validation performance: Overall accuracy = 99.2%, sensitivity = 99%, specificity = 99.2%, and AUC for fatigue and non-fatigue condition = 1.00.

A) Total observations table

B) Confusion matrix

C) Fatigue ROC

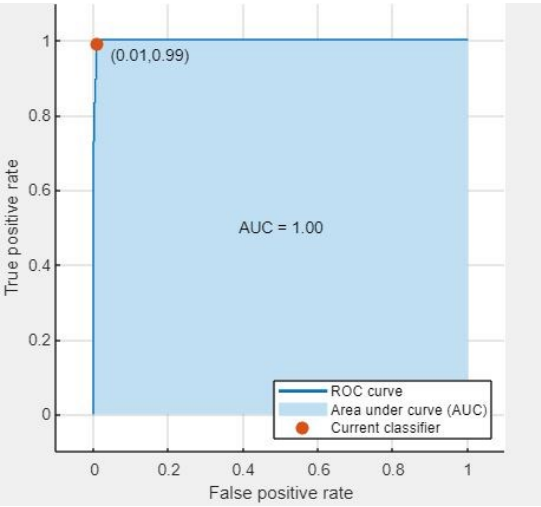

D) Non-Fatigue ROC

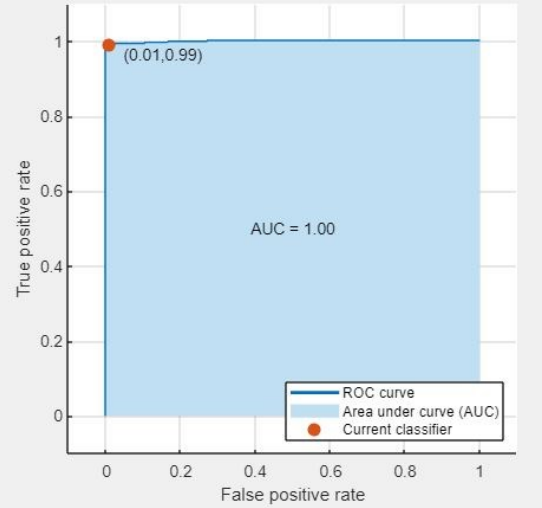

E) Minimum classification error

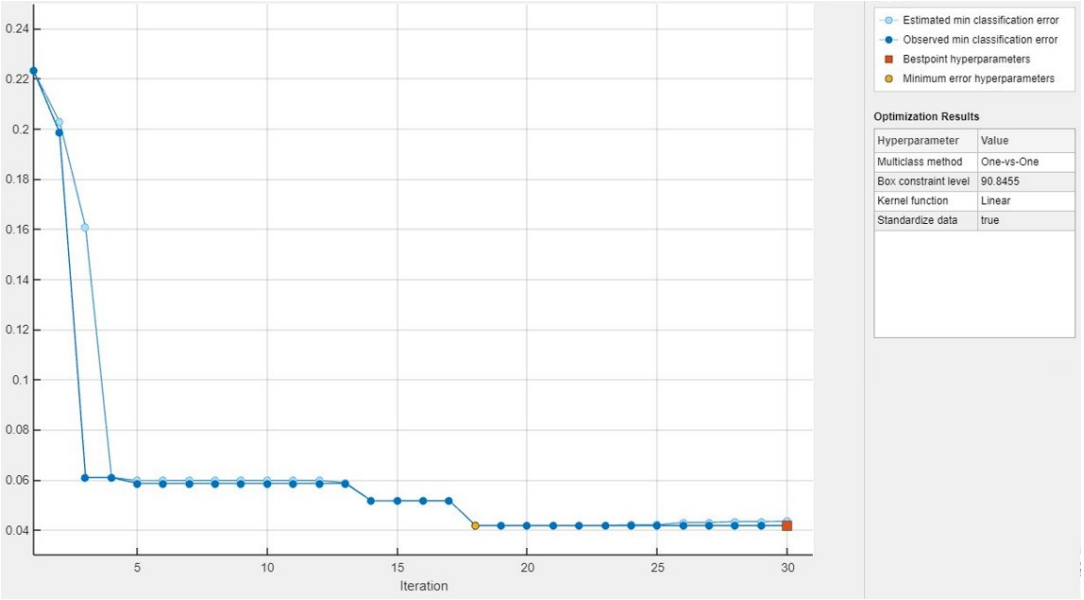

Figure 3.23: Validation performance of optimized SVM classifier: A) Total number of observations table, B) Confusion matrix of the trained model, C) ROC curve for fatigue condition, D) ROC curve for non-fatigue, and E) Minimum classification error of the optimized SVM model.

Overall classification accuracy = 99.2%

The true positive rate (TRP) is the fatigue classification rate of 99%, whereas the false-negative rate (FNR) is only 1%.

To explore the tradeoff between different kinds of misclassification, we use a total observation table and a confusion matrix. The total number of observations table shows that out of 96 fatigue samples, the OSVM classifier misclassified only 1 (One) sample, which is the clinically acceptable range to implement this system in the clinic for real-time detection of fatigue. The confusion matrix represents that the OSVM classifier can accurately identify the fatigue samples up to 99%. The classification accuracy of non-fatigue samples slightly higher (99.2%) because of the imbalance between the non-fatigue and fatigue samples. The non-fatigue samples are four times higher than the fatigue samples. To enhance performance for classification problems in imbalance conditions,

we optimize the bias and misclassification-cost of the classifier by tuning hyperparameters to minimize the misclassification of fatigue samples. For this current classifier, only a 0.2% accuracy imbalance can be acceptable.

The receiver operating characteristics (ROC) curve is 0.99 for both conditions, whereas the area under the curve (AUC) is maximum (1.00). The AUC value represents the classifier's overall consistency for sample classification. The larger the area under the curve, the better the classifier's accuracy and minimum the classification error. Figure 3.23 (E) represented the trained classification error of the OSVM classifier based on the current optimizer. The model automatically chooses hyperparameter values that minimize the upper confidence interval of the classification error with the iterations. The OSVM classifier gained the highest accuracy with a linear kernel function.

Testing performance of the OSVM: The TRP for fatigue classification is 100% and FNR is zero for this classifier. The result is very promising.

The OSVM classifier's classification performance with the new dataset is exceptional, where it can detect all fatigue samples precisely with 100% accuracy for fatigue classification. The total observation table shows that the OSVM model classified all of the fatigue samples perfectly. The model detected all of 15 fatigue trails correctly as fatigue samples during testing with new data.

Testing performance: overall accuracy = 99%, sensitivity (TPR) = 100%, specificity = 98.2%, and AUC for fatigue and non-fatigue classification =1.00.

A) Total number of observations table

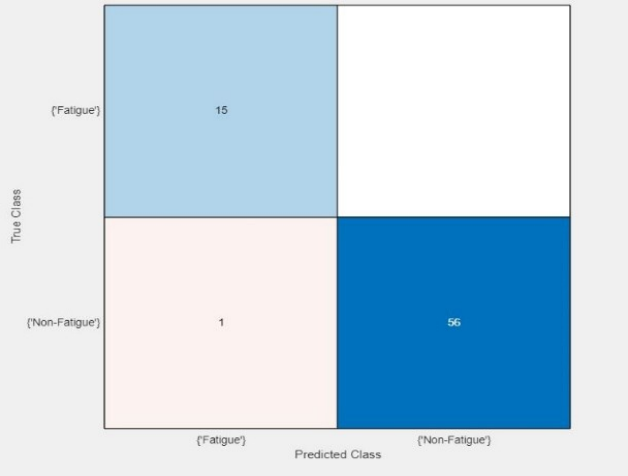

B) Confusion matrix

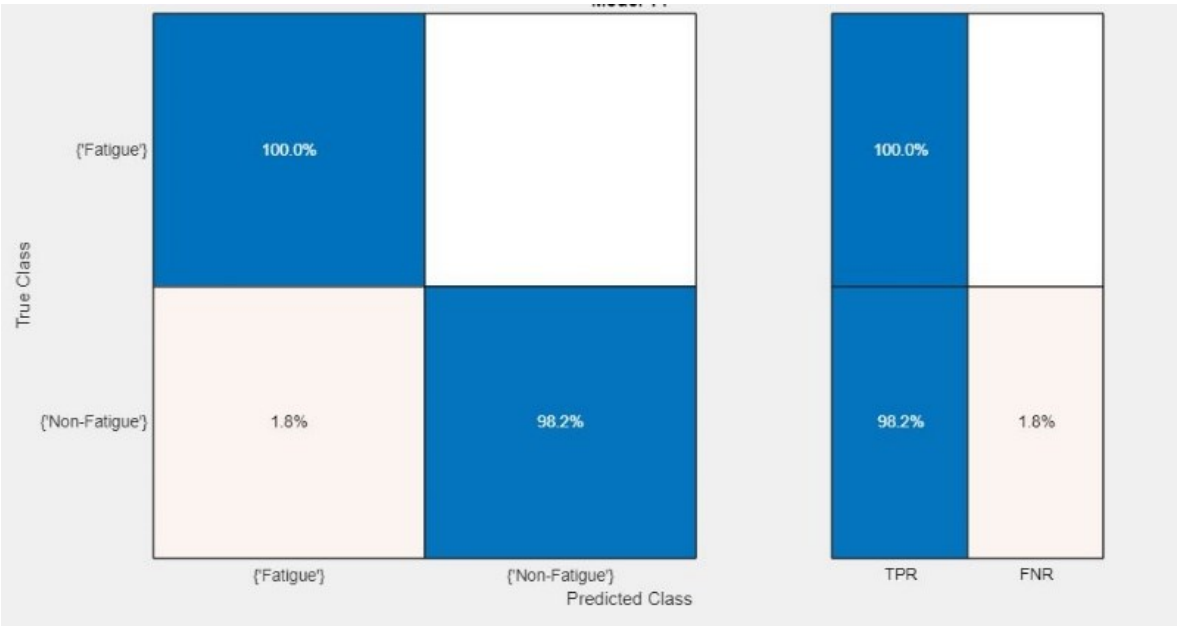

C) Fatigue ROC curve

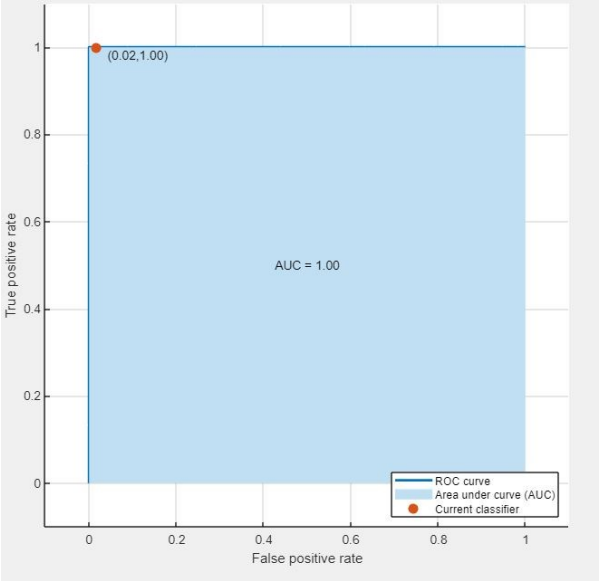

D) Non-Fatigue ROC Curve

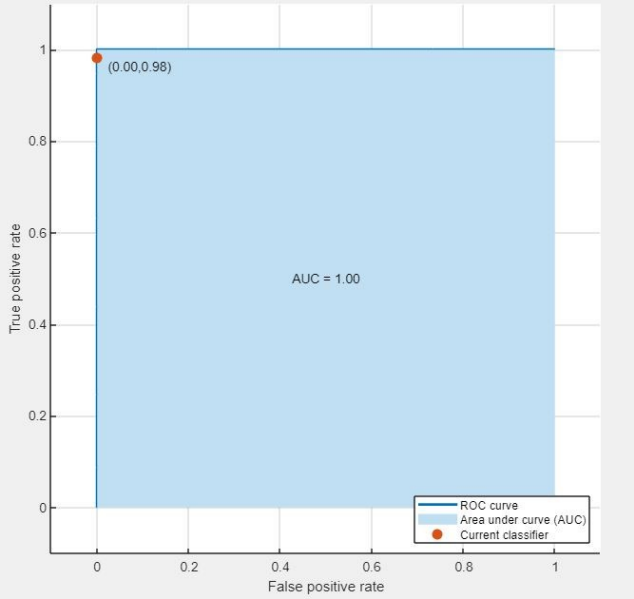

Figure 3.24: Test performance of optimized SVM classifier: A) Total number of observations table, B) Confusion matrix of the trained model, C) ROC curve for fatigue condition, and D) ROC curve for non-fatigue

The classification rate for non-fatigue is 98.2% of the current model. Only 1 non-fatigue sample was misclassified as a fatigue sample; however, we will double-check the sample with an expert clinician for further evidence at the time of the clinical application. The OSVM overall testing

accuracy achieves up to 99%, denotes excellent generalization and convergence to the problem classification. For the classification of fatigue samples in real-time, the ROC curve reached the maximum region, and AUC is gained to 1.00 (unity). The testing results demonstrate that this OSVM algorithm can perfectly classify fatigue samples from the new sEMG data.

Classification Performance of Each ML Algorithm with Different Epochs Approach

Table 3.2: Classification performance of the selected ML models with different epochs system

No. of Epoch	Fatigue Epoch	ML Model	Validation Performance							Test Performance						
			Fatigue Case			Non-Fatigue Case			Model Validation Accuracy	Fatigue Case			Non-Fatigue Case			Model Test Accuracy
			TPR (%)	FNR (%)	AUC-F	TNR (%)	FPR (%)	AUC-NF		TPR (%)	FNR (%)	AUC-F	TNR (%)	FPR (%)	AUC-NF	
5	5th	LDA	89	11	0.94	96	4	0.98	95%	95	5	0.99	98	2	0.99	97.8%
		SVMs[a]	96	4	0.99	98	2	0.99	98	97	3	1.00	98	2	1.00	98.7%
		OSVM	**99**	**1**	**1.00**	**99.2**	**0.8**	**1.00**	**99.2%**	**100**	**0**	**1.00**	**98.2**	**1.8**	**1.00**	**99%**
		LR	81.5	18.5	0.89	98.8	1.2	0.89	95.3%	97	3	0.98	93.0	7	0.98	94.4%
		Optimized Ensemble	93.9	6.1	0.94	90.3	9.7	0.94	90.7%	96	4	0.97	96.6	3.4	0.98	97.2%
5	4th and 5th	LDA	78.5	21.5	0.87	75.8	24.2	0.87	76.9%	80	20	0.89	78.6	21.4	0.89	79.2%
		SVMs[a]	73.3	26.7	0.90	88.1	11.9	0.90	82.2%	93.3	6.7	0.96	73.7	26.3	0.96	77.8%
		OSVM	73.3	26.7	0.90	88.1	11.9	0.90	82.2%	94	6	0.96	82.1	17.9	0.96	79.2%
		LR	70.3	29.7	0.87	81.7	20.9	0.87	80.8%	70	30	0.89	89.3	10.7	0.89	81.2%
		Optimized Ensemble	87.8	12.2	0.87	76.2	23.8	0.87	80.8%	80	20	0.86	71.4	28.6	0.86	75%
10	8th, 9th, and 10th	LDA	73	27	0.88	86.7	13.3	0.88	79%	80	20	0.90	89	11	0.90	78.5%
		SVMs[a]	75	25	0.87	87	13	0.87	80%	85	15	0.95	93	7	0.95	85%
		OSVM	80	20	0.92	90	10	0.92	87%	87	13	0.97	94	6	0.97	90%
		LR	65	35	0.83	83.9	16.1	0.83	76.1%	63.8	36.2	0.79	80.2	19.8	0.79	73.6%
		Optimized Ensemble	70.6	29.4	0.83	82.4	17.6	0.83	77.7%	55.2	77.9	0.76	77.9	22.1	0.76	68.8%
10	6th to 10th	LDA	94.5	5.5	0.96	79.5	20.5	0.96	88.5%	95.4	4.6	0.98	87.7	12.3	0.98	92.4%
		SVMs[a]	96.1	3.9	0.97	85.3	14.7	0.97	91.8%	96.6	3.4	0.98	93	7	0.98	95.1%
		OSVM	97.3	2.7	0.99	94.5	5.5	0.99	96.2%	95.4	4.6	0.99	94.7	5.3	0.99	95.1%
		LR	91.2	8.8	0.92	93	7	0.92	91.9%	95.4	4.6	0.99	96.5	3.5	0.99	95.8%
		Optimized Ensemble	98.4	1.6	0.99	95.4	4.6	0.99	97.2%	97	3	0.99	98	2	0.99	99%

a= SVM with polynomial and radial kernel

Each of the ML classifiers' performance index was mapped in Table 3.2 for 5 and 10 epochs. During the training session of the ML algorithms, it is also crucial to check the algorithm's performance for different epoch numbers. It is essential to train the classifier for both the 5 and 10 epoch cases to determine which classifier obtains the highest accuracy for which case. The technical feasibility of the five epochs case showed the highest performance.

Table 3.2 shows both the validation and testing performance of each algorithm classifier. The SVM classifier presented here is based on the non-linear polynomial and radial kernel, whereas OSVM performs based on the linear kernel function. Table 3.2 shows that the classification accuracy of the OSVM classifier outperforms regular SVM.

Unlike the OSVM, the performance of the ensemble algorithm is not consistent for the two epoch cases. The LDA and LR algorithm achieved overall accuracy up to 97.8% and 95.1%, respectively. However, the fatigue classification rate (TPR) of the OSVM is higher than other algorithms. Therefore, based on the comparison Table 3.3, the OSVM classifier shows the highest overall performance for fatigue classification.

3.3.4: Selection of the Most Promising Algorithm for Developing the Proposed Model

A requirement was that the proposed model be embedded in a wearable device to detect fatigue in real-time. The most promising algorithm can be selected based on two primary criteria:

(i) Adaptability to be embedded in a wearable device

(ii) exhibit superior fatigue classification performance.

Table 3.3 was included to evaluate each algorithm's performance on the aforementioned two criteria.

The MATLAB Research Team identified five distinct properties for justifying the adaptiveness of an algorithm in a wearable device (Suhm, 2021). The characteristics properties are prediction speed, training time, required memory, tuning or level of adjustment, and adaptability to the problem applications. Table 3.3 depicts performance of each algorithm on these properties as well as fatigue classification accuracy. Instead of overall accuracy, each algorithm's fatigue classification accuracy is significant for the identification of muscle fatigue research.

Table 3.3: Criteria for selection of the most promising algorithm for the sEMG based fatigue prediction

Algorithm	Adaptability to a Wearable Device					Algorithm Performance
	Fatigue Prediction Speed	Training Speed	Memory Usage	Required Tuning	General Assessment (Adaptability to problems)	Fatigue Classification Accuracy (TPR) %
LDA	Fast	Fast	Small	Minimal	Good for small problems with linear decision boundaries. But fails in non-linear applications like muscle fatigue.	**95**
LR	Fast	Fast	Small	Minimal	Good with less classification level either two (0, 1) binary classifiers	**97**
Ensemble	Moderate	Slow	Varies (Problem complexity)	Some	High accuracy and good performance for small- to medium-sized datasets	**96**
SVM (Polynomial, Radial kernel)	Slow	Slow	Medium	Some	Good for many binary problems, and handles high-dimensional data well	**97**
OSVM (Linear kernel)	Fast	Fast	Small	Minimal	Excellent performance on both small and large dataset. Popular classifier	**100**

Notably, the OSVM is trained based on the linear kernel. However, the SVM is trained with two non-linear kernels: polynomial and radial kernels, separately. In both cases, the SVM produced the same results.

For LDA, LR, and OSVM, the features of fatigue prediction speed, training speed, memory allocation, and tuning are nearly identical. The LDA and LR work both well for simple linear

problems where the number of classification level in the data are two or fewer. However, they often fail to perform in a non-linear system like fatigue classification problem. Additionally, as compared to OSVM, the fatigue classification accuracy of these two algorithms is lower. Therefore, LDA and LR will not be suitable for muscle fatigue research associated with an isometric contraction.

The Ensemble can handle high-dimensional data and complex issues, but it demands a lot of memory and processing time. In addition, the performance accuracy of the ensemble algorithm is not consistent and lower.

Similarly, SVMs based on polynomial and radial kernels require much memory and are sluggish. The Ensemble and SVMs with polynomial and radial kernels increase the computational burden to a wearable device for the fatigue classification problem.

To conclude, the OSVM is the most promising algorithm for our proposed muscle fatigue research. Therefore, the OSVM is used to develop a model embedding in a wearable device to detect muscle fatigue in real-time based on sEMG data associated with a sustained single 80% MVC.

3.3.5: Performance of the OSVM with Reduced Features

One of the challenges of the current embedded devices is to lower computational power and require less memory for processing. Larger numbers of features increase the computational burden. Therefore, it is vital to reduce features that are either redundant or not contributing significantly to the predictive performance of the model, in order to achieve faster processing.

In the validation state, the fatigue classification accuracy of the OSVM is outstanding and reaches 99% shown in Table 3.4, with the selected 14 features. The fatigue classification accuracy achieved

100% when testing with test dataset mentioned in Table 3.2. The results we obtained achieved the highest performance accuracy for the classification of muscle fatigue in the literature, and with a large diverse dataset.

To reduce the computation overhead of 14 features, we tested the performance of the OSVM model with the most promising 5, 3, and then only 1 feature. The reduced number of features will enhance the processing time for fatigue prediction significantly. Some muscle fatigue applications, such as prosthesis and driver fatigue during driving, need a requires faster response.

Table 3.4: Performance comparison of the median frequency with our proposed selected features technique

Algorithm	**No. of Features**	**Validation Performance of Classifier**
OSVM	Total **14** features selected by NCA	TRP (%) = 99 FNR (%) = 1 AUC-F = 1.00 Overall Accuracy = 99.2%
	5 (IEMG, RMS, IMDF, MF, MDF)	TRP (%) = 92 FNR (%) = 8 AUC-F = 0.92 Overall Accuracy = 90%
	3 (IEMG, MDF, IMDF)	TRP (%) = 85 FNR (%) = 15 AUC-F = 0.85 Overall Accuracy = 85%
	MDF	TRP (%) = 83 FNR (%) = 17 AUC-F = 0.83 Overall Accuracy = 81%

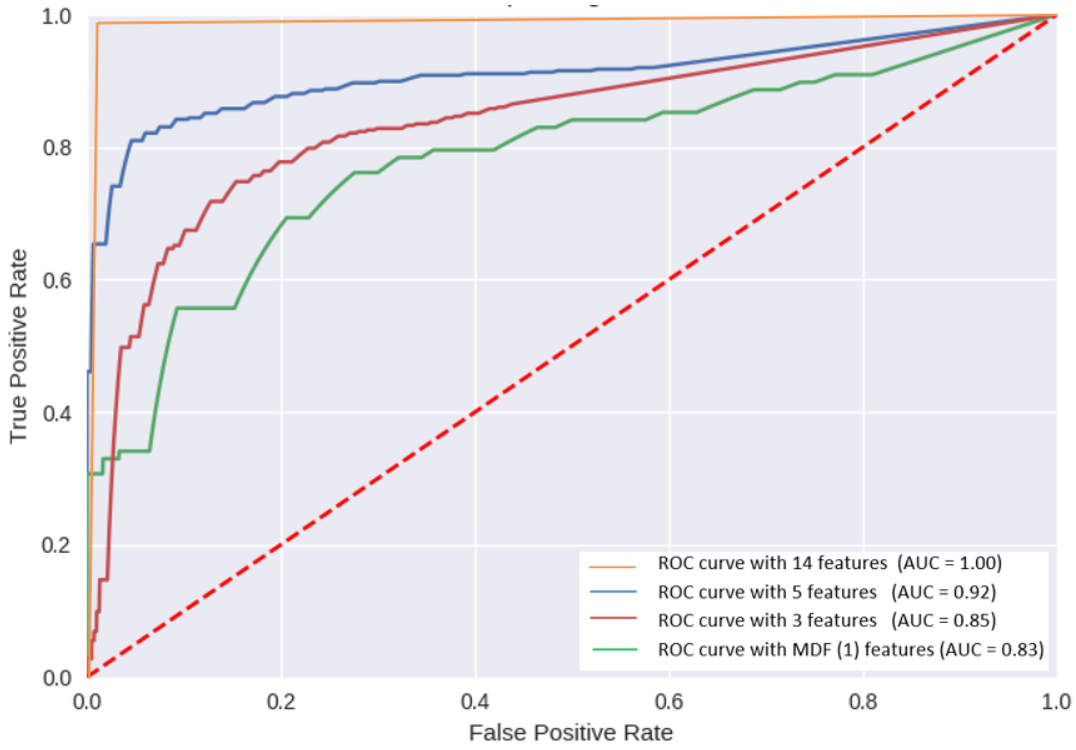

Figure 3.25: Performance of the classifier with different features (No. of features vs ROC curve for fatigue state)

With the 5 features (IEMG, RMS, IMDF, MF, MDF), the model is able to detect muscle fatigue with at least 92% accuracy. This result is likely to be satisfactory in clinical settings. Furthermore, the processing time will be half that required with 14 features.

Using the 3 most promising features (IEMG, MDF, IMDF), the classifier achieved 85% fatigue classification accuracy. Additionally, we investigated the fatigue classification accuracy utilizing only the median frequency feature and subsequently, the OSVM achieved 83% overall validation accuracy. Table 3.3 shows how performance accuracy changes with the number of features. Figure 3.24 indicates the trend of the ROC curve with the different number of selected features.

3.3.6: Development of the Proposed Model

The OSVM algorithm shows outstanding performance for classifying muscle fatigue in real-time and is adaptable to be embedded in a wearable device.

To prepare and develop the final application model for deployment, C code is generated from the model by performing the following steps:

(i) To save the trained model as a compact model

(ii) To launch MATLAB Coder for C-code generation.

(iii) To create an entry point function that takes raw sensor data as input and classifies the raw sEMG data into fatigue or non-fatigue state in real-time.

The output of the final model can be displayed in a dashboard or mobile app.

3.3.7: Computational Requirements of the Model

One of the novelties of this research is that this model can used in the laboratory setting and at the same time can be used as a compact model with same performance and accuracy. Using the MATLAB C Coder tool, the OSVM based model was exported as a compact model. Now, the final model is ready to deploy in a wearable device. The challenge of the current wearable devices that they possess less memory, clock frequency, and processing power. The OSVM gained 100% fatigue classification accuracy during the testing phase with 14 features for our current model. We developed the compact model using these 14 features.

We used Fourier Transform for power spectrum, Detrend for removing noises, remove outliers using default function, OSVM based final model and 14 features. The size of the RAM depends on all of those functions, tools, and properties.

The sEMG sampling frequency = 1000 Hz

The processing interval of EMG signal = 10 seconds each epoch

Timestamp for each epoch = 4 Bytes

For FFT = $1024*\log_2 2048 \cong 16$ KB

Overall, Detrend and Outlier removal function requires maximum = 2 KB

For Compact model of SVM = 31058 bytes $\cong$ 32 KB

Overall utilities and function libraries = 32 KB

We need $= (1000 \times 10 \times 2 \times 4) = 80$ KB memory for storing 10 seconds of data each time.

Total RAM requirement for the entire processing $= 80 + 16 + 2 + 32 + 32 =$ **162 KB**

ARM-based wearable microcontrollers have RAM capacity up to 32 KB, so ARM-microcontrollers will not be suitable for the deployment of this model.

However, 'Raspberry Pi Zero W' is a wearable microcontroller with 512 MB RAM and a clock frequency of 1 GHz. Due to its high clock frequency, it has a higher processing capability. The detailed specifications of Pi zero are given in Appendix B.

As a result, our current model can be embedded in a '**Raspberry Pi Zero W'** device. The Pi Zero W is very compact and so it is aesthetically feasible and attractive as a wearable device. Therefore, this study suggested to embed the model in a 'Pi Zero W' device to make a wearable device.

Parallel processing is available in an 8-core Parallax microcontroller unit (MCU) and is used for processing very high dimensional data including arrays. This type of MCU unit maybe indicated for faster response fatigue classification applications like Olympic weightlifting, and prosthetics applications for real-time operation.

3.4: Discussion

3.4.1: Summary and Strength of the Research

This research presents a comprehensive method for detecting muscle fatigue in real-time applications where the model is intended to be embedded in a wearable device. The feature extraction, features selection, development of a real-time model using ML algorithm, and deployment in an embedded, wearable device, are the novelty of this research. In this research project, we used 96 participants' fatigue data which is considerably larger than previously published models.

A limitation of previous studies is that they do not represent a diverse population of users (Häkkinen & Komi, 1983; Komi & Tesch, 1979; Q. Liu et al., 2021; Moniri et al., 2021; Phinyomark et al., 2013, 2018; Qi et al., 2011; Wu et al., 2016; Yang et al., 2014). and the model becomes overfitted. A fundamental practice in computing science is to avoid over-training ML models on small amounts of data (Pham & Triantaphyllou, 2008). The relatively large dataset was used in this study was less susceptible to these concerns, but even so would be more valuable if a larger dataset is generated.

Figure 3.18 and Figure 3.19 show how the MF, MDF, IMDF change during fatigue and non-fatigue conditions. At the beginning of the test, the IMDF increase from 65 to 90 Hz. The reason is that at the beginning of the test, both fast and slow fibres contribute to sustaining the task and the power

spectrum moves to a higher frequency region. The IMDF drops from 63 to 35 Hz in the fatigue condition shown in Figure 3.19, as the slow fibres recruitment become the dominant influence. The fast-twitch fibres fatigue first when fatigue occurs, while the slow-twitch fibres remain. Then the force drops off and the test ends. Consequently, MF, MDF, and IMDF reduce abruptly to the lower range. For the sustained task, the magnitude of the sEMG signal increases during the fatigue condition while the frequency reduces.

3.4.2: Predictive Performance of the Model.

The OSVM shows the highest classification accuracy in both validation and testing phase. Trained with 14 selected features, the overall validation accuracy of the proposed OSVM model showed 99.2% correct classification on all samples. The sensitivity of the current model for fatigue classification rate is 99% and specificity is obtained 99.2%. Furthermore, during testing with new data, the current model classified fatigue sample 100% accurately (sensitivity). The OSVM model has proven that the ability to classify fatigue samples successfully. In both validation and testing conditions, the AUC of the current model perfectly gained unity (1.00) and is the excellent performance of the model. The sensitivity or fatigue classification rate of the OSVM model achieved 92% with the most promising 5 features. With the reduced number of features, the fatigue prediction and processing time of the controller changes enormously in real-time application.

3.4.3: Model Performance with Previous Literature

The performance of the OSVM model is highest and outstanding compared to the other studies in the previous literature. Table 3.5 depicts the performance comparison of the OSVM with other studies.

Table 3.5: Performance comparison of our proposed model with previous studies

Directed studies	**Model Classification Performance**	**Real-Time Approach**
Al Mulla et al. (20111)	LDA = 90.3%	Yes
Wu et al. (2015)	BF-PSO-FSVCM = 96.55%	Real-time but Not feasible for wearable
Liu et al. (2019)	EMD model but did not report any accuracy	Yes
Moniri et al. (2020)	CNN = 82.8%	Not feasible for wearable
Our proposed system	**OSVM = 99.2%**	**For real-time and wearable**

LDA model shows good performance up to 90.3%. However, the study was conducted based on 5 participants data (Al-Mulla et al., 2011a). As a result, in our large dataset with 96 participants, the LDA fails to outperform the performance accuracy of the OSVM model. Indeed, LDA works well for small data and more straightforward problems but fails to conclude and is overfitted in non-linear problems.

The Bacterial Foraging Optimization (BFO) based PSO-FSVCM model recommended in the study (Wu et al., 2016) achieved excellent accuracy up to 96.55%, which is less than the classification rate of our proposed OSVM model. At the same time, the BFO model requires large computational memory and processing time. However, the method is still challenging for implementing in a laboratory setting to forecast fatigue in real-time. Besides, it is not feasible to deploy in a wearable device.

Therefore, it is obvious that the performance of the proposed OSVM model is higher than any other studies in the literature. As a result, it is concluded that the OSVM model has the potential to be used in real-time for the fatigue classification application and the model can be utilized to generate a model to detect muscle fatigue in a wearable device.

3.5: Conclusion

In this proposed research, we developed a comprehensive method for predicting muscle fatigue in real-time applications, with the model designed to be deployed in a wearable device. The feasibility of embedding this model in a suitable microcontroller based on its technical features has been measured. Our research has demonstrated the possibility of implementing this model in a wearable device for detecting muscle fatigue with exceptional accuracy in the clinical setting.

CHAPTER 4: **THESIS DISCUSSION AND CONCLUSION**

4.1: Discussion

4.1.1: General Overview

Muscle fatigue adversely impacts individuals with several health conditions in daily life and reduces the ability of muscles to contract and exert force overtime during a sustained task (Wan et al., 2017). Muscle fatigue manifests itself as a state of exhaustion, affecting a person's ability to perform voluntary tasks such as those in the workplace or prolonged strenuous exercise or activity (Al-Mulla et al., 2011a; Dayan et al., 2012; Kumar et al., 2003). At present, individuals generally have to rely on their own perception of muscle fatigue which can be inaccurate and unreliable. From the Olympic event to the rehabilitation area, obtaining the balance between enhancing performance and preventing injury is a large part of planning the training applicable to undertake a specific competitive task. Detecting fatigue during exercise in real-time allows individuals to ascertain their limit before progression of the fatigue and prevents injury (Kumar et al., 2003). A wearable device could provide valuable fatigue feedback directly to individuals during exercises, activities, and training sessions. Although muscle fatigue research has been conducted for more than 40 years, most methods for detecting fatigue require post-processing and have not been applied in real-time (Lindstrom & Magnusson, 1977). Therefore, there is a significant deficit in the literature to indicate how to detect muscle fatigue using a wearable device in real-time.

The primary motivation of this project was to develop a model that could be embedded in a wearable device to detect muscle fatigue in real-time while performing sustained tasks. To develop a model for a wearable device, a ML based algorithm is required that has high adaptiveness in embedded devices; however, current wearable devices have limited memory size, low

computational power, and lower clock frequencies. Consequently, the challenge in developing a fatigue detecting wearable is to find a potential algorithm that could work within these computational limits.

4.1.2: Summary of Most Relevant Findings from the Scoping Review

Following that, we conducted a scoping review to see whether any potential algorithms or wearable systems existed in the current literature—the scoping review identified a total of 67 studies that reported numerous algorithms techniques for detecting muscle fatigue.

However, most of the techniques were utilized to detect fatigue during post-processing. Very few algorithms identified could be used to develop an automated fatigue detection system in a wearable device.

Among the 67 included studies, a total of 27 studies reported the FT (7), WT(13), ICA(1), HHT(6) methods that were used to decompose the EMG signal into the frequency domain. The WT, ICA, HHT are the time-frequency analysis tools, and FT is the frequency analysis method. Besides, the HHT and EMD are technically linked with each other where the HHT is the mother tool, and the EMD is the revised version of HHT. The FT, HHT, WT, and ICA are not automated methods for detecting muscle fatigue in real-time. Instead, they could be used to extract features from the EMG signal to train an automated fatigue detection model. An expert clinician or trained person is required to analyze fatigue when these methods are used. However, all these methods are reliable tools to decompose the EMG signal and provides detailed frequency information. These methods are robust tools to convert the EMG signal into the frequency domain. The WT, HHT, and ICA algorithms can be used to extract time-frequency domain features simultaneously. Unfortunately, these methods need more computational memory and processing time, making them the least likely

to be deployed in a wearable device. Aside from providing frequency domain information, the FFT is technically feasible for use in a wearable device.

Operating in the time domain, prior research of five different time domain characteristics showed the ANN attained a maximum accuracy of 70% (MacIsaac et al., 2006). This research was carried out in 2006, and we were unable to locate any further studies that focused solely on time domain aspects. The processing of time domain features is relatively faster than frequency domain features (Phinyomark et al., 2013). However, because of the random and non-linear fluctuation of the amplitude of the EMG signal in the time domain, it is unlikely to attain sufficient accuracy using time domain features solely. Furthermore, the ANN-based system shows more robust performance in noisy signals and might be automated in laboratory settings with high processor hardware to identify fatigue in real-time. Nevertheless, given its multilayer perceptron and computational weight, the ANN is unlikely to be technically practical for integrating the current wearable devices.

A total of 22 studies reported the combination of FT, WT, HHT, ICA with the ML and DL method to detect muscle fatigue. In this approach, either the Fourier Transform (Fast Fourier Transform) or Wavelet Transform and HHT were used to extract frequency domain features. Then, based on the identified features, ML and DL algorithms were trained to detect fatigue. Among different ML algorithms for identifying fatigue, t5rained on both time and frequency domain features, the ML methods show superior fatigue classification performance than other methods. For example, The BF-PSO-FSVCM algorithm with a combination of FFT, HHT, WT achieved high fatigue classification accuracy (BF-PSO-FSVCM = 96.55% with WT) (Wu et al., 2016) yet. However, the BF-PSO-FSVCM with WT, HHT is technically unlikely to be applied in a wearable device. Moreover, the scoping review recommended that the LDA, LR, SVM, and Ensemble algorithms

using the FT technique have the potential to be embedded in a wearable device to detect muscle fatigue in real-time.

According to the scoping review, the muscle fatigue detection systems have obtained maximal fatigue classification accuracy by incorporating both time and frequency domain features, rather than employing only time or frequency domain features. Furthermore, the review suggested the four most promising algorithms that could provide the potential to embed in a wearable device.

The scoping review investigated that only 4 studies attempted to develop a wearable device for detecting fatigue in real-time. However, the four studies that were undertaken were mainly feasibility analyses rather than the development of a wearable device: no performance matrix or validation study was reported in the 4 studies. In addition, the technology readiness level is inferior and most unlikely to reach a satisfactory conclusion. Furthermore, there was no indication of clinical acceptance of those wearable devices mentioned in the 4 included studies. Consequently, we did not find any ML model currently available to be embedded in a wearable. Most significantly, based on the scoping review, there is no wearable device currently used to detect fatigue in real-time. However, the scoping review demonstrates that the demand for wearable devices in sports, rehabilitation, and health applications is rising to detect muscle fatigue in real-time during performing activities. Therefore, the scoping review recommends conducting research for developing a wearable device to detect muscle fatigue in real-time.

4.1.3: Summary of the Substantial Findings from the Development and Validation of the Model

This research presents comprehensive methods for detecting muscle fatigue in real-time during a sustained single 80% MVC test. The significant steps for the development of the real-time muscle fatigue detection system included sEMG signal grooming, feature extraction, feature selection, trained the selected algorithms utilizing the above features, selecting the most promising algorithm and validating its performance, and then the development of the wearable model, with the assessment of the technical potential of the model. This is a novel research investigation.

We extracted 35 features from the previously recorded sEMG data and evaluated the contribution of each feature in forecasting muscle fatigue in a real-time fashion. The NCA tool was then used to choose the most relevant features, removing any that were redundant or did not provide meaningful fatigue information. As a result, the NCA picked 14 most promising features out of 35 features.

During the feature's analysis stage, we observed notable characteristics of the sEMG signal during fatigue conditions. For a sustained single isometric maximum voluntary contraction, the magnitude of the EMG signal increases during the fatigue state. As a result, the magnitude of IEMG and RMS also increases. However, the power spectrum of the sEMG signal transferred to lower frequency components for the duration of fatigue. Consequently, median, mean, and instantaneous median frequencies reduce. However, the frequencies were higher values in the non-fatigue state. Figure 3.19 shows instantaneous median frequencies from the higher frequency range to the lower frequency range. In the fatigue state, the IMDF varies from 35 to 63 Hz, which is the slow fibres

recruitment range, and in the non-fatigue state, it ranges from 65 to 90 Hz. As a result, it is concluded that for the sustained single isometric MVC, as the muscle fatigues, the sEMG signal transitions to the higher magnitude, and the frequency component changes to lower frequencies. As a result, the total power exerted by the individuals to sustain the task increases in the fatigue condition compared to the normal state. However, the work performed is most likely less than the amount of work done in a normal state with less exertional power.

Considering the recommendation of the scoping review, the classification performance of the LDA, LR, SVM and Ensemble algorithms was evaluated. Both the LR and LDA achieved acceptable fatigue classification accuracy. Furthermore, the LDA and LR are lightweight algorithms with a quicker processing time. However, these algorithms failed to complete during the processing of large amounts of real-time data with the different sEMG features. Similarly, the performance of the Ensemble method was not consistent in our fatigue classification task. In addition, the Ensemble algorithm requires a medium amount of memory and processing time. Comparably, the regular SVM with a polynomial or a radial kernel requires more significant processing and forecasting time.

By contrast, linear kernel SVM has a quicker processing time and uses less computing memory. Significantly, our proposed OSVM model is trained on a linear kernel and outperformed previous techniques. The proposed OSVM model shows a maximum of 99.2 % overall classification accuracy with the selected 14 features by the NCA. In the validation stage, the sensitivity of the OSVM is 99%, and the specificity of the model is 99.2%. Testing with new data showed our model having 100% (sensitivity) fatigue classification accuracy.

Compared to the other studies in the muscle fatigue research, our developed OSVM model achieved maximum outstanding classification accuracy. Additionally, the model obtained 92% fatigue classification accuracy with the 5 (five) most prevalent features. The fatigue forecasting speed of the model with 5 features was boosted by more than double compared to processing time with 14 features; however, the model's classification performance with 5 features remains promising and clinically acceptable. Additionally, this proposed OSVM model can be used to detect muscle fatigue in a laboratory setting using routine hardware. We assessed the technical requirement of this model to be embedded in the embedded devices. Therefore, the proposed model is technically able to be embedded in a wearable device.

4.1.4: Limitation of This Research

There are some limitations of this research. The limitations are following:

i) The model developed is based only on sEMG data recorded from the biceps brachii muscle during static sustained single isometric contraction.

ii) Only two classification states were used in the study: fatigue and non-fatigue. We did not identify the progression of the fatigue state by recording perceived exercise reported by the participant. It is essential to identify the onset of fatigue to define the maximum range of training sessions. Time of the onset of fatigue will help precisely to determine the optimal exercise and train period without progression of fatigue.

iii) To achieve maximum fatigue classification accuracy, the processing time of the model likely needs to be higher.

4.1.5: Future Research

This research suggests that future research should be conducted to build a practical wearable device using the proposed model. Therefore, the following research is recommended with the following specific aims:

i) Immediate research is needed to embed the model in a wearable device and validate its real-time performance.

ii) Future research is required to evaluate how the model works to function the number of sEMG signal features.

iii) Defining a universal fatigue index during the wearable application is necessary, making it easily interpreted by non-expert users. Furthermore, it is desirable to create this fatigue index rather than predict the binary fatigue state.

iv) Research is required to design this model as an easy-to-use, aesthetically pleasing wearable product that can be used in the market.

4.1.6: Clinical Implications of This Research For Neuro-degenerative Conditions

The proposed machine learning (ML) model was developed based on the sEMG data recorded from 100 participants, all of whom were free of neuromuscular disease and any upper extremity injury within the past year. Subsequently, certain clinical conditions such as spinal cord injury (SCI) and muscular dystrophy create neuromuscular changes that would exclude the use of the ML model developed in this study to assess muscle fatigue for them. In the case of SCI, the damage to the spinal cord prevents neurological control of muscles, and so contractions that do occur are usually the result of spasticity (Adams & Hicks, 2005). In muscular dystrophy, muscle mass is gradually lost due to protein deficiency associated with a genetic mutation (Lovering et al., 2005). .

Therefore, the ML model developed in this study is unlikely to be applicable to neurodegenerative conditions such as muscular dystrophy. However, a similar approach, but explicitly using data acquired from people with these conditions, could provide an effective and sensitive way to measure the progression of the disease and the effectiveness of treatments.

4.1.7: Fatigue and Injury

Muscle fatigue often causes direct or indirect injury, including musculoskeletal and strain injuries in athletes and similarly non-athletes while performing different tasks in everyday life (Slobounov, 2008). Specifically, muscular fatigue is also common in heavy work environments, and there is extensive evidence that prolonged low-level contractions induce muscle fatigue that can be harmful (Wan et al., 2017).

Fatigue in the trunk muscles is one of the causes of low back pain (LBP), which is one of the leading causes of disability worldwide, impacting more than 500 million people at any given moment (Moniri et al., 2021).

When playing soccer games and other similar competitive team sports, continuous dynamic contractions reduce dynamic control due to fatigue (Pinniger et al., 2000). In addition, when the muscles of the lower limbs are fatigued, the loss of muscle strength increases the risk of hamstring injury (Cohen et al., 2015).

The study (Khal et al., 2020) proposed that fatigue-induced changes in the lower trapezius might put the infraspinatus at risk of damage. They found that muscle fatigue in the glenohumeral external rotation can also lead to shoulder injuries. In endurance sports, such a marathon running, when fatigue sets in the proper alignment of the joint can be compromised. This increases

potentially damaging loading of the cartilage and ligaments, which, if sustained over many races and training sessions, can result in osteoarthritis.

Construction workers are at risk of physical strain and muscle fatigue, increasing the risk of musculoskeletal injuries (Anwer et al., 2020) worldwide. The Transportation Safety Board (TSB) of Canada has reported that Canadians are experiencing unprecedented levels of workplace fatigue, 60% of which is attributed to muscular fatigue (Dawson et al., 2015; Statistics-Canada, n.d.). They suggest that a real-time wearable device has the potential to automatically alert the individuals as fatigue occurs while performing tasks and will help to prevent work-related injuries.

4.1.8: Detection of the Onset of Fatigue

The ML based model developed in this study was intended to classify the sEMG signal associated with a sustained contraction into fatigue and non-fatigue states. However, fatigue occurs progressively and therefore, in the context of predictive model development should ideally be considered to be continuous. However, the sEMG dataset available for this study was intended to demonstrate proof of concept, only accommodating two conditions reported by the participant:

1. Non-fatigue state at the start of the test
2. End-stage fatigue when the participant can no longer sustain the 80% MVC

Recent research by Qi et al. (2012) in our lab has shown that the Borg Rating of Perceived Exertion (RPE) scale (Williams, 2017) can be used to correlate sEMG parameters with the subjective assessment of the level of fatigue. For future studies, this subjective measurement would enhance the practical usefulness of ML fatigue prediction models. Previous studies have reported fatigue classification accuracy ranges from 68 to 78% by utilizing a single feature (e.g. median frequency of the power spectrum) of the sEMG signal (Elshafei & Shihab, 2021; Wu et al., 2016). Our study

set out to determine if ML models which combine multiple features extracted from the sEMG signal could improve on previous fatigue classification accuracy results of single variable studies. The goal was to train a model to increase fatigue classification accuracy to levels that would be more acceptable for clinical interpretation. One of the strengths of ML modelling is its ability to combine input parameters and relate them non-linearly, thereby optimizing the predictive power of the model. Furthermore, the computational requirements of ML models have the potential to embed the model into wearable, real-time sensors, which increases the usefulness in clinical and sports performance applications.

The model developed in this study achieved 100% fatigue classification accuracy when utilizing 14 features and 92% for 5 features; both are clinically acceptable results (Suhm, 2021). Thus, we concluded that OSVM is an adaptive algorithm that works well for training models to detect end-stage muscle fatigue. The performance accuracy of the model was shown to be effective in detecting the end-stage fatigue state for a relatively large and diverse cohort of healthy participants when performing a single, sustained 80% maximum voluntary contraction.

4.2: Impact of the Proposed Research

Currently, there is no wearable device that can detect muscle fatigue in real-time accurately and precisely for large groups of people in sports, rehabilitation, and health applications. Therefore, the wearable system to monitor muscle fatigue in real-time is highly desirable for human-computer interactions, prosthetics, occupational science, ergonomics, rehabilitation, biomedical and kinesiology research. This research is the very first developed ML model that can be used to detect muscle fatigue in real-time precisely, and the model can be incorporated in a wearable device. Using the wearable device, an athlete may decide their race strategy by tracking the level of muscle fatigue in the coming days. By developing a wearable device using this developed model,

researchers and therapists could measure fatigue in real-time. Remarkably, the system will also help clinicians decide optimal test limits and calculate test periods for clients during training and exercise sessions toward injury prevention in various settings (e.g., sport, occupation).

4.3: Conclusion

First and foremost, this research represents a comprehensive method to detect muscle fatigue in real-time during a sustained single isometric task. The trained model can be used in the laboratory setting as well as a wearable device to detect muscle fatigue in real-time. The features reduction mechanism facilitates the model to perform adaptively based on the task's performance requirement and the system's response requirement. This automated model can classify fatigue samples with exceptional accuracy in real-time, which is clinically acceptable for consumer applications. Machine learning has real potential for developing a wearable device to detect muscle fatigue in real-time. Therefore, this research demonstrated that we can generate an effective machine learning model to detect muscle fatigue in real-time, and it is deployable in a wearable device. Based on the evaluation in this thesis, the proposed model has the potential to be embedded in a low-cost microcontroller such as the "Raspberry Pi Zero W". It is most likely to conclude that that embedding this model in a wearable device system will contribute to preventing injury in the coming days.

BIBLIOGRAPHY

Adams, M. M., & Hicks, A. L. (2005). Spasticity after spinal cord injury. In *Spinal Cord* (Vol. 43, Issue 10, pp. 577–586). Nature Publishing Group. https://doi.org/10.1038/sj.sc.3101757

Al-Mulla, M. R., & Sepulveda, F. (2010). Novel feature modelling the prediction and detection of sEMG muscle fatigue towards an automated wearable system. *Sensors*, *10*(5), 4838–4854. https://doi.org/10.3390/s100504838

Al-Mulla, M. R., Sepulveda, F., & Colley, M. (2011a). An autonomous wearable system for predicting and detecting localised muscle fatigue. *Sensors*, *11*(2), 1542–1557. https://doi.org/10.3390/s110201542

Al-Mulla, M. R., Sepulveda, F., & Colley, M. (2011b). A review of non-invasive techniques to detect and predict localised muscle fatigue. *Sensors*, *11*(4), 3545–3594. https://doi.org/10.3390/s110403545

Allen, D. G., & Westerblad, H. (2001). Role of phosphate and calcium stores in muscle fatigue. In *Journal of Physiology* (Vol. 536, Issue 3, pp. 657–665). J Physiol. https://doi.org/10.1111/j.1469-7793.2001.t01-1-00657.x

Anwar, H., Qamar, U., & Muzaffar Qureshi, A. W. (2014). Global optimization ensemble model for classification methods. *Scientific World Journal*, *2014*. https://doi.org/10.1155/2014/313164

Anwer, S., Li, H., Antwi-Afari, M. F., Umer, W., & Wong, A. Y. L. (2020). Cardiorespiratory and thermoregulatory parameters are good surrogates for measuring physical fatigue during a simulated construction task. *International Journal of Environmental Research and Public*

Health, *17*(15), 1–12. https://doi.org/10.3390/ijerph17155418

Arksey, H., & O'Malley, L. (2005). Scoping studies: Towards a methodological framework. *International Journal of Social Research Methodology: Theory and Practice*, *8*(1), 19–32. https://doi.org/10.1080/1364557032000119616

Barbero, M., Merletti, R., & Rainoldi, A. (2012). Generation, Propagation, and Extinction of Single-Fiber and Motor Unit Action Potentials. In *Atlas of Muscle Innervation Zones* (pp. 21–38). Springer Milan. https://doi.org/10.1007/978-88-470-2463-2_3

Beck, T. W., Stock, M. S., & Defreitas, J. M. (2014). Shifts in EMG spectral power during fatiguing dynamic contractions. *Muscle & Nerve*, *50*(1), 95–102. https://doi.org/10.1002/mus.24098

Bilgin, G., Hindistan, E., Özkaya, Y. G., Köklükaya, E., Polat, Ö., & Çolak, Ö. H. (2015). Determination of Fatigue Following Maximal Loaded Treadmill Exercise by Using Wavelet Packet Transform Analysis and MLPNN from MMG-EMG Data Combinations. *Journal of Medical Systems*, *39*(10), 1–10. https://doi.org/10.1007/s10916-015-0304-5

Boser, B. E., Guyon, I. M., & Vapnik, V. N. (1992). Training algorithm for optimal margin classifiers. *Proceedings of the Fifth Annual ACM Workshop on Computational Learning Theory*, 144–152. https://doi.org/10.1145/130385.130401

Brownlee, J. (2019). *Master Machine Learning Algorithms: Discover How They work and Implement Them Scratch.* Machine learning mastery. https://machinelearningmastery.com/master-machine-learning-algorithms/

Bukhari, W. M., Yun, C. J., Kassim, A. M., & Tokhi, M. O. (2020). Study of K-Nearest Neighbour classification performance on fatigue and non-fatigue EMG signal features. *International Journal of Advanced Computer Science and Applications*, *11*(8), 41–47. https://doi.org/10.14569/IJACSA.2020.0110806

Caffier, G., Heinecke, D., & Hinterthan, R. (1993). Surface EMG and load level during long-lasting static contractions of low intensity. *International Journal of Industrial Ergonomics*, *12*(1–2), 77–83. https://doi.org/10.1016/0169-8141(93)90039-G

Cao, H., El Hajj Dib, I., Antoni, J., & Marque, C. (2007). Analysis of muscular fatigue during cyclic dynamic movement. *Annual International Conference of the IEEE Engineering in Medicine and Biology - Proceedings*, 1880–1883. https://doi.org/10.1109/IEMBS.2007.4352682

Chang, J., Chablat, D., Bennis, F., & Ma, L. (2016). Estimating the EMG response exclusively to fatigue during sustained static maximum voluntary contraction. *Advances in Intelligent Systems and Computing*, *489*, 29–39. https://doi.org/10.1007/978-3-319-41694-6_4

Chen, S. W., Liaw, J. W., Chan, H. L., Chang, Y. J., & Ku, C. H. (2014). A real-time fatigue monitoring and analysis system for lower extremity muscles with cycling movement. *Sensors (Switzerland)*, *14*(7), 12410–12424. https://doi.org/10.3390/s140712410

Chowdhury, I Reaz, M. B., & Ali, M. L. (2019). Advanced simple and robust technique for detecting localized early muscular fatigueDETECTING LOCALIZED EARLY MUSCLE FATIGUE. *Journal of Engineering Science and Technology*, *14*(6), 3536–3550.

Chowdhury, Kanti, S., & Nimbarte, A. D. (2015). Comparison of Fourier and wavelet analysis for

fatigue assessment during repetitive dynamic exertion. *Journal of Electromyography and Kinesiology*, *25*(2), 205–213. https://doi.org/10.1016/j.jelekin.2014.11.005

Chowdhury, & Reaz, M. B. I. (2015). Fatigue contraction analysis using empirical mode decomposition and wavelet transform. *Jurnal Teknologi*, *77*(6), 83–89. https://doi.org/10.11113/jt.v77.6232

Chowdhury, Reaz, M. B. I., & Ali, M. A. M. (2014). Determination of muscle fatigue in SEMG signal using empirical mode decomposition. *IECBES 2014, Conference Proceedings - 2014 IEEE Conference on Biomedical Engineering and Sciences: "Miri, Where Engineering in Medicine and Biology and Humanity Meet," December*, 932–937. https://doi.org/10.1109/IECBES.2014.7047649

Cifrek, M., Medved, V., Tonković, S., & Ostojić, S. (2009). Surface EMG based muscle fatigue evaluation in biomechanics. *Clinical Biomechanics*, *24*(4), 327–340. https://doi.org/10.1016/j.clinbiomech.2009.01.010

CLA: pathophysiology. (n.d.). Scanning Surface Electromyography and the Vertebral Subluxation - INSiGHT CLA - Chiropractic Leadership Alliance. Retrieved May 2, 2021, from https://insightcla.com/scanning-surface-electromyography-and-the-vertebral-subluxation/

Clancy, E. A., Bertolina, M. V., Merletti, R., & Farina, D. (2008). Time- and frequency-domain monitoring of the myoelectric signal during a long-duration, cyclic, force-varying, fatiguing hand-grip task. *Journal of Electromyography and Kinesiology*, *18*(5), 789–797. https://doi.org/10.1016/j.jelekin.2007.02.007

Cohen, D. D., Zhao, B., Okwera, B., Matthews, M. J., & Delextrat, A. (2015). Angle-specific

eccentric hamstring fatigue after simulated soccer. *International Journal of Sports Physiology and Performance*, *10*(3), 325–331. https://doi.org/10.1123/ijspp.2014-0088

Cortes, C., & Vapnik, V. (1995). Support-vector networks. *Machine Learning*, *20*(3), 273–297. https://doi.org/10.1007/bf00994018

Daudt, H. M. L., Van Mossel, C., & Scott, S. J. (2013). Enhancing the scoping study methodology: A large, inter-professional team's experience with Arksey and O'Malley's framework. In *BMC Medical Research Methodology* (Vol. 13, Issue 1, p. 48). BioMed Central. https://doi.org/10.1186/1471-2288-13-48

Dawson, D., Mayger, K., Thomas, M. J. W., & Thompson, K. (2015). Fatigue risk management by volunteer fire-fighters: Use of informal strategies to augment formal policy. *Accident Analysis and Prevention*, *84*, 92–98. https://doi.org/10.1016/j.aap.2015.06.008

Dayan, O., Spulber, I., Eftekhar, A., Georgiou, P., Bergmann, J., & McGregor, A. (2012). Applying EMG spike and peak counting for a real-time muscle fatigue monitoring system. *2012 IEEE Biomedical Circuits and Systems Conference: Intelligent Biomedical Electronics and Systems for Better Life and Better Environment, BioCAS 2012 - Conference Publications*, 41–44. https://doi.org/10.1109/BioCAS.2012.6418474

De Luca, C. J., Donald Gilmore, L., Kuznetsov, M., & Roy, S. H. (2010). Filtering the surface EMG signal: Movement artifact and baseline noise contamination. *Journal of Biomechanics*, *43*(8), 1573–1579. https://doi.org/10.1016/j.jbiomech.2010.01.027

De Rocha, V. A., Do Carmo, J. C., & Assis De Nascimento, F. O. (2018). Weighted-Cumulated S-EMG Muscle Fatigue Estimator. *IEEE Journal of Biomedical and Health Informatics*,

22(6), 1854–1862. https://doi.org/10.1109/JBHI.2017.2783849

Dias, D., & Cunha, J. P. S. (2018). Wearable health devices—vital sign monitoring, systems and technologies. In *Sensors (Switzerland)* (Vol. 18, Issue 8). MDPI AG. https://doi.org/10.3390/s18082414

Duan, S., Wang, C., Li, Y., Zhang, L., Yuan, Y., & Wu, X. (2020). A Quantifiable Muscle Fatigue Method Based on sEMG during Dynamic Contractions for Lower Limb Exoskeleton. *2020 IEEE International Conference on Real-Time Computing and Robotics, RCAR 2020*, 20–25. https://doi.org/10.1109/RCAR49640.2020.9303284

Elipot, S., & Gille, S. T. (2009). Ekman layers in the Southern Ocean: Spectral models and observations, vertical viscosity and boundary layer depth. *Ocean Science*, *5*(2), 115–139. https://doi.org/10.5194/os-5-115-2009

Elshafei, M., & Shihab, E. (2021). Towards detecting biceps muscle fatigue in gym activity using wearables. *Sensors (Switzerland)*, *21*(3), 1–18. https://doi.org/10.3390/s21030759

Engel, W. K., & Warmolts, J. R. (2015). The Motor Unit. *New Concepts of the Motor Unit, Neuromuscular Disorders, Electromyographic Kinesiology*, 141–177. https://doi.org/10.1159/000394034

Enoka, R. M., & Duchateau, J. (2008). Muscle fatigue: What, why and how it influences muscle function. In *Journal of Physiology* (Vol. 586, Issue 1, pp. 11–23). John Wiley & Sons, Ltd. https://doi.org/10.1113/jphysiol.2007.139477

Esposito, F., Veicsteinas, A., Orizio, C., & Malgrati, D. (1996). Time and frequency domain

analysis of electromyogram and sound myogram in the elderly. *European Journal of Applied Physiology and Occupational Physiology*, *73*(6), 503–510. https://doi.org/10.1007/BF00357671

Fidalgo-Herrera, A., Miangolarra-Page, J. C., & Carratalá-Tejada, M. (2021). Electromyographic traces of motor unit synchronization of fatigued lower limb muscles during gait. *Human Movement Science*, *75*(July 2020). https://doi.org/10.1016/j.humov.2020.102750

Fisher, R. A. (1936). The use of multiple measurements in taxonomic problems. *Annals of Eugenics*, *7*(2), 179–188. https://doi.org/10.1111/j.1469-1809.1936.tb02137.x

Fu, J., Ma, L., Tsao, L., & Zhang, Z. (2019). Continuous measurement of muscle fatigue using wearable sensors during light manual operations. In *Lecture Notes in Computer Science (including subseries Lecture Notes in Artificial Intelligence and Lecture Notes in Bioinformatics): Vol. 11581 LNCS*. Springer International Publishing. https://doi.org/10.1007/978-3-030-22216-1_20

Georgiou, P., & Koutsos, E. (2017). Microelectronics for muscle fatigue monitoring through surface EMG. In *CMOS Circuits for Biological Sensing and Processing* (pp. 133–162). Springer International Publishing. https://doi.org/10.1007/978-3-319-67723-1_6

Ghosh, D. M., & Swaminathan, R. (2017). Fatigue analysis in biceps brachii muscles using semg signals and polynomial chirplet transform. *ACM International Conference Proceeding Series*, 43–47. https://doi.org/10.1145/3155077.3155090

Gokcesu, K., Ergeneci, M., Ertan, E., Alkilani, A. Z., & Kosmas, P. (2018). An sEMG-based method to adaptively reject the effect of contraction on spectral analysis for fatigue tracking.

Proceedings - International Symposium on Wearable Computers, ISWC, 80–87. https://doi.org/10.1145/3267242.3267292

Häkkinen, K., & Komi, P. V. (1983). Electromyographic and mechanical characteristics of human skeletal muscle during fatigue under voluntary and reflex conditions. *Electroencephalography and Clinical Neurophysiology*, *55*(4), 436–444. https://doi.org/10.1016/0013-4694(83)90132-3

Han, J. (2017). Application of EMG fatigue detection algorithm in portable DSP system. *Acta Technica CSAV (Ceskoslovensk Akademie Ved)*, *62*(3), 85–94.

Hari, L. M., Jero, S. E., Venugopal, G., & Ramakrishnan, S. (2021). Model-Based Simulation of Surface Electromyography Signals and Its Analysis Under Fatiguing Conditions Using Tunable Wavelets. In *Lecture Notes in Mechanical Engineering*. Springer Singapore. https://doi.org/10.1007/978-981-15-8315-5_9

Hari, L. M., Venugopal, G., & Ramakrishnan, S. (2020). Analysis of Isometric Muscle Contractions using Analytic Bump Continuous Wavelet Transform. *Proceedings of the Annual International Conference of the IEEE Engineering in Medicine and Biology Society, EMBS*, *2020-July*, 732–735. https://doi.org/10.1109/EMBC44109.2020.9176203

Hastie, T., Tibshirani, R., & Friedman, J. (2009). *The Elements of Statistical Learning, Data Mining, Inference, and Prediction.* (Second Edi). Springer. https://doi.org/978-0387848570

Hegedus, A., Trzaskoma, L., Soldos, P., Tuza, K., Katona, P., Greger, Z., Zsarnoczky-Dulhazi, F., & Kopper, B. (2020). Adaptation of Fatigue Affected Changes in Muscle EMG Frequency Characteristics for the Determination of Training Load in Physical Therapy for Cancer

Patients. *Pathology and Oncology Research*, *26*(2), 1129–1135. https://doi.org/10.1007/s12253-019-00668-3

Hotta, Y., & Ito, K. (2013). Detection of muscle fatigue during low-level isometric contraction by recurrence quantification analysis and monopolar configuration. *Transactions of Japanese Society for Medical and Biological Engineering*, *51*(5), 292–299. https://doi.org/10.11239/jsmbe.51.292

Ibitoye, M. O., Estigoni, E. H., Hamzaid, N. A., Wahab, A. K. A., & Davis, G. M. (2014). The effectiveness of FES-Evoked EMG potentials to assess muscle force and fatigue in individuals with spinal cord injury. *Sensors (Switzerland)*, *14*(7), 12598–12622. https://doi.org/10.3390/s140712598

Jamaluddin, F. N., Ahmad, S. A., Nor, S. B. M., Hasan, W. Z. W., & Shair, E. F. (2019). A new threshold estimation method of SEMG wavelet de-noising for prolonged fatigue identification. *International Journal of Integrated Engineering*, *11*(3), 51–59. https://doi.org/10.30880/ijie.2019.11.03.006

Jawadwala, R. (2012). *The role of supplementary calcium in submaximal exercise and endurance performance*. https://bit.ly/3cnhxOz

Jero, S. E., & Ramakrishnan, S. (2019). Analysis of Muscle Fatigue Conditions in Surface EMG Signal with A Novel Hilbert Marginal Spectrum Entropy Method. *Proceedings of the Annual International Conference of the IEEE Engineering in Medicine and Biology Society, EMBS*, 2675–2678. https://doi.org/10.1109/EMBC.2019.8857077

Jordanic, M., & Magjarevic, R. (2012). Estimation of muscle fatigue during dynamic contractions

based on surface electromyography and accelerometry. *MIPRO 2012 - 35th International Convention on Information and Communication Technology, Electronics and Microelectronics - Proceedings*, 201–205.

Jun, P., Pagé, I., Vette, A., & Kawchuk, G. (2020). Potential mechanisms for lumbar spinal stiffness change following spinal manipulative therapy: A scoping review. In *Chiropractic and Manual Therapies* (Vol. 28, Issue 1, p. 15). BioMed Central Ltd. https://doi.org/10.1186/s12998-020-00304-x

Kahl, L., & Hofmann, U. G. (2016). Comparison of algorithms to quantify muscle fatigue in upper limb muscles based on sEMG signals. *Medical Engineering and Physics*, *38*(11), 1260–1269. https://doi.org/10.1016/j.medengphy.2016.09.009

Karthick, P. A., Ghosh, D. M., & Ramakrishnan, S. (2018). Surface electromyography based muscle fatigue detection using high-resolution time-frequency methods and machine learning algorithms. *Computer Methods and Programs in Biomedicine*, *154*, 45–56. https://doi.org/10.1016/j.cmpb.2017.10.024

Karthick, P. A., Venugopal, G., & Ramakrishnan, S. (2016). Analysis of Muscle Fatigue Progression using Cyclostationary Property of Surface Electromyography Signals. *Journal of Medical Systems*, *40*(1), 1–11. https://doi.org/10.1007/s10916-015-0394-0

Kavya, N., Sriraam, N., Usha, N., Sharath, D., Hiremath, B., Menaka, M., & Venkatraman, B. (2020). Feature Selection Using Neighborhood Component Analysis with Support Vector Machine for Classification of Breast Mammograms. *Lecture Notes in Electrical Engineering*, *637*, 253–260. https://doi.org/10.1007/978-981-15-2612-1_24

Khal, K. M., Moore, S. D., Pryor, J. L., & Singh, B. (2020). Changes in infraspinatus and lower trapezius activation in volleyball players following repetitive serves. *International Journal of Sports Physical Therapy*, *15*(2), 196–202. https://doi.org/10.26603/ijspt20200196

Komi, P. V., & Tesch, P. (1979). EMG frequency spectrum, muscle structure, and fatigue during dynamic contractions in man. *European Journal of Applied Physiology and Occupational Physiology*, *42*(1), 41–50. https://doi.org/10.1007/BF00421103

Koutsos, E. (2017). Spiral: Real time sEMG based muscle fatigue monitoring using low power integrated circuits. In *PhD dissertation, University College of London, 2017*. https://doi.org/10044/1/57110

Koutsos, E., Cretu, V., & Georgiou, P. (2016). A Muscle Fibre Conduction Velocity Tracking ASIC for Local Fatigue Monitoring. *IEEE Transactions on Biomedical Circuits and Systems*, *10*(6), 1119–1128. https://doi.org/10.1109/TBCAS.2016.2520563

Kumar, D. K., Pah, N. D., & Bradley, A. (2003). Wavelet Analysis of Surface Electromyography to Determine Muscle Fatigue. *IEEE Transactions on Neural Systems and Rehabilitation Engineering*, *11*(4), 400–406. https://doi.org/10.1109/TNSRE.2003.819901

Lévesque, J.-C., Gagné, C., & Sabourin, R. (2016). Bayesian Hyperparameter Optimization for Ensemble Learning. *32nd Conference on Uncertainty in Artificial Intelligence 2016, UAI 2016*, 437–446. http://arxiv.org/abs/1605.06394

Li, K., Hogrel, J. Y., Duchêne, J., & Hewson, D. J. (2012). Analysis of fatigue and tremor during sustained maximal grip contractions using Hilbert-Huang Transformation. *Medical Engineering and Physics*, *34*(7), 832–840. https://doi.org/10.1016/j.medengphy.2011.09.025

Li, Z., Sheng, X., Jiao, S., University, T., Kwon, C. S., Zhao, J., She, J., Fukushima, E. F., Wang, D., Wu, M., & Pan, K. (2020). Muscle Fatigue Analysis With Optimized Complementary Ensemble Empirical Mode Decomposition and Multi-Scale Envelope Spectral Entropy. *Frontiers in Neurorobotics | Www.Frontiersin.Org*, *14*, 566172. https://doi.org/10.3389/fnbot.2020.566172

Lindstrom, L. H., & Magnusson, R. I. (1977). Interpretation of Myoelectric Power Spectra: A Model and Its Applications. *Proceedings of the IEEE*, *65*(5), 653–662. https://doi.org/10.1109/PROC.1977.10544

Liu, Q., Liu, Y., Zhang, C., Ruan, Z., Meng, W., Cai, Y., & Ai, Q. (2021). sEMG-Based Dynamic Muscle Fatigue Classification Using SVM with Improved Whale Optimization Algorithm. *IEEE Internet of Things Journal*. https://doi.org/10.1109/JIOT.2021.3056126

Liu, S. H., Huang, J., Huang, Y. F., Tan, T. H., & Huang, T. S. (2020). A Wearable Device for Monitoring Muscle Condition During Exercise. In *Communications in Computer and Information Science: Vol. 1178 CCIS*. Springer Singapore. https://doi.org/10.1007/978-981-15-3380-8_35

Liu, S. H., Lin, C. B., Chen, Y., Chen, W., Huang, T. S., & Hsu, C. Y. (2019). An EMG patch for the real-time monitoring of muscle-fatigue conditions during exercise. *Sensors (Switzerland)*, *19*(14). https://doi.org/10.3390/s19143108

Lovering, R. M., Porter, N. C., & Block, R. J. (2005). The muscular dystrophies: From genes to therapies. In *Physical Therapy* (Vol. 85, Issue 12, pp. 1372–1388). American Physical Therapy Association. https://doi.org/10.1093/ptj/85.12.1372

Luebke, J. I., Weaver, C. M., Rocher, A. B., Rodriguez, A., Crimins, J. L., Dickstein, D. L., Wearne, S. L., & Hof, P. R. (2010). Dendritic vulnerability in neurodegenerative disease: Insights from analyses of cortical pyramidal neurons in transgenic mouse models. In *Brain Structure and Function* (Vol. 214, Issues 2–3, pp. 181–199). NIH Public Access. https://doi.org/10.1007/s00429-010-0244-2

MacIsaac, D. T., Parker, P. A., Englehart, K. B., & Rogers, D. R. (2006). Fatigue estimation with a multivariable myoelectric mapping function. *IEEE Transactions on Biomedical Engineering*, *53*(4), 694–700. https://doi.org/10.1109/TBME.2006.870220

Madeleine, P., Jørgensen, L. V., Søgaard, K., Arendt-Nielsen, L., & Sjøgaard, G. (2002). Development of muscle fatigue as assessed by electromyography and mechanomyography during continuous and intermittent low-force contractions: Effects of the feedback mode. *European Journal of Applied Physiology*, *87*(1), 28–37. https://doi.org/10.1007/s00421-002-0578-4

Medicine LibreTexts. (n.d.). Types of Contraction. Retrieved May 26, 2021, from https://med.libretexts.org/Bookshelves/Anatomy_and_Physiology/Book%3A_Anatomy_and_Physiology_(Boundless)/11%3A_Central_Nervous_System

Ming, D., Wang, X., Xu, R., Qiu, S., Zhao, X., Qi, H., Zhou, P., Zhang, L., & Wan, B. (2014). SEMG feature analysis on forearm muscle fatigue during isometric contractions. *Transactions of Tianjin University*, *20*(2), 139–143. https://doi.org/10.1007/s12209-014-2181-2

Mitra, S., & Cumming, D. R. S. (2017). CMOS circuits for biological sensing and processing. In

CMOS Circuits for Biological Sensing and Processing. Springer International Publishing. https://doi.org/10.1007/978-3-319-67723-1

Moniri, A., Terracina, D., Rodriguez-Manzano, J., Strutton, P. H., & Georgiou, P. (2021). Real-Time Forecasting of sEMG Features for Trunk Muscle Fatigue Using Machine Learning. *IEEE Transactions on Biomedical Engineering*, *68*(2), 718–727. https://doi.org/10.1109/TBME.2020.3012783

Moschovakis, Y. N. (2001). What Is an Algorithm? In *Mathematics Unlimited — 2001 and Beyond* (pp. 919–936). Springer Berlin Heidelberg. https://doi.org/10.1007/978-3-642-56478-9_46

Munn, Z., Peters, M. D. J., Stern, C., Tufanaru, C., McArthur, A., & Aromataris, E. (2018). Systematic review or scoping review? Guidance for authors when choosing between a systematic or scoping review approach. *BMC Medical Research Methodology*, *18*(1), 143. https://doi.org/10.1186/s12874-018-0611-x

Naeije, M., & Zorn, H. (1982). Relation between EMG power spectrum shifts and muscle fibre action potential conduction velocity changes during local muscular fatigue in man. *European Journal of Applied Physiology and Occupational Physiology*, *50*(1), 23–33. https://doi.org/10.1007/BF00952241

Nagai, H. (2017). A method for real-Time estimation of local muscular fatigue in exercise using redundant discrete wavelet coefficients. *2016 3rd International Conference on Systems and Informatics, ICSAI 2016*, *Icsai*, 819–825. https://doi.org/10.1109/ICSAI.2016.7811064

Nahid, N., Rahman, A., & Ahad, M. A. R. (2020). Deep Learning Based Surface EMG Hand Gesture Classification for Low-Cost Myoelectric Prosthetic Hand. *2020 Joint 9th*

International Conference on Informatics, Electronics and Vision and 2020 4th International Conference on Imaging, Vision and Pattern Recognition, ICIEV and IcIVPR 2020. https://doi.org/10.1109/ICIEVicIVPR48672.2020.9306613

Nugent, N. S., Majeski, J. B., Choe, R., & Rashedi, E. (2020). Investigating the effect of fatigue on muscle microvasculature blood flow during intermittent isometric contraction. *Proceedings of the Annual International Conference of the IEEE Engineering in Medicine and Biology Society, EMBS*, *2020-July*, 3220–3223. https://doi.org/10.1109/EMBC44109.2020.9175709

O'Sullivan, C., Pinkoski, A., & Ferguson-Pell, M. (2018). How much gas is left in the tank? The analysis of EMG to detect fatigue in real-time. In *Unpublished thesis work, RRL Lab* (p. April).

Orizio, C., Gobbo, M., Veicsteinas, A., Baratta, R. V., Zhou, B. H., & Solomonow, M. (2003). Transients of the force and surface mechanomyogram during cat gastrocnemius tetanic stimulation. *European Journal of Applied Physiology*, *88*(6), 601–606. https://doi.org/10.1007/s00421-002-0765-3

Patel, S. (2017). *Chapter 2 : SVM (Support Vector Machine) — Theory | by Savan Patel | Machine Learning 101 | Medium*. 2017. https://medium.com/machine-learning-101/chapter-2-svm-support-vector-machine-theory-f0812effc72

Peng, B., Jin, X., Min, Y., & Su, X. (2006). The study on the sEMG signal characteristics of muscular fatigue based on the Hilbert-Huang transform. *Lecture Notes in Computer Science (Including Subseries Lecture Notes in Artificial Intelligence and Lecture Notes in*

Bioinformatics), *3991 LNCS*, 140–147. https://doi.org/10.1007/11758501_23

Pham, H. N. A., & Triantaphyllou, E. (2008). The impact of overfitting and overgeneralization on the classification accuracy in data mining. *Soft Computing for Knowledge Discovery and Data Mining*, 391–431. https://doi.org/10.1007/978-0-387-69935-6_16

Phinyomark, A., Khushaba, R. N., & Scheme, E. (2018). Feature extraction and selection for myoelectric control based on wearable EMG sensors. *Sensors (Switzerland)*, *18*(5). https://doi.org/10.3390/s18051615

Phinyomark, A., Quaine, F., Charbonnier, S., Serviere, C., Tarpin-Bernard, F., & Laurillau, Y. (2013). EMG feature evaluation for improving myoelectric pattern recognition robustness. *Expert Systems with Applications*, *40*(12), 4832–4840. https://doi.org/10.1016/j.eswa.2013.02.023

Pilarski, P. M., Qi, L., Ferguson-pell, M., & Grange, S. (2013). *Determining the Time until Muscle Fatigue using Temporally Extended Prediction Learning*. 6–9. https://sites.ualberta.ca/~pilarski/docs/papers/Pilarski_2013_IFESS_Postprint

Pinniger, G. J., Steele, J. R., & Groeller, H. (2000). Does fatigue induced by repeated dynamic efforts affect hamstring muscle function? *Medicine and Science in Sports and Exercise*, *32*(3), 647–653. https://doi.org/10.1097/00005768-200003000-00015

Qi, L. (2009). *Use of wavelet analysis techniques with surface EMG and MMG to characterise motor unit recruitment patterns of shoulder muscles during wheelchair propulsion and voluntary contraction tasks.* (Issue (Doctoral Dissertation), October) [University College London, UK]. https://discovery.ucl.ac.uk/id/eprint/1310439/

Qi, L., Ferguson-Pell, M., & Lu, Y. (2019). The effect of manual wheelchair propulsion speed on users' shoulder muscle coordination patterns in time-frequency and principal component analysis. *IEEE Transactions on Neural Systems and Rehabilitation Engineering*, *27*(1), 60–65. https://doi.org/10.1109/TNSRE.2018.2886826

Qi, L., Wakeling, J., Grange, S., & Ferguson-Pell, M. (2012). Changes in surface electromyography signals and kinetics associated with progression of fatigue at two speeds during wheelchair propulsion. *Journal of Rehabilitation Research and Development*, *49*(1), 23–34. https://doi.org/10.1682/JRRD.2011.01.0009

Qi, L., Wakeling, J. M., & Ferguson-Pell, M. (2011). Spectral properties of electromyographic and mechanomyographic signals during dynamic concentric and eccentric contractions of the human biceps brachii muscle. *Journal of Electromyography and Kinesiology*, *21*(6), 1056–1063. https://doi.org/10.1016/j.jelekin.2011.08.011

Qi, L., Zhang, L., Lin, X. B., & Ferguson-Pell, M. (2020). Wheelchair propulsion fatigue thresholds in electromyographic and ventilatory testing. *Spinal Cord*, *58*(10), 1104–1111. https://doi.org/10.1038/s41393-020-0470-2

R., M., Sepulveda, F., & Colley, M. (2012). sEMG Techniques to Detect and Predict Localised Muscle Fatigue. *EMG Methods for Evaluating Muscle and Nerve Function*. https://doi.org/10.5772/25678

Rezki, M., Griche, I., & Ayad, M. (2017). Study of muscle fatigue across typical physical exercise by using different techniques of analysis. *2017 5th International Conference on Electrical Engineering - Boumerdes, ICEE-B 2017*, *2017-Janua*, 1–4. https://doi.org/10.1109/ICEE-

B.2017.8192193

Rocca, J. (2021). *Ensemble methods: bagging, boosting and stacking | by Joseph Rocca | Towards Data Science*. 2021. https://towardsdatascience.com/ensemble-methods-bagging-boosting-and-stacking-c9214a10a205

Rogers, D. R., & MacIsaac, D. T. (2013). A comparison of EMG-based muscle fatigue assessments during dynamic contractions. *Journal of Electromyography and Kinesiology*, *23*(5), 1004–1011. https://doi.org/10.1016/j.jelekin.2013.05.005

Rong, Y., Hao, D., Han, X., Zhang, Y., Zhang, J., & Zeng, Y. (2013). Classification of surface EMGs using wavelet packet energy analysis and a genetic algorithm-based support vector machine. *Neurophysiology*, *45*(1), 39–48. https://doi.org/10.1007/s11062-013-9335-z

Seshadri, D. R., Davies, E. V., Harlow, E. R., Hsu, J. J., Knighton, S. C., Walker, T. A., Voos, J. E., & Drummond, C. K. (2020). Wearable Sensors for COVID-19: A Call to Action to Harness Our Digital Infrastructure for Remote Patient Monitoring and Virtual Assessments. *Frontiers in Digital Health*, *2*(8), 8. https://doi.org/10.3389/fdgth.2020.00008

Seunggu, H. (2017). *Neurons: What are they and how do they work?* Medical News Today. https://www.medicalnewstoday.com/articles/320289.php#neurons_look_like

Slobounov, S. (2008). Fatigue-Related Injuries in Athletes. In *Injuries in Athletics: Causes and Consequences* (pp. 77–95). Springer US. https://doi.org/10.1007/978-0-387-72577-2_4

Smale, K. B., Shourijeh, M. S., & Benoit, D. L. (2016). Use of muscle synergies and wavelet transforms to identify fatigue during squatting. *Journal of Electromyography and*

Kinesiology, *28*, 158–166. https://doi.org/10.1016/j.jelekin.2016.04.008

Soo, Y., Sugi, M., Yokoi, H., Arai, T., Nakamura, T., Du, R., & Ota, J. (2008). The relationship between changes in amplitude and instantaneous mean frequency at low and high frequency bands during dynamic contraction. *2nd International Conference on Bioinformatics and Biomedical Engineering, ICBBE 2008*, 1413–1416. https://doi.org/10.1109/ICBBE.2008.682

Srhoj-Egekher, V., Cifrek, M., & Medved, V. (2011). The application of Hilbert-Huang transform in the analysis of muscle fatigue during cyclic dynamic contractions. *Medical and Biological Engineering and Computing*, *49*(6), 659–669. https://doi.org/10.1007/s11517-010-0718-7

Statistics-Canada. (n.d.). *Fatigue Risk Management System for the Canadian Aviation Industry - Fatigue Management Strategies for Employees - TP 14573*. Retrieved June 28, 2021, from https://tc.canada.ca/en/aviation/publications/fatigue-risk-management-system-canadian-aviation-industry-fatigue-management-strategies-employees-tp-14573

Subasi, A., & Kiymik, M. K. (2010). Muscle fatigue detection in EMG using time-frequency methods, ICA and neural networks. *Journal of Medical Systems*, *34*(4), 777–785. https://doi.org/10.1007/s10916-009-9292-7

Suhm, B. (2021). *Heart Sound Classifier*. MATLAB Central File Exchange. May 17, 2017. https://doi.org/https://www.mathworks.com/matlabcentral/fileexchange/65286-heart-sound-classifier

Taylor, A. D., Bronks, R., & Bryant, A. L. (1997). The relationship between electromyography and work intensity revisited: A brief review with references to lacticacidosis and hyperammonia. *Electromyography and Clinical Neurophysiology*, *37*(7), 387–398.

https://www.scienceopen.com/document?vid=38c9dbf7-8cb1-4abc-bc69-89cdc12a4bf3

Toledo-Peral, C. L., Gutiérrez-Martínez, J., Mercado-Gutiérrez, J. A., Martín-Vignon-Whaley, A. I., Vera-Hernández, A., & Leija-Salas, L. (2018). SEMG signal acquisition strategy towards hand FES control. *Journal of Healthcare Engineering*, *2018*(6). https://doi.org/10.1155/2018/2350834

Too, J., Abdullah, A. R., Saad, N. M., & Tee, W. (2019). EMG feature selection and classification using a Pbest-guide binary particle swarm optimization. *Computation*, *7*(1). https://doi.org/10.3390/computation7010012

Vigotsky, A. D., Halperin, I., Lehman, G. J., Trajano, G. S., & Vieira, T. M. (2018). Interpreting signal amplitudes in surface electromyography studies in sport and rehabilitation sciences. *Frontiers in Physiology*, *8*(JAN). https://doi.org/10.3389/fphys.2017.00985

Waly, S. M., Asfour, S. S., & Khalil, T. M. (1996). Effects of time windowing on the estimated EMG parameters. *Computers and Industrial Engineering*, *31*(1–2), 515–518. https://doi.org/10.1016/0360-8352(96)00188-x

Wan, J. J., Qin, Z., Wang, P. Y., Sun, Y., & Liu, X. (2017). Muscle fatigue: General understanding and treatment. In *Experimental and Molecular Medicine* (Vol. 49, Issue 10, p. 384). Nature Publishing Group. https://doi.org/10.1038/emm.2017.194

Wang, J., Sun, Y., & Sun, S. (2020). Recognition of Muscle Fatigue Status Based on Improved Wavelet Threshold and CNN-SVM. *IEEE Access*, *8*, 207914–207922. https://doi.org/10.1109/ACCESS.2020.3038422

Williams, N. (2017). The Borg Rating of Perceived Exertion (RPE) scale. *Occupational Medicine*, *67*(5), 404–405. https://doi.org/10.1093/occmed/kqx063

Wu, Q., Mao, J. F., Wei, C. F., Fu, S., Law, R., Ding, L., Yu, B. T., Jia, B., & Yang, C. H. (2016). Hybrid BF-PSO and fuzzy support vector machine for diagnosis of fatigue status using EMG signal features. *Neurocomputing*, *173*, 483–500. https://doi.org/10.1016/j.neucom.2015.06.002

Xie, H., & Wang, Z. (2006). Mean frequency derived via Hilbert-Huang transform with application to fatigue EMG signal analysis. *Computer Methods and Programs in Biomedicine*, *82*(2), 114–120. https://doi.org/10.1016/j.cmpb.2006.02.009

Yang, Z., Wu, Q., & Fu, S. (2014). Spectral analysis of surface EMG based on empirical mode decomposition. *Optik*, *125*(23), 7045–7052. https://doi.org/10.1016/j.ijleo.2014.08.109

Yochum, M., Bakir, T., Lepers, R., & Binczak, S. (2012). Estimation of muscular fatigue under electromyostimulation using CWT. *IEEE Transactions on Biomedical Engineering*, *59*(12), 3372–3378. https://doi.org/10.1109/TBME.2012.2215031

Yochum, M., Binczak, S., Bakir, T., Jacquir, S., & Lepers, R. (2010). A mixed FES/EMG system for real time analysis of muscular fatigue. *2010 Annual International Conference of the IEEE Engineering in Medicine and Biology Society, EMBC'10*, 4882–4885. https://doi.org/10.1109/IEMBS.2010.5627264

Zhang, G., Morin, E., Zhang, Y., & Etemad, S. A. (2018). *Non - invasive detection of low - level muscle fatigue using surface EMG with wavelet decomposition*. 5648–5651.

Zhang, L., Huang, M.-J., & Wang, H.-J. (2019). A Novel Technique for Fetal Heart Rate Estimation Based on Ensemble Learning. *Modern Applied Science*, *13*(10), 137. https://doi.org/10.5539/mas.v13n10p137

Zhao, S., Liu, J., Gong, Z., Lei, Y., Ouyang, X., Chan, C. C., & Ruan, S. (2020). Wearable physiological monitoring system based on electrocardiography and electromyography for upper limb rehabilitation training. *Sensors (Switzerland)*, *20*(17), 1–17. https://doi.org/10.3390/s20174861

Zhou, Y., Bi, Z., Ji, M., Chen, S., Wang, W., Wang, K., Hu, B., Lu, X., & Wang, Z. (2020). A Data-Driven Volitional EMG Extraction Algorithm during Functional Electrical Stimulation with Time Variant Parameters. *IEEE Transactions on Neural Systems and Rehabilitation Engineering*, *28*(5), 1069–1080. https://doi.org/10.1109/TNSRE.2020.2980294

APPENDIX A: SEARCH PARAMETERS

Search Criteria and Search string	
sEMG	Electromyography Electromyogram electromyogram surface electromyography sEMG EMG SEMG electromyo*
Muscle fatigue	Muscle fatigue muscle fatigue fatigue fatigue*
Activity or exercise	exercises exercise exercise* training activity activit* activities physical activities physical activity dynamic contraction dynamic contractions dynamic contraction* contraction contract** repetitive exercise repetitive repetitive training repetitive
Detection	identification diagnosis assesses assessment quantify analysis detect detection record recognition

	forecast prediction determine*
Non-invasive	non-invasive non-invasively non-invasiv* noninvasive noinvas*
Wearable	autonomous auto* real-time real time automatic standalone

APPENDIX B: TECHNICAL SPECIFICATIONS OF PI ZERO W

Pi zero w: (Pi Zero official website)

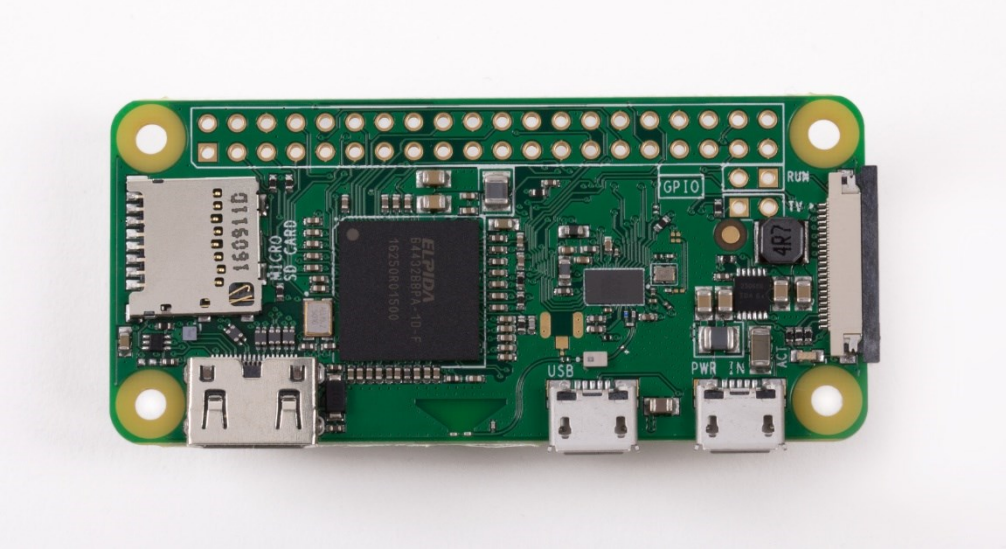

Raspberry Pi Zero W specs

- **Dimensions:** 65mm × 30mm × 5mm
- **SoC:** Broadcom BCM2835
- **CPU:** ARM11 running at 1GHz
- **RAM:** 512MB
- **Wireless:** 2.4GHz 802.11n wireless LAN
- **Bluetooth:** Bluetooth Classic 4.1 and Bluetooth LE
- **Power:** 5V, supplied via micro USB connector
- **Video & Audio:** 1080P HD video & stereo audio via mini-HDMI connector
- **Storage:** MicroSD card
- **Output:** Micro USB
- **GPIO:** 40-pin GPIO, unpopulated
- **Pins:** Run mode, unpopulated; RCA composite, unpopulated
- Camera Serial Interface (CSI)

APPENDIX C: INDEX OF MUSCLE FATIGUE

Liu et al. (2019) introduced a fatigue index reporting a formula. The level of fatigue is given below:

$$Level_{Muscle\_Fatigue} = \left[\frac{Baseline - MF_{average}}{Baseline} \times 100\right]_{10}$$

According to the equation, the average of the first MDF values would be the baseline, and an average of the other MDF values was used to calculate the level of fatigue. If the average value of the MDF was more significant than the baseline value, then the average MDF is replaced with the baseline value.

APPENDIX D: POWER SPECTRUM OF THE sEMG SIGNAL WITH DETREND

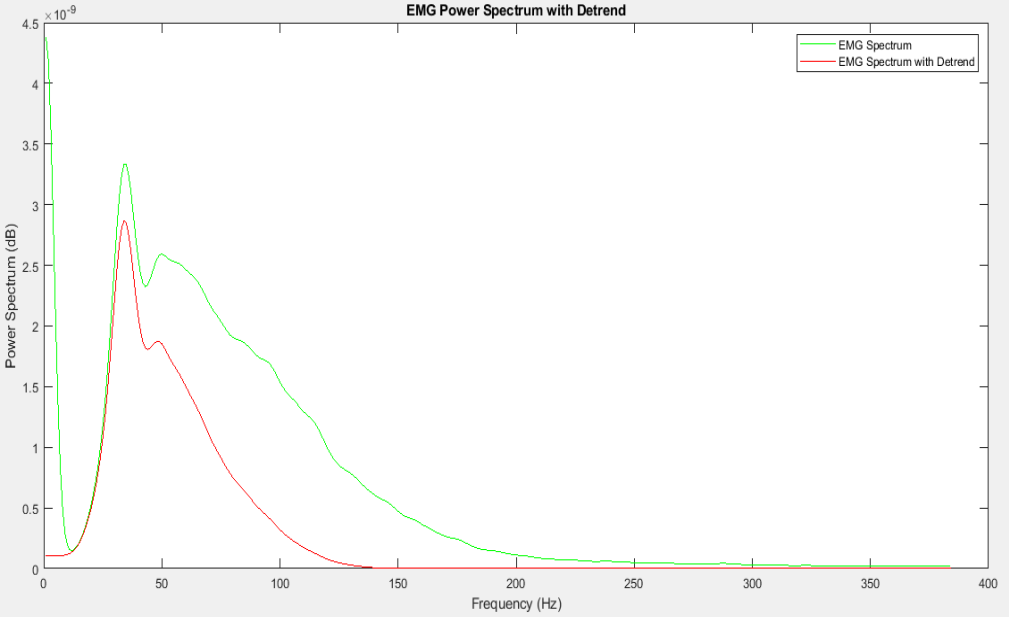

Figure 2: the power spectrum of the EMG signal with and without Detrend.

APPENDIX E: NECESSARY CODE

Code for selected algorithms.

```
import pandas as pd
from matplotlib import pyplot as plt
import numpy as np
from sklearn.preprocessing import MinMaxScaler, RobustScaler, StandardScaler
from sklearn.model_selection import train_test_split
from sklearn import metrics
from sklearn import svm
from sklearn.metrics import precision_recall_curve
from sklearn.metrics import f1_score
from sklearn.metrics import auc
from sklearn.metrics import roc_curve
from sklearn.metrics import roc_auc_score
from sklearn.metrics import plot_confusion_matrix
from sklearn.ensemble import RandomForestClassifier
from sklearn.linear_model import LogisticRegression
from sklearn.model_selection import GridSearchCV
from sklearn.svm import SVC
from sklearn.metrics import classification_report
```

```
### Dropping participants ID and epochs

dataset = dataset.drop('Participant_ID',axis=1)
dataset = dataset.drop('Test_Length', axis=1)
dataset = dataset.drop('Epoch',axis=1)
print("Dataset Shape After Dropping Epochs and ID : ", dataset.shape)
```

```
Dataset Shape After Dropping Epochs and ID :  (479, 36)
```

```
x = dataset.iloc[:,0:35] ### Taking only first 37 columns as input
```

```
: ### Scaling the data between 0 and 1

scaler = MinMaxScaler()
x = scaler.fit_transform(x)
```

```
: y = dataset.iloc[:,35:36] ### Taking last columns for target
y = np.squeeze(y,axis=1)
```

```
: x_train, x_test, y_train, y_test = train_test_split(x, y, test_size = 0.5,␣
 ↪random_state=10)
```

Applying Grid Search

```
: # Set the parameters by cross-validation
tuned_parameters = [{'kernel': ['rbf'], 'gamma': [1e-3, 1e-4],
                     'C': [1, 10, 100, 1000]},
                    {'kernel': ['linear'], 'C': [1, 10, 100, 1000]}]

scores = ['precision', 'recall']


for score in scores:
    print("# Tuning hyper-parameters for %s" % score)
    print()

    clf = GridSearchCV(
        SVC(), tuned_parameters, scoring='%s_macro' % score
    )
    clf.fit(x_train, y_train)

    print("Best parameters set found on development set:")
    print()
    print(clf.best_params_)
    print()
    print("Grid scores on development set:")
    print()
    means = clf.cv_results_['mean_test_score']
    stds = clf.cv_results_['std_test_score']
    for mean, std, params in zip(means, stds, clf.cv_results_['params']):
        print("%0.3f (+/-%0.03f) for %r"
              % (mean, std * 2, params))
    print()

    print("Detailed classification report:")
    print()
    print("The model is trained on the full development set.")
    print("The scores are computed on the full evaluation set.")
```

```
    print()
    y_true, y_pred = y_test, clf.predict(x_test)
    print(classification_report(y_test, y_pred))
    print()
```

Code for aggregated power spectrum plot

```
clc
clear vars

numParticipants = 96;
tableLength = numParticipants*1+1;
tableWidth = 33;
dataTable = zeros(tableLength,tableWidth);

for i=1:96

    Variable = readmatrix([pwd,'\', strcat(num2str(i)),'.xlsx']);
    data=Variable;
    Time=data(1:end,1);
    EMG=data(1:end,2);
    [Time, EMG] = trimzeros(Time, EMG);    %% eliminate unwanted zeros from the lower part of the excel
    EMG=filloutliers(EMG,'nearest','median');

    N=length (EMG);
    Resulotion=fix(N/5);
    aa=Resulotion;
    bb=2*aa;
    cc=3*aa;
    dd=4*aa;
    ee=5*aa;

    EMG_1=EMG(1:cc, 1);
    Time_1=Time(1:cc, 1);
    xTable_1=timetable(seconds(Time_1), EMG_1);
    [pxx_1, f_1]=pspectrum (xTable_1);

    maxFreq = 150;

    Frequency_Range_1 =(0:5:maxFreq).';

    % This array will store the locations of the closest frequency to match with members of fivesArray
    PowerLocs_1 = zeros((length(Frequency_Range_1)),1);

    % This array will store the values from the table corresponding to the locations
    PowerMagnitude_1 = zeros((length(Frequency_Range_1)),1);

    for j = 1:numel(Frequency_Range_1)

    % Find the location of the element in f closest to the element i of fivesArray
```

```
    [val_1, PowerLocs_1(j)] = min(abs(f_1-Frequency_Range_1(j)));
    % Extract pxx value of that index
    PowerMagnitude_1(j) = pxx_1(PowerLocs_1 (j));

    end

    FinalTable_1 = [Frequency_Range_1, PowerMagnitude_1];


    Epoch_1= 1;
    State_1="Non-Fatigue";
    P_ID=i;
    rowIdx_1 =(2*i-1)+ Epoch_1;
    dataTable(rowIdx_1,:) = [P_ID, State_1, PowerMagnitude_1'];

  %%%%%%%%%%%%%%%%%%%%   2 %%%%%%%%%%%%%%%%%%%%%%%


    EMG_2=EMG(cc:ee, 1);
    Time_2=Time(cc:ee, 1);
    xTable_2 = timetable(seconds(Time_2),EMG_2);
    [pxx_2,f_2] = pspectrum (xTable_2);

    xTable_2=[f_2 pxx_2];


    maxFreq = 150;



% Get an array going from 0 to maximum frequency in steps of 5
Frequency_Range_2 = (0:5:maxFreq).';

% This array will store the locations of the closest frequency to match with members of fivesArray
PowerLocs_2 = zeros((length(Frequency_Range_2)),1);

% This array will store the values from the table corresponding to the locations
PowerMagnitude_2 = zeros((length(Frequency_Range_2)),1);

  for k = 1:numel(Frequency_Range_2)

    % Find the location of the element in f closest to the element i of fivesArray

    [val_2, PowerLocs_2(k)] = min(abs(f_2-Frequency_Range_2(k)));
```

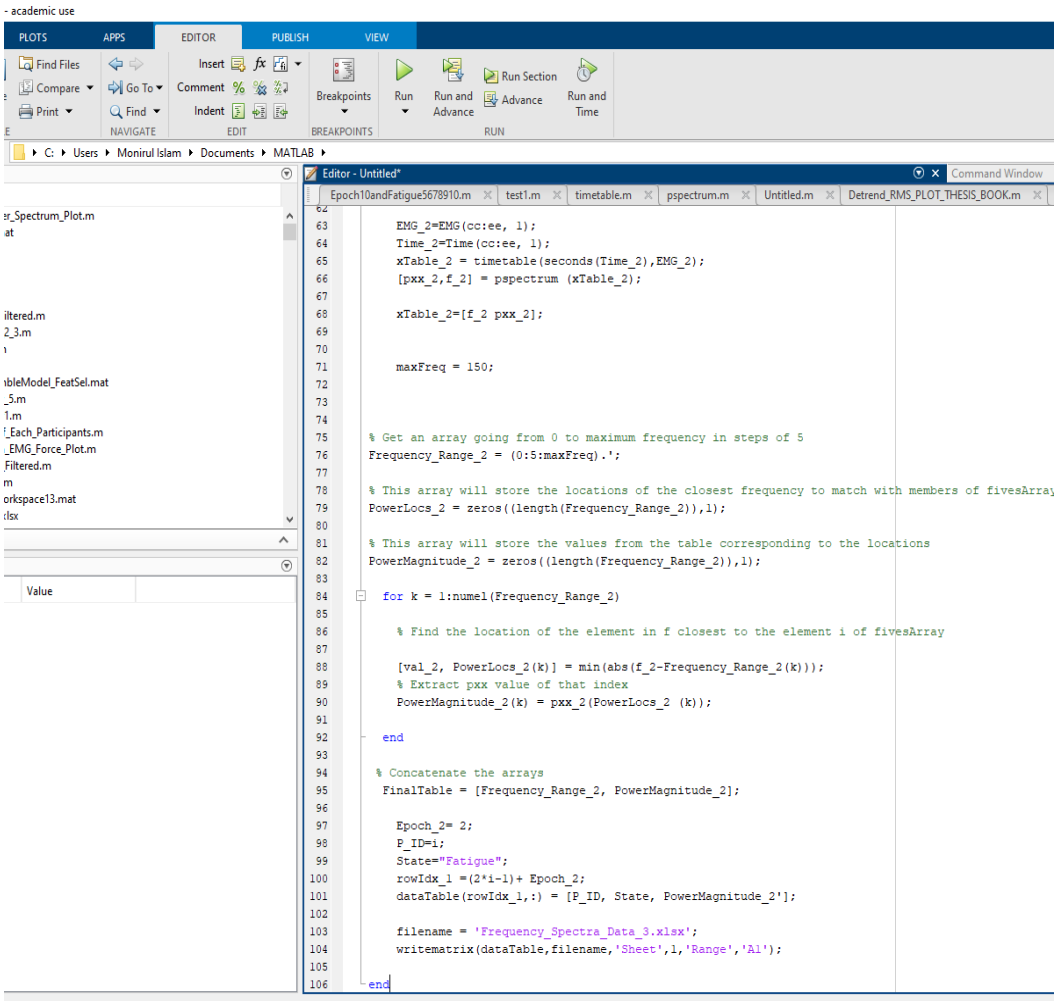
- academic use
PLOTS
APPS
EDITOR
PUBLISH
VIEW
Find Files
Compare
Print
Go To
Find
NAVIGATE
Insert
Comment
Indent
EDIT
Breakpoints
BREAKPOINTS
Run
Run and Advance
Run Section
Advance
Run and Time
RUN
C: ▸ Users ▸ Monirul Islam ▸ Documents ▸ MATLAB ▸
Editor - Untitled*
Command Window
Epoch10andFatigue5678910.m
test1.m
timetable.m
pspectrum.m
Untitled.m
Detrend_RMS_PLOT_THESIS_BOOK.m
Value
EMG_2=EMG(cc:ee, 1);
Time_2=Time(cc:ee, 1);
xTable_2 = timetable(seconds(Time_2),EMG_2);
[pxx_2,f_2] = pspectrum (xTable_2);
xTable_2=[f_2 pxx_2];
maxFreq = 150;
% Get an array going from 0 to maximum frequency in steps of 5
Frequency_Range_2 = (0:5:maxFreq).';
% This array will store the locations of the closest frequency to match with members of fivesArray
PowerLocs_2 = zeros((length(Frequency_Range_2)),1);
% This array will store the values from the table corresponding to the locations
PowerMagnitude_2 = zeros((length(Frequency_Range_2)),1);
for k = 1:numel(Frequency_Range_2)
% Find the location of the element in f closest to the element i of fivesArray
[val_2, PowerLocs_2(k)] = min(abs(f_2-Frequency_Range_2(k)));
% Extract pxx value of that index
PowerMagnitude_2(k) = pxx_2(PowerLocs_2 (k));
end
% Concatenate the arrays
FinalTable = [Frequency_Range_2, PowerMagnitude_2];
Epoch_2= 2;
P_ID=i;
State="Fatigue";
rowIdx_1 =(2*i-1)+ Epoch_2;
dataTable(rowIdx_1,:) = [P_ID, State, PowerMagnitude_2'];
filename = 'Frequency_Spectra_Data_3.xlsx';
writematrix(dataTable,filename,'Sheet',1,'Range','A1');
end

APPENDIX F: PARTICIPANT CONSENT FORM AND STUDY PROTOCOL

Title of Project: DEMA-Dash: Real time EMG relay and fatigue detection

Name of Principal Investigator: Dr. Martin Ferguson-Pell
Contact Information: Phone: 780-492-4383, Email: martin.ferguson-pell@ualberta.ca
Name of Undergraduate Student: Adam Pinkoski
Contact Information: Phone: 780-222-5575, Email: apinkosk@ualberta.ca

	Yes	No
Do you understand that you have been asked to participate in a research study?	☐	☐
Have you received and read a copy of the attached Information Sheet?	☐	☐
Do you understand the benefits and risks involved in taking part in this research study?	☐	☐
Have you had an opportunity to ask questions and discuss this study?	☐	☐
Do you understand that you are free to refuse to participate or withdraw from the study at any time, without having to give reason, and that your information will be withdrawn at your request?	☐	☐
Has the issue of confidentiality been explained to you? Do you understand who will have access to your records/information?	☐	☐

This study was explained to me by: _____

I agree to take part in this study. Yes ☐ No ☐

_____ _____ _____
Signature of Research Participant **Date** **Witness**

I believe that the person signing this form understands what is involved in the study and voluntarily agrees to participate.

_____ _____
Signature of Investigator or Designee **Date**

Martin Ferguson Pell's Office
5-375 Edmonton Clinic Health Academy • University of Alberta • Edmonton • Canada • T6G 1C9
Telephone: (780) 492-4383

Last name _____

First name _____

Email address _____

Telephone Number _____

Year of Birth (Age) _____

A copy of the consent form must be given to the participant

Martin Ferguson Pell's Office
5-375 Edmonton Clinic Health Academy • University of Alberta • Edmonton • Canada • T6G 1C9
Telephone: (780) 492-4383

Study protocol

DEMA-Dash: Real time EMG relay and fatigue detection

Principal Investigator and Contact Information:

Dr. Martin Ferguson-Pell Telephone 780-492-4383 or Email: martin.ferguson-pell@ualberta.ca

Overview of the study

Electrical signals make muscles move. Measuring these electrical signals will allow us to tell how well the muscle is working. When muscles have been working very hard or for a long period of time, the muscle will get tired and the electrical signals will slow down, making the muscle weaker. This process is known as fatigue. Fatigue is useful for researchers but is difficult to detect as it happens. This study was designed to produce an index of fatigued signals to use for the detection of fatigue as the muscular contraction is occurring. We will be recruiting approximately 100 participants. As a participant in this study you will be invited to the lab for a single visit lasting about 30 minutes.

What will be done if you take part in this research study?

As a participant in this study, you will be invited to the lab for a single visit. Upon arrival you will be asked to complete a Physical Activity Readiness Questionnaire (PARQ+) (2 minutes) to ensure you are healthy and capable of participating in the test. Once completed, you will perform a test to measure the maximal strength (MVC) of your biceps. This test involves pulling on a stationary strap as hard as possible for a duration of 3 seconds. This will be repeated 3 times with a rest period of 1 minute between each trial (10 minutes). After the final MVC trial, you will rest for 5 minutes while you recover. The next step involves pulling on the strap at a force of 40% of your maximum strength. For this step you will be required to pull on the strap for as long as possible at the target force. Once you can no longer physically sustain the target force the test will finish (15 minutes) and you will be free to leave. All testing will involve use of some instruments that will be attached to you. These instruments include:

- Surface Electromyography (sEMG): This device is used to read the electrical activity of your muscles. For this, a single electrode will be placed on the skin over the biceps of your dominant arm while a reference electrode will be placed on the skin on the back of your non dominant arm. Double sided and medical tape will be used to stick the electrodes onto the skin.
- A force transducer: This device measures the amount of force that you produce by pulling on a strap. This information will be available to you throughout the testing process.

What are the possible discomforts and risks of participation?

This is a low risk study applying low level exercise testing. There is no adverse effects to be expected by participating in this study. There are no expected risks and discomforts associated with this study, other than those normally associated with sustained muscular contractions and can be felt as physical fatigue immediately following the completion of testing.

There will be at least 1 minute between each MVC trial. The next trial will not be started until you feel as though you have had as much rest as needed. The same will apply during the rest period between the final MVC trial and the 40% exertion trial. A minimum of 5 minutes recovery between these trials is scheduled but if more time is needed to recover, you are more than welcome to take longer.

What are the possible benefits to you or to others?

There is no direct immediate benefit to the participants. This study will help researchers and clinicians to build an index of fatigue that can potentially be used in real time detection of fatigue during various muscular activities.

How will your privacy and the confidentiality of your research records be protected?

Personal records relating to this study will be kept confidential. Any research data collected about participants during this study will not identify by participants' name, only by participants' initials and a coded number. Participants' name will not be disclosed outside the research office (ECHA, 2-545). No one would have access to your identifying information other than this study research team, unless the investigator gets a written permission from you. None of your identifying information will be published, and your confidentiality will remain protected. Any report published as a result of this study will not identify by participants by name. A minimum period of 7 years the data will be stored by the researchers.

Can you withdraw from this study?

Taking part in this study is completely up to you. You can refuse to take part or withdraw from the study at any time and such a decision will not affect you in any way. You can also ask for stopping the experiment if you experience motion sickness.

What if you do not want to answer a particular question?

You are not required to answer any question if you do not want to.

Who may you contact if you have concerns about this research study?

- If you have questions about your rights as a research participant, please contact the Health Research Ethics Board at 780-492-0302.
- If you have any questions feel free to ask the investigator: Adam Pinkoski,
    - cell: (780) 222-5575
    - email: apinkosk@ualberta.ca